Understanding and predicting storage stability of UHT milk

A thesis submitted in fulfillment of the requirements of the degree of

Doctor of Philosophy

By

Manpreet Kaur Grewal

B.Tech. (Agril. Engg.), M.Tech. (Food Process Engg.)

College of Health and Biomedicine

Institute of Sustainable Industries and Liveable Cities

2018

Dedicated to my beloved husband Sukhjiwan, parents S. Balwinder Singh and Smt. Sukhmeet Kaur, parents-in-law S. Inderjeet Singh and Smt. Bhupinder Kaur and kids Harjas and Tejal

CERTIFICATE

Todor Vasiljevic (BEng., PhD)

Professor

College of Health & Biomedicine

Institute of Sustainable Industries and Liveable Cities

Victoria University

Werribee Campus, VIC Australia

This is to certify that the thesis entitled "Understanding and predicting storage stability of UHT milk" submitted by Manpreet Kaur Grewal in partial fulfilment of the requirement for the award of the Doctor of Philosophy in Food Science at Victoria University is a record of the bonafide research work carried out by her under my personal guidance and supervision and the thesis has not previously formed the basis for the award of any degree, diploma or other similar title.

Prof. Todor Vasiljevic

Date 12/03/2018

DECLARATION

I, Manpreet Kaur Grewal, declare that the PhD thesis by publication entitled "Understanding and predicting storage stability of UHT milk" is no more than 100,000 words in length including quotes and exclusive of tables, figures, appendices, bibliography, references and footnotes. This thesis contains no material that has been submitted previously, in whole or in part, for the award of any other academic degree or diploma. Except where otherwise indicated, this thesis is my own work.

Manpreet Kaur Grewal

Dated: 13/03/18

ACKNOWLEDGEMENT

I would like to express my sincere gratitude to my principal supervisor, Todor Vasiljevic, Professor of Food Science and Leader, Advanced Food Systems Research Unit, College of Health and Biomedicine, Victoria University for his professional guidance, scientific contribution, vision and encouragement. I am grateful to him for listening with patience to my ideas and steering me into the right direction with his ability to think clearly in all sort of situations. His 'question for a question' style has honed my thinking skills and helped developing capability to handle research projects independently. Because of him, I am now confident to write a research paper on my own. His supervision fulfilled a lot of expectations, I had from my PhD degree.

I also acknowledge scientific contribution, technical support and constructive feedback of my co-supervisors by Dr. Osaana Donkor, Prof Vasso Appostopoulos and Prof. Lily Stojanovska. I sincerely acknowledge timely academic and moral support of Dr. Jayani Chandrapala in my PhD degree. She has always been supportive and willing to discuss different challenges I faced in experimentation, analysis and interpretation. I cannot thank you enough for making a positive impact on my personal and professional development.

I gratefully acknowledge the contribution and technical assistance of the laboratory manager, Mrs. Stacey Lloyd and the laboratory technicians Joseph Pelle and Charmaine DiQuattro. Special thanks to Joseph Pelle for his technical training for different instruments and prompt support with their troubleshooting. Special thanks to colleagues at Victoria University, Manjula Nishanthi, Nuwan Vithanage, Narges Dargahi, Winston Liyanaarachchi for healthy discussions. Special thanks to Muditha for training me with different scientific protocols.

I would like to express my heartiest gratitude to my lunch friends Swati Garg, Anthony, Robin and Derrick Dsouza. Mere thanks will not be enough for my dear friends Anthony and Robin for moral support and healthy arguments and discussions over these years. Your invaluable time and efforts has helped me enormously to overcome difficult emotions, focus on my study and succeed. Another valuable friend I gained during this PhD journey is Zeinab Ahmed, whose kindness is matchless.

I will like to express gratitude to my supervisor Dr. SN Jha during my role as Food Scientist at CIPHET, ICAR, India who introduced me to FTIR spectroscopy and chemometrics. Without his mentorship and guidance, I would not have been able to acquire expertise and skill in the area of spectroscopy, which helped me to sail smoothly throughout my PhD.

Finally, I would like to express my heartiest and sincerest gratitude to my husband, Sukhjiwan, for always been positive, supportive, strongly believing in me and standing by my side in every situation. Your love, enthusiasm, encouragement and moral support is the main reason I survived the PhD course. No words would describe how grateful I am for the patience exhibited by my kids Harjas and Tejal. I wish to thank my mother-in-law Bhupinder Kaur for her continuous love and support over the last few years. I have to thank my dad Balwinder Singh for constant reminder that I cannot quit. I acknowledge love and encouragement provided by my mother Sukhmit Kaur.

I acknowledge the Australian India Institute for bestowing me with the Victoria India Doctoral scholarship and state government of Victoria for providing me child care rebate and benefits, without which the PhD journey with a family to support could have been real tough.

VICTORIA UNIVERSITY
MELBOURNE AUSTRALIA

PART A:

DETAILS OF INCLUDED PAPERS: THESIS BY PUBLICATION

Please list details of each Paper included in the thesis submission. Copies of published Papers and submitted and/or final draft Paper manuscripts should also be included in the thesis submission

Item/ Chapter No.	Paper Title	Publication Status (e.g. published, accepted for publication, to be revised and resubmitted, currently under review, unsubmitted but proposed to be submitted)	Publication Title and Details (e.g. date published, impact factor etc.)
3	Electrophoretic characterization of protein interactions suggesting limited feasibility of accelerated shelf-life testing of ultra-high temperature milk	Published	**Published online 11 November 2016 in Journal of Dairy Science, SJR Q1**
4	Fourier transform infrared spectroscopy analysis of physicochemical changes in UHT milk during accelerated storage	Published	**Published online 2 December 2016 in International Dairy Journal, SJR Q1**
5	Predicting sediment formation in ultra high temperature-treated whole and skim milk using attenuated total reflectance-Fourier transform infrared spectroscopy	Published	**Published online 4 Februray 2017 in International Dairy Journal, SJR Q1**
6	FTIR fingerprinting of structural changes of milk proteins induced by heat treatment, deamidation and dephosphorylation	Published	Published online 8 February 2018 in Food Hydrocolloids, SJR Q1

Declaration by [candidate name]: Manpreet Kaur Grewal

Signature: [redacted]

Date: 28.02.18

ORAL PRESENTATION

Grewal M.K., C. J., Donkor O., Apostolopoulos V., Vasiljevic T. (2016). *Predicting storage stability of UHT milk proteins using FTIR spectroscopy*. Paper presented at the NIZO Dairy Conference - Asia Pacific. Milk protein ingredients, Singapore.

TABLE OF CONTENTS

LIST OF FIGURES

LIST OF TABLES

ABSTRACT

UHT milk is gaining market share worldwide for being a healthy, safe and convenient food product with a long shelf life at room temperature. However, the UHT treatment (usually 140-150 °C for 2-10 s) contributing to its long shelf life may induce some changes, which may make it unstable during storage. Considerable levels of sedimentation (up to 1 % dry weight basis) of proteinaceous material at the bottom of the storage container, or formation of a gel (age-gelation), or both, can mark the end of shelf life of UHT milk, and hence affect its market potential and incur financial losses to the UHT dairy processors. Irrespective of a mechanism, gelation or sedimentation appears to be governed and preceded by changes in the extent and nature of interactions among milk proteins leading to their aggregation. Though recent investigations have added significantly to the understanding of the different protein interactions, the exact mechanism involving changes in these molecular interactions leading to sedimentation and gelation, is not clear yet. Moreover, less is known about the role of protein-lipid interactions in the development of a storage instability. In addition, the need of a rapid technique which can detect the shelf life of UHT milk has been emphasised in recent years. This is mainly because applying full-length shelf life tests in a product such as UHT milk would be time- and resource-intensive. Thus, the overall objective of this project was to understand and rapidly predict the storage stability of UHT milk.

Accelerated shelf life testing is one such rapid alternative applied to a variety of food products to save time. The industry has not been successful in applying this approach to ultra-high temperature (UHT) milk because of the chemical and physical changes in the milk proteins that take place during its processing and storage. Thus, the first objective of the study was to investigate the feasibility of applying accelerated shelf life principles to UHT milk samples with different fat levels to elucidate changes in interactions of milk proteins at ambient

temperature using electrophoretic analysis (Native- and Sodium dodecyl sulfate-polyacrylamide gel electrophoresis). Samples of UHT skim (SM) and whole milk (WM) were stored at 20, 30, 40, and 50 °C for 28 days. Irrespective of fat content, UHT treatment had a similar effect on the electrophoretic patterns of milk proteins. At the start of testing, proteins were bonded mainly through disulphide and noncovalent interactions. However, storage at and above 30 °C enhanced protein aggregation via covalent interactions. The extent of aggregation appeared to be influenced by fat content, implying aggregation via melted or oxidized fat, or both. Based on the reduction in loss in the absolute quantity of individual proteins, covalent crosslinking in WM was facilitated mainly by products of lipid oxidation. Whereas, Maillard and dehydroalanine products appeared to be the main contributors to protein changes in SM. Protein crosslinking appeared to follow a different pathway at higher temperatures (≥40 °C), making it difficult to extrapolate these changes to lower temperatures. The changes identified under the accelerated shelf life conditions using electrophoretic analysis assisted in evaluating the potential of using another rapid technique, Fourier transform infrared spectroscopy (FTIR) in detecting changes in structure and interactions of milk proteins (the second objective).

The feasibility of using FTIR to detect changes in conformational rearrangements, protein-protein and protein-lipid interactions was studied with accelerated shelf life protocols. WM and SM were stored at 20, 30, 40 and 50 °C for 28 days. The changes in FTIR spectra were observed concomitant with increased sedimentation in SM (by 50 %) and WM (by 20 %) at higher temperatures (40 °C) after 14 days of the storage period. Milk samples stored at 40 and 50 °C showed marked changes in the bands corresponding to the conformations of milk lipids and formation of intermolecular β-sheets, indicating protein-lipid interactions and aggregation. Dried sediment contained fat confirming protein-lipid participation in the sedimentation. FTIR was also able to detect changes that led to increased sedimentation in SM at temperatures lower than 40 °C, but only after 28 days. However, to establish appropriateness

of accelerated shelf life testing and FTIR as a tool for prediction of stability of UHT milk, the observed correlation between spectral changes and sediment formation at accelerated temperatures has to align with that at normal storage temperature (third objective of the study).

SM and WM were stored at 20 °C for 9 months to investigate the feasibility of using FTIR to predict sedimentation in UHT milk. Identified spectral marker variables corresponding to changes in the structure and interactions of lipids, proteins and carbohydrates successfully predicted sedimentation in SM (R^2 -0.92) and WM (R^2 - 0.60). Low predictability in WM may be due to the influence of fat. These markers were similar to those observed during accelerated shelf life testing, hence implying that the accelerated shelf life testing could be used in UHT milk.

Among several changes in milk protein interactions during its heating and storage, conformational changes specific to an interaction remain largely unknown. Hence, the fourth objective of the project evaluated the possibility of fingerprinting two selected changes, i.e., deamidation and dephosphorylation, using FTIR. Enzymatic deamidation and dephosphorylation were carried out prior to heat treatment. Principal component analysis revealed that the heat treatment induced different changes in the secondary structure of control, deamidated and dephosphorylated milk samples. In contrast to a significant ($P<0.05$) decrease in β-sheet (1624 cm^{-1}) and a rise in β-turns (1674 cm^{-1}) in heated control samples, both deamidation and dephosphorylation of SM before heat treatment created more ordered secondary structure (significant ($P<0.05$) increase in α-helix (1650-52 cm^{-1}) and β-sheet at the expense of 3_{10}-helix (1661 cm^{-1}), random (1645-46 cm^{-1}) and β-turn (1674 cm^{-1}). The only difference between heated deamidated and dephosphorylated samples was decrease in large loops (1656 cm^{-1}) in the latter opposed to the increase in the former.

The project therefore established that the accelerated shelf life testing in combination with FTIR spectroscopy has a potential as a rapid tool to forecast sedimentation and other instabilities in UHT milk, and hence the shelf life of UHT milk. Further, a complete understanding of the conformational changes affecting the storage stability of UHT milk could also be attained by studying the structural changes specific to different known interactions using FTIR spectroscopy

CHAPTER 1

Introduction

1.1 Introduction

UHT milk has gained acceptance worldwide for being a healthy, safe and convenient food product with a long shelf life at room temperature (Newswire, 2014; Malmgren et al., 2017). It owes its long shelf life to ultra-high temperature (UHT) treatment involving heating of milk at high temperature (usually 140-150 °C) for 2-10 s followed by aseptic packaging (Deeth & Lewis, 2016). The treatment and packaging renders UHT milk as a 'commercially sterile' product with minimal changes to its quality. More importantly elimination of the requirement of cold chain and refrigeration facilities for transportation and storage contributes in reducing energy loads and the greenhouse gas emissions. However, UHT milk might get unstable during storage and experience physical defects like sedimentation of proteinaceous material at the bottom of the storage container or formation of a gel (age-gelation), or both (Andrews & Cheeseman, 1972; McMahon, 1996; Deeth & Lewis, 2016). Occurrence of considerable levels of sedimentation (up to 1 % dry weight basis (Deeth & Lewis, 2016)) or gelation can mark the end of the shelf life of UHT milk. Hence, the appearance of these defects in UHT milk could affect its market potential and incur financial losses to the UHT dairy processors.

Sedimentation and gelation in UHT milk can be a result of non-enzymatic changes induced by thermal (UHT) treatment, mainly whey protein denaturation, Maillard reaction and mineral imbalance. Likewise, indigenous or exogenous enzyme induced proteolysis, another main underlining mechanism of gelation, also induces protein network formation (i.e., interaction or linking between proteins or their fragments) (Deeth & Lewis, 2016). Irrespective of mechanism, gelation or sedimentation appears to be governed and preceded by changes in the extent and nature of interactions among milk proteins leading to their aggregation.

Changes in protein interactions primarily involve noncovalent interactions, via either weak bonding (such as hydrophobic, van der Waals, or electrostatic interactions) or covalent crosslinking with other proteins through formation of disulphide bonds, advanced Maillard products (AMP), and dehydroalanine (Singh, 1991; Friedman, 1999; Wang, Nema, & Teagarden, 2010; Holland, Gupta, Deeth, & Alewood, 2011). The most assessed pathway of protein aggregation is mediated by denaturation of whey proteins as a result of UHT treatment (Singh, 1991). Denaturation exposes a free sulphydryl group of β-lactoglobulin (β-Lg), which is involved in intramolecular and intermolecular thiol-disulphide exchange reactions with other whey proteins and caseins [κ-Casein (k-CN) and α_{s2}-Casein (α_{s2}-CN)] present on the surface and the interior of the casein micelles, respectively, and homogenised fat globules (Sharma & Dalgleish, 1993). Though recent investigations have expanded the understanding of the above-mentioned interactions, the exact mechanism leading to sedimentation and gelation in UHT milk, is not clear yet. Moreover, the focus has been mainly on the protein-protein linking, less is known about the role of protein-lipid interactions in the initiation and buildup of sediment or a gel. All that is known is that there is lower extent of proteolysis (López-Fandiño, Olano, Corzo, & Ramos, 1993; Garcia-Risco, Ramos, & Lopez-Fandino, 1999), and the formation of Maillard reaction products (Valero, Villamiel, Miralles, Sanz, & Martínez-Castro, 2001) in stored UHT milk with higher fat content. These reports however give an indication that the milk fat plays some role in the extent of protein interactions during storage, and hence needs to be further explored, which would be undertaken in this project.

In addition to exploring the progression and extent of changes in different protein interactions in context of shelf life of UHT milk, the need of a rapid technique which can detect and predict

these changes and hence predict their development in advance has been emphasised in recent years. This is mainly because applying full-length shelf life tests for the purpose in a product such as UHT milk would be time- and resource-intensive. Additionally, it is estimated that 40 % of the cost of developing a new food emulsion is incurred in shelf life testing (Robins, 2000). Accelerated shelf life tests could be one of the suitable alternative for predicting shelf life of UHT milk in comparably short time. By accelerating the rate of deterioration of sensory attributes with the use of elevated storage temperatures, Richards, De Kock, and Buys (2014) successfully developed a model to predict shelf life of UHT milk. Likewise, changes in protein-protein interactions linked to shelf life ending defects such as sediment or gelation can be enhanced using higher storage temperatures (Al-Saadi & Deeth, 2008). Proteomic analysis in combination with accelerated shelf life testing have added information about different types of prospective crosslinking during storage of UHT milk at elevated temperatures, but these techniques are still limited in their approach (Holland et al., 2011). Main reason being the fairly laborious sample preparation accompanied with a complex analysis, all of which require highly trained experts. In recent years, application of vibrational spectroscopy techniques has increased in the food industry. This has been due to these techniques being rapid, non-invasive, non-destructive, requiring very less sample preparation and relatively low cost as compared to the conventional techniques. These techniques are based on the unique spectral analysis of stretching and bending of molecular bonds, and thus collectively producing fingerprint spectra for a particular molecule (Wang, He, Labuza, & Ismail, 2013). Among these techniques, FTIR (Fourier Transform Infrared Spectroscopy) is most accepted and is sensitive to changes in covalent bonding and non-covalent electrostatic and hydrophobic interactions, which are hallmarks of thermal treatment and subsequent storage. Additionally, FTIR

has already been successfully used to study ageing of pharmaceuticals (Masmoudi, Dréau, Piccerelle, & Kister, 2005) and oil in water emulsions (Whittinghill, Norton, & Proctor, 1999) by determination of changes in molecular structure and interactions, but has not been used in UHT milk.

Hence, the project for the first time envisaged studying feasibility of using FTIR technique and accelerated shelf life testing to detect changes in protein structure and interactions, which lead to storage instability mainly sedimentation in UHT milk. Besides tracking the development of storage instabilities in milk using FTIR, the project would also focus on developing a rapid method for prediction of sedimentation in advance. To achieve this, a new approach correlating changes in FTIR spectral profiles and sedimentation using multivariate analysis tools (chemometrics) would be developed. The appropriateness of the developed approach using FTIR and accelerated shelf life testing would be established by comparing the findings to those obtained during full length shelf life testing.

The focus was only on build-up of sediment and not on gelation because higher storage temperatures (>40 °C) inhibit age-gelation (Kocak & Zadow, 1985; McMahon, 1996; Deeth & Lewis, 2016) and result in increased non-dispersible sediment (Nieuwenhuijse & van Boekel, 2003). Thus, accelerated shelf life testing in UHT milk could only be used to predict sedimentation. The results could be extrapolated to predict aggregation mechanisms at lower storage temperatures, avoiding lengthy real-time analysis. The developed approach can also be used to determine and predict storage instabilities in other dairy and non-dairy emulsions.

Besides having an idea of overall changes in the secondary structure and related protein interactions leading to storage instability in UHT milk, conformational adjustments corresponding

to individual protein interactions needs to be known in order to improve the predictive ability of model developed to predict sedimentation in UHT milk and identify the main interactions responsible for this storage instability.

Thus, the overall objective of this project was to understand and predict the storage stability of UHT milk using FTIR spectroscopy and accelerated storage temperatures. The main objectives of this research were:

i) To investigate feasibility of using elevated temperatures during storage of UHT milk containing different fat content to elucidate changes in interactions of milk proteins at ambient temperature using electrophoretic analysis

ii) To determine the feasibility of FTIR technique to detect changes in protein structure and interactions leading to sedimentation under accelerated storage temperatures in skim and whole UHT milk.

iii) To develop a rapid method for detection and prediction of sedimentation in UHT milk using FTIR and multivariate analysis (chemometrics) by comparing findings obtained under accelerated storage temperatures with a long storage study at room temperature.

iv) To detect specific changes in milk protein structure and interactions held responsible for sedimentation using FTIR spectroscopy

1.1 Thesis outline

This thesis comprises of seven chapters. Chapter 1 presents introduction of the project and its aims. A thorough literature review of the current scientific knowledge on the scope of the thesis is provided in chapter 2. Chapter 3-6 are full length published research articles

addressing the four objectives in the same sequence mentioned. An overall conclusion from the study with future research directions is presented in chapter 7.

CHAPTER 2

Literature review

2.1 Literature review

2.2 Milk as a 'complete' food

Milk, a fluid secreted by females of all mammals, is designed to meet the complete nutritional requirement of their neonates. Mainly, milk contains ~90 % water, life's vital requirement, lactose and lipids for energy, proteins and peptides (immunoglobulins, enzymes, enzyme inhibitors, growth factors, hormones, antibacterial agents) for growth, immunity and other physiological functions (O'Mahony & Fox, 2013). Furthermore, milk is free from toxins and antinutritional factors and has a pleasant and attractive flavour and mouthfeel. Such a nutritional and sensory profile has given milk the label of 'complete' food and is not restricted only to meet the nutritional requirements of neonates. Milk from domesticated cows (mainly) has become an integral part of human diet in many parts of the world. In addition, the ease with which it can be converted to a wide range (several thousands) of different and attractive products has made it a favourite ingredient for food industry. As a result, in the USA, Canada, Australia and New Zealand and many European countries, about 30 % of dietary protein is supplied by milk and dairy products (O'Mahony & Fox, 2013). In this thesis, unless otherwise stated, the word *milk* refers to bovine milk.

2.3 Milk composition and structure

Milk, a white or yellowish white complex fluid, contains on average mainly water (91 %), sugar (lactose) (4.6 %), lipids (3.9 %), proteins (3.25 %) and mineral substances (0.65 %) (Walstra, Jenness, & Badings, 1984; Walstra, Wouters, & Geurts, 2005). Milk also contains organic acids such as citrate, enzymes and a range of vitamins that do not fit into the previously mentioned major categories. The composition of milk varies between individual animals, breeds, seasons, feed,

stages of lactation and animal's health. However, this biological variability will not be discussed in detail here.

Milk structure is mainly due to colloidal existence of its lipids as fat globules (fat droplets stabilized by mixture of lipoproteins and bilayer structures), protein casein as casein micelles sterically stabilized by hairy layer of κ-CN and whey proteins as oligomers. These structural components are mainly responsible for optical properties, viscosity and physical stability of milk. These components will be discussed in more detail in section 2.3.1. Typical constituents of milk and their distribution between the colloidal and serum, defined as milk depleted of caseins and fat globules, phases is summarised in Table 2.1.

2.4 Major milk constituents

2.4.1 Lipids

Almost 99 % of milk lipid exists as milk fat globules (MFG) (Heid & Keenan, 2005), which are lipid spheres with diameter ranging from 0.1 to 15 μm (average 4 μm) and surrounded by a multilayered structure called milk fat globule membrane (MFGM) (Leser & Michel, 2008). The membrane comprises about 2 % of the fat globules and is composed of a phospholipid monolayer, an inner protein coat, a bilayered phospholipid membrane, and a glycosylated surface (Mather & Keenan, 1998). MFGM acts as a natural emulsifying agent preventing flocculation and coalescence of fat globules. The membrane also prevents hydrolysis of fat by enzymes. Approximately 95-98 % of the total lipids in these globules consist of triacylglycerides, with lesser amounts of partial glycerides, sterols, phospholipids, glycolipids, and hydrocarbons (Table 2.1) (Mather & Keenan, 1998; Walstra et al., 2005). The remaining portion occurs as membrane-

fragments in the skim milk phase. A detailed review has been published recently about MFG and MFGM (Singh & Gallier, 2017).

Table 2.1 Composition of bovine milk (adapted from Walstra et al., (1984) and Walstra et al. (2005))

Component	**Average content (w/w, %)**		
	Total	**Colloidal**	**Serum phase**
Water	**87**	**8**	**79**
Lipids	**4.07**	**4.058**	**0.016**
Triglycerides	4.0	-	-
Diglycerides	0.01	0.01	-
Phospholipids	0.035	0.025	0.01
Sterols	0.014	0.012	0.002
Free fatty acids	0.01	0.008	0.002
Cerebrosides	0.005	0.003	0.002
Protein	**3.23**	**2.67**	**0.56**
Casein	2.6	2.6	-
α_{s1}-Casein	1.02	1.02	-
α_{s2}-Casein	0.28	0.28	-
β-Casein	0.93	0.93	-
κ-Casein	0.37	0.37	-
Whey protein	0.56	-	0.56
β-Lactoglobulin	0.32	-	0.32
α-Lactalbumin	0.12	-	0.12
Bovine serum albumin	0.04	-	0.04
Immunoglobulins	0.08	-	0.08
Others	0.07	0.07*	
Carbohydrates (lactose)	**4.6**	-	**4.6**
Mineral substance	**0.7**	**0.2**	**0.481**
Calcium	0.117	0.080	0.037
Phosphate	0.21	0.1	0.11
Potassium	0.143	0.011	0.132
Magnesium	0.011	0.004	0.007
Sodium	0.048	0.002	0.046
Chloride	0.11	-	0.11
Sulphate	0.01	-	0.01
Bicarbonate	0.01	-	0.01
Organic acids	**0.189**	**0.026**	**0.161**
Citrate	0.175	0.014	0.161
Others	0.012	0.012	-
Miscellaneous		0.14	

* Proteins in fat globule membrane

** The values are average of the biological variability between individual animals, breeds, seasons, feed, stages of lactation and animal's health

2.4.2 Protein-Caseins

Casein is the main milk protein constituting about 80 % of the total protein in milk. It is a milk specific group of proteins that precipitates upon acidification to pH 4.6. These proteins are also coagulated by action of rennet (chymosin and other proteinases). Caseins are phosphorylated proteins, containing an average of 0.85 % phosphorous, and thus having an ability to bind relatively large amounts of calcium (Fox, Uniacke-Lowe, McSweeney, & O'Mahony, 2015b). Caseins exist in the milk in a form of large colloidal aggregates called casein micelles (10^6-10^9 Da) which include all four types of caseins namely α_{s1}, α_{s2}, β and κ-caseins, along with the colloidal calcium phosphate and water (Table 2.1). The key properties of these four types of caseins are listed in Table 2.2.

Caseins are relatively heat stable. However, heating above 120 °C induces some chemical changes which render them insoluble (Walstra et al., 2005). Heat stability of caseins can be attributed to their less order structural organization including secondary and tertiary structures, which is further owed to high proline content. However, the full secondary and tertiary structure of caseins has not been fully elucidated yet, because of their unsuccessful crystallization.

Table 2.2 Key characteristics of four caseins (adapted from Huppertz (2013) and Fox, Uniacke-Lowe, McSweeney, and O'Mahony (2015a))

	α_{s1}-Casein α_{s1}-CN B-8P	α_{s2}-Casein α_{s2}-CN A-11P	β-Casein β-CN A^2-5P	κ-Casein κ-CN A-1P
Molecular weight (Da)	23599	25206	23973	19052
Number of amino acid residues	199	207	209	169
Serine	16	17	16	13
Proline	17	10	35	20
Cysteine	0	2	0	2
Lysine	14	24	11	9
Positively charged residues	25	33	20	17
Negativley charged residues	40	39	28	28
Aromatic residues	20	20	14	14
Grand average of hydropathicity (GRAVY)	-0.704	-0.918	-0.355	-0.557

2.4.2.1 α_{s1}-Casein

α_{s1}-Casein (α_{s1}-CN) is the most abundant of all caseins contributing about 40 % to the total casein in milk (Huppertz, 2013). It is moderately hydrophobic protein with two predominantly hydrophobic regions and one highly charged polar zone (Fox et al., 2015a). Around eight genetic variants have been detected until now with 8-9 phosphorylated amino acid residues (mostly serine). More details about these variants can be found elsewhere (Huppertz, 2013). α_{s1}-CN is characterized by a lack of cysteine residue and is a calcium sensitive casein precipitating at 3-8 mM $CaCl_2$. At pH 6.6 and ionic strength of 0.003, α_{s1}-CN exists as a monomer. With increase in ionic strength to 0.01 at same pH, a monomer-dimer equilibrium exists. Further increase in ionic strength to 0.2 at the same pH favours formation of dimers and tetramers. However, increase in pH above 6.6 suppresses degree of association.

2.4.2.2 α_{s2}-Casein

α_{s2}-Casein constitutes upto 10 % of the total casein in milk. It exhibits varying levels of phosphorylation with 10-13 phosphates (Thompson, Boland, & Singh, 2009) and intermolecular disulphide bonding due to the presence of two cysteine residues per mole. It is the most hydrophilic of the caseins with a dipolar structure where the N terminus is negatively charged and the C terminus is positively charged (Fox et al., 2015a). At neutral pH, α_{s2}-CN self-associates with increase in ionic strength with maximum at 0.2. α_{s2}-CN has also the highest number of phosphorylated residues and is also most sensitive to calcium-induced precipitation. It is insoluble in calcium solution over 2 mM.

2.4.2.3 β-Casein

β-Casein (β-CN) constitutes about 35 % to the total caseins in milk (Huppertz, 2013). It has amphipathic properties due to a strong negatively charged N-terminal portion with all the phosphorylated residues (4-5) and apolar C terminal characterized by little charge and high hydrophobicity. It is most hydrophobic casein and thus its self-association is strongly dependent on temperature, only a monomeric form is present at 4 °C but large polymers are assembled at room temperature. Compared to α_{s1}- and α_{s2}-CN, β-CN is less sensitive to calcium-induced precipitation. At 37 °C, it precipitates in the range of 8-15 mM calcium ions. However, at 1 °C, it does not precipitate up to 400 mM of $CaCl_2$.

2.4.2.4 κ-Casein

κ-Casein is the smallest of the caseins with low levels of phosphorylation (1-3P) and low sensitivity to calcium. Of all the caseins, only κ-CN is glycosylated (Huppertz, 2013). κ-CN has an amphipathic (detergent like structure) with strongly hydrophilic glycosylated C-terminal

without any aromatic and a few apolar residues and a strongly hydrophobic N-terminus. This is an important characteristic of κ-CN, which explains its presence on the surface of the casein micelle and its micelle size determinations and stabilizing properties (Swaisgood, 2003). κ-CN is rapidly hydrolyzed by an enzyme chymosin and other proteases at Phe (105)-Met (106) yielding N-terminal fragment (para κ-CN) with two cysteine residues and C-terminal fragment (macropeptide) containing all carbohydrate and phosphate groups. Hydrolysis of κ-CN is the first step in the manufacturing of most cheese varieties. In a naturally occurring mixture, κ-CN polymerizes into subunits containing 3-8 monomers through S-S linkages, which further polymerize into complexes with 1180 kDa. Self-association of κ-CN has a lower sensitivity to temperature when compared to β-CN (Huppertz, 2013).

2.4.2.5 Casein micelle

Above mentioned four caseins, α_{s1}, $\alpha_{s2,}$ β and κ casein associate with each other in an approximate ratio of 4: 1: 3.5: 1.5, respectively, in presence of Ca^{2+} and produce a dominant feature of milk, the casein micelle, a macromolecular assembly with an average size of 200 nm (Dalgleish, 2011). In addition to caseins (approx. 94 %), micelles also contain inorganic minerals (~6 %) (Fox et al., 2015a). Inorganic minerals mainly include calcium bound to phosphorus in calcium phosphate nanoclusters referred to as colloidal calcium phosphate (CCP) and lower levels of magnesium and citrate. This ability of integrating CCP into the micelle makes them a primary transport vehicle for calcium and phosphorus, essential minerals (Singh, 2014). In addition, the presence of CCP also avoids the risk of significant increase in milk viscosity due to open structure of its casein components. Above all, casein micelles scatter light and responsible for the white

colour of the milk. The micelles are very stable and can withstand heat treatment, commercial homogenization and high calcium concentration (Singh, 2014).

2.4.2.6 Casein micelle structure

Casein micelle structure is a topic of continuing research over the last thirty years. Different models have been proposed to explain the structure of casein micelle. The main idea, supporting experimental observations, strengths and limitations of different models are discussed in Table 2.3.

Table 2.3 Different models proposed for casein micelle structure

Model	Main idea	Can explain	Cannot explain
Submicelle model (Schmidt, 1982; Walstra et al., 1984; Walstra, 1999)	Casein micelles composed of smaller protein subunits linked via CCP. κ-CN deficient submicelles are in the interior of the micelle while those with high κ-CN levels are on the surface. CCP interacts with phophoseryl residues of α_s and β-casein on the surface of κ-CN deficient submicelles present in the core of the micelle. Negatively charged hydrophilic parts (glycosylated) of κ-CN extend from the surface of micelles as 'hairs' and stabilise the micelle against coagulation by steric and electrostatic repulsion. Later on observation of CCP throughout the micelle, Walstra (1999) proposed that CCP is inside the submicelle and submicelle are linked via hydrophobic interaction	1. Early electron micrographs 2. Chemical and physical measurements of casein micelles 3. Coagulation or precipitation of casein micelles on specific hydrolysis of κ-CN 4. Dissociation of micelles into smaller particles 5. Analysis of particles (~20 nm diameter) made from sodium caseinate and their growth into larger supramolecules (~100 to 200 nm diameter) upon addition of calcium.	1. Electron micrographs produced using cryoppreapration electron microscopy stereo-imaging technique (McMahon & McManus, 1998; Trejo, Dokland, Jurat-Fuentes, & Harte, 2011) 2. Dissociation behavior of casein supramolecules on either removal of CCP or treatment with excess k-casein or urea (Holt, 1998)
Dual−binding model (Horne, 1998, 2002; Horne, 2006, 2008, 2014)	Individual caseins are cross-linked through hydrophobic regions of the caseins and calcium phosphate clusters act as bridges for the assembly of the casein supramolecule. Processes of protein polymerization and calcium binding of casein molecule would occur simultaneously. Growth of hydrophobically bonded proteins is inhibited by electrostatic repulsive interactions. k-casein is linked into the casein supramolecule by hydrophobic bonding of its N-terminal region. k-casein ends the chain as it does not possess either a phosphoserine cluster for linkage via CCP or another hydrophobic anchor point to extend the chain.	1. Chemical and physical measurements of casein micelles 2. Coagulation or precipitation of casein micelles on specific hydrolysis of κ-CN 3. TEM and SEM micrographs	1. Highly hydrated casein micelle interior 2. Clefts in electron microscopic observations 3. Interior structure of the micelle
Internal structure model (Dalgleish, 2011)	κ-CN distributed unevenly on the surface of casein micelle leaving clefts where other caseins were exposed to serum. Micelle interior contains subassemblies of α_s, some β-casein and CCP. β-casein act as surfactant to stabilize the water in the micelles	1. Hydration of casein micelle 2. β-casein exiting on cooling and re-entering on warming. 3. Large molecules entering the casein micelle e.g. hydrolysis of β-casein present in micelle interior by trypsin and papain 4. Chemical and physical measurements of casein micelles 5. Coagulation or precipitation of casein micelles on specific hydrolysis of κ-CN	
Nanocluster model (Holt, 1992; Holt & Horne, 1996; Holt, 1998; De Kruif & Holt, 2003; de Kruif, Huppertz, Urban, & Petukhov, 2012)	Casein micelle as a homogeneous matrix of caseins in which the CCP nanoclusters are dispersed as "cherry stones" (about 2 nm) at an average distance of 18.6 nm. Centres of phosphorylation (3-5 nearby phosphorylated amino acid residues) of the caseins are attached to the surface of the nanoclusters. The tails of these caseins protruding from the clusters associate to form a protein matrix (polymer mesh with density fluctuations at the 2 nm scale) via co-operative weak interactions (hydrophobic interactions, hydrogen bonding, ion bonding, weak electrostatic Van der Waals attraction and other factors). κ-CN limits the process of self-association leading to stabilization of the native casein micelle. The binding of caseins to calcium phosphate nanoclusters initiates the formation of the casein supramolecule.	1. TEM and SEM micrographs 2. Chemical and physical measurements of casein micelles 3. Coagulation or precipitation of casein micelles on specific hydrolysis of κ-CN 4. Dissociation of casein micelles on removal of CCP or treatment with excess k-casein or urea (Holt, 1998) 5. Observations of SANS and SAXS scatering experiments which imply a heterogeneous internal structure.	

2.4.3 Whey proteins

Whey proteins constitute 20 % of the total protein content in bovine milk. The term 'whey proteins' encompasses five different groups of proteins, namely, β-lactoglobulin (β-Lg), α-lactalbumin (α-La), lesser amounts of bovine serum albumin (BSA), immunoglobulins (Ig) and proteose peptones (pp). These proteins have a globular to ellipsoid structure and are relatively soluble. These proteins are more heat sensitive and less sensitive to calcium than caseins.

2.4.3.1 β-Lactoglobulin

β-Lg is the most abundant (~ 60 %) whey protein in milk (Table 2.1). It is a globular protein with 162 amino acid residues and a molecular weight of approximately18 kDa. Ten genetic variants of β-Lg have been known with most common being named A and B (Edwards & Jameson, 2014). β-Lg can self-associate to varying degrees depending on temperature, pH, protein concentration and ionic strength. At ambient temperature and natural pH of milk, β-Lg exists as dimer. A β-Lg monomer contains two intra-molecular disulphide bonds and a free sulfhydryl group (-SH, Cys_{121}). β-Lg (Figure. 2.1) denatures at temperatures above 65 °C at pH 6.7 exposing its free thiol group, which can undergo thiol-disulphide exchange reactions with other denatured β-Lg and/or milk proteins such as κ-CN and α-La. Denaturation and following crosslinking reactions of β-Lg affect the rennet coagulation and heat stability of the milk. Denaturation temperature of β-Lg depends on pH. It is most heat sensitive near pH 4.0 and most stable at pH 6.0 (Sawyer, 2003). The physiological role of β-Lg is not known. However, due to the presence of a hydrophobic cavity, it is considered as transporter for small hydrophobic molecules like vitamin A (Fox et al., 2015a). In addition, β-Lg is one of the milk proteins responsible for milk protein intolerance or allergy in humans (Downs, Kabourek, Baumert, & Taylor, 2013).

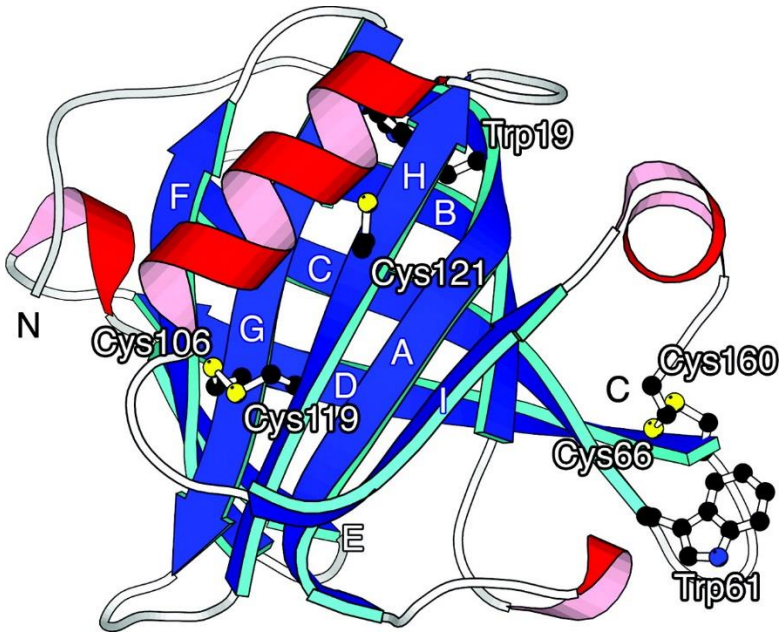

Figure 2.1 Structure of bovine β-Lg indicating disulphide bonds and thiol group (Yagi, Sakurai, Kalidas, Batt, & Goto, 2003)

2.4.3.2 α-Lactalbumin

α-Lactalbumin (α-La) constitutes 20 % of whey proteins and has two genetic variants A (most common in bovine milk) and B with a molecular weight of 14.147 kDa and 14.175 kDa, respectively (Fox et al., 2015a). α-La is composed of 123 amino acid residues and has an oblate ellipsoid tertiary structure with a deep cleft dividing the protein in two lobes (α and β). The cleft is binding site for Ca^{2+}, an integral part of its molecular structure, which plays a role in its stability and minimized susceptibility to denaturation. The α-lobe has three α-helices and three short 3_{10}-helices whereas the β-lobe contains three stranded β sheets and a short 3_{10}- helix. α-La contains four disulphide bonds and lacks free thiol group, which further adds to its heat stability. α-La is a component of enzyme lactose synthetase which defines its physiological role being transferring galactose to glucose required for lactose synthesis (Fox et al., 2015a).

2.4.3.3 Other whey proteins

Bovine serum albumin (BSA), immunoglobulins (Ig) and proteose peptone (pp) are minor proteins present in the serum at low levels (Table 2.1). BSA accounts for 6 % of whey proteins and has a molecular weight of ~65 kDa with 582 amino acid residues. Ig are antibodies synthesised in response to foreign antigens. These proteins provide immunity to the young and thus their concentration is high in colostrum but decreases rapidly after postpartum. Proteose peptones is a complex mixture of peptides, most of which produced by the action of indigenous enzyme plasmin (Fox et al., 2015a).

The contributions of these whey proteins to the physio-chemical changes in milk during UHT processing and subsequent storage are considered relatively minor, compared to α-La and β-Lg and therefore not discussed in detail here. Detailed information about these proteins can be found elsewhere (Hurley & Theil, 2013; O'mahony & Fox, 2013; Wynn & Sheehy, 2013; Fox et al., 2015a).

2.4.4 Minerals

Milk minerals occur in one or more chemical forms, including ions and salts (organic and inorganic), complexes or constituents of organic molecules like proteins. They constitute only a small fraction (8-9 g/L) of milk and includes cations (mainly calcium, magnesium, sodium and potassium) and anions (mainly inorganic phosphate, citrate and chloride) (Gaucheron, 2005). These cations and anions are partitioned between the colloidal and aqueous phase of milk. About one third of calcium, two thirds of magnesium, half of the inorganic phosphate and over 90 % citrate is in aqueous phase whereas the rest is associated with casein molecules and are an integral part of casein micelle.

CCP, as discussed in previous sections 2.4.2.5 and 2.4.2.6, plays a pivotal role in the casein micelle structure and stability. There is an equilibrium between calcium in the colloidal and aqueous phase. Partition of calcium in milk between different phases has been tabulated in Table 2.4. The formation of CCP is an effective way of "burying" a considerable amount of Ca and phosphate within casein micelles, therefore determines to a large extent the physicochemical properties of casein micelles (Lucey, 2003). About 70 % of total Ca and 30 % of total phosphate as principle colloidal salt are in the colloidal phase, which combines with four major caseins (α_{s1}-, α_{s2}-, β- and k-CN) in the casein micelle (Gaucheron, 2005).

Table 2.4 Calcium partition in cow milk by Holt and Jenness (1984).

Component	Mean* value (mM)
Total Ca	29.4
Ionic Ca	2.0
Soluble Ca	9.2
% Soluble Ca	31 %
Micellar Ca	20.2
Micellar Ca / g of casein	0.77

*Mean values include the biological variability over different breeds of cows

2.4.5 Sugars

Main sugar of milk is lactose, a reducing disaccharide composed of glucose and galactose. Lactose is responsible for slight sweet taste of milk. Being the principal carbon source for microorganisms in milk, it is indispensable for manufacture of fermented dairy products like cheese and yogurt. In addition to lactose, a large number of free saccharides mainly

oligosaccharides and small amount of monosaccharides and glycosylated proteins κ-CN, mucins and glycoproteins in fat globule membrane are also present (O'Mahony & Fox, 2014)

2.4.6 Vitamins and enzymes

Milk is a source of fat soluble (A, D and E) and the water-soluble vitamins (C, B1, B2, B6, B12, pantothenic acid, niacin, biotin and folic acid). Milk also contains a large number of enzymes including proteases, lipases and oxidoreductases. Plasmin is the major serine protease in milk and its concentration increases during very early or very late lactation or in animal with mastitis. Plasmin is heat stable at pH of milk and can retain substantial activity after pasteurisation and thus affect protein stability of milk. Lipoprotein lipase in the major lipase in milk. The enzyme is heat labile and thus of no significance in heat treated milk. Lactoperoxidase is one of the main oxidoreductases present in milk and is able to catalyze oxidation of unsaturated fatty acids resulting in oxidized taste. Lactoperoxidase is also a component of potentially important lactoperoxidase/thiocyanate/hydrogen peroxide system. Alkaline phosphatase does not affect milk stability but is important due to its widespread use as index of adequate heat treatment (Varnam & Sutherland, 2001; Walstra et al., 2005).

2.5 Secondary structure of milk proteins

In last 30 years, spectral studies and predictive modelling has thrown some light on secondary structure of different caseins individually and in micellar state (Huppertz, 2013) (Table 2.5). This has uplifted their status from 'random coil proteins' to 'rheomorpic proteins' with an open, flexible and mobile conformation (Holt & Sawyer, 1993). Contents of secondary structures of different caseins individually and in the micellar state determined using different methods in comparison to well elucidated structure of whey proteins are tabulated in Table 2.5. κ-CN appears

to be the one with the highest amount of secondary structure among caseins. The C-terminal half of α_{s2}-CN is suggested to be having a globular conformation with α-helix and a β-sheet whereas the N-terminal region forms a randomly structured hydrophilic tail. α_{s1}-CN contains little α-helix but considerable amount of β-sheets and β-turns (Fox et al., 2015a). β-Lg has a lower proportion of α-helix (~ 12 %) compared to α-La (36 %) (Figure 2.1). However, β-sheet content in β-Lg (50 %) is far greater than that in α-La. β-Lg is a typical lipocalin (family of proteins found in gram negative bacteria, vertebrate cells, and invertebrate cells, and in plants which transport small hydrophobic molecules such as steroids, bilins, retinoids and lipids) with a structure that contains a β-barrel with eight antiparallel β-strands, labelled A–H and a three-turn α-helix that lies parallel to three of the β strands. Strands A–D form one surface of the barrel while strands E–H form the other (Kontopidis et al., 2004).

2.6 Milk processing

Raw milk is highly perishable and may contain pathogenic bacteria. Therefore, in order to make it safe for drinking and extending its shelf life, milk is generally heat-treated. Heat treatment may vary in its intensity, which is a combination of temperature and the duration of heating. Heating processes are classified into different categories on the basis of their intensity.

2.6.1 Thermisation

Thermisation is a heat treatment (20 s, 60-69 °C) of intensity lower than pasteurisation aimed to kill bacteria, especially psychrotrophs. Many psychrotrophs produce heat resistant lipases and proteinases that may eventually deteriorate quality parameters of milk. Thermisation kills many vegetative microorganisnms and partially inactivates some enzymes with negligible changes in the milk.

Table 2.5 Secondary Structure of milk proteins

Protein	Method	α-helix (%)	β-sheet (%)	β- turn (%)	Unspecified structure (%)	Reference
α_{s1}-CN	Raman	8–13	18–20	29–35	33-40	Byler, Farrell, and Susi (1988)
	CD	13-15	34-46	18-25	27-28	Malin, Brown, Wickham, and Farrell (2005)
	FTIR					
	3D model	15	22	45	18	Kumosinski, Brown, and Farrell (1991)
α_{s2}-CN	Predictive	54	15	19	13	Garnier, Osguthorpe, and Robson (1978)
	CD	24	30	24	22	Hoagland, Unruh, Wickham, and Farrell (2001)
	FTIR	32	27	31	9	Hoagland et al. (2001)
	3D model	46	9	12	7	Farrell, Malin, Brown, and Mora-Gutierrez (2009)
β-CN	Raman	6-14	20-23	31-36	30-36	Byler et al. (1988)
	CD	20	32	28	21	Farrell, Wickham, Unruh, Qi, and Hoagland (2001)
	FTIR	29	34	32	4	Farrell et al. (2001)
	3D Model	10	20	30	34	Kumosinski, Brown, and Farrell (1993)
κ-CN	CD	15-19	32-38	23-27	19-27	Farrell et al. (1996)
	FTIR	8-10	39-41	25-27	23-25	Farrell et al. (1996)
	3D model	10	30	32	30	Farrell Jr, Brown, and Malin (2013)
β-Lg	FTIR	9	54	27	9	Yang, Yang, Kong, Dong, and Yu (2015)
	FTIR	12	53	22	13	Qi, Ren, Xiao, and Tomasula (2015)
	CD	10.5	47.8	16.1	25.6	Qi, Wickham, and Garcia (2014)
α-La	FTIR	36	18	20	26	Qi et al. (2015)
Lyophilized micellar casein	Raman	14	27	41	18	Byler et al. (1988)
Lyophilized submicellar casein	Raman	18	27	39	16	Byler et al. (1988)
Whey from Raw Milk	FTIR	15	51	20	15	Qi et al. (2015)
Whey from Homogenized UHT milk	FTIR	10	47	21	22	Qi et al. (2015)
Milk	FTIR	15.3	17.7	19.2	7.6	Carbonaro, Maselli, and Nucara (2012)

2.6.2 Low Pasteurisation

Low pasteurisation is a heat treatment with intensity (30 min, 63 °C or 15 s, 72 °C) optimized to inactivate enzyme alkaline phosphastase. The treatment kills all yeasts and moulds, almost all pathogens specifically *Mycobacterium tuberculosis* and some vegetative bacteria. In addition, only some enzymes are inactivated and there are no alterations in flavour, cold agglutination and bacteriostatic properties of milk. Whey proteins are also not denatured with low pasteurisation treatment, thus no significant effect on their secondary structure.

2.6.3 High pasteurisation

High pasteurisation is a heat treatment (20 s, 85 °C) sufficient to destroy activity of enzyme lactoperoxidase. The treatment kills virtually all vegetative microorganisms but no spores and inactivates most of the enzymes except plasmin and some bacterial proteinases and lipases. In addition to a cooked flavour, the treatment denatures partly the whey proteins and destroys the bacteriostatic properties of milk.

2.6.4 Sterilisation

Sterilisation is a heat treatment designed to eliminate most of the microorganisms and bacterial spores present in milk. This can be sufficed by either in-container sterilisation (30 min, 110 °C) (Walstra et al., 2005) or Ultra high temperature (UHT) short time treatment (1-10 s, 135-145 °C) (Deeth & Lewis, 2016). In-container sterilisation inactivates all milk enzymes except bacterial lipases and proteinases. However, it results in browning due to extensive Maillard reactions, a sterilized milk flavour, loss of some available lysine, denaturation of whey proteins and even changes in the caseins, loss of vitamins and decrease in milk pH by 0.2 units. UHT

treatment results in less chemical changes and a weak cooked flavour with no inactivation of plasmin, proteinases and bacterial lipases**.**

2.7 UHT processing

UHT heat treatment in combination with aseptic packaging can extend shelf life of milk up to 12 months with less chemical changes compared to in-container sterilization. Time-temperature combination or intensity of UHT process are decided to achieve inactivation of heat resistant spores of *Bacillus stearothermophilus* with minimum chemical changes so that sensory and nutritional qualities of the 'commercially sterile' UHT milk are not lowered.

UHT heating can be achieved using either 'direct' or 'indirect' heating methods. Direct heating results in rapid heating due to mixing with superheated steam and rapid cooling using vacuum flash cooling process. Indirect heating process involves slower heating and cooling as the heat transfer occurs across wall of stainless steel plate or tube exchanger. The comparison between direct heating and indirect heating systems in terms of their heating profiles, economics and changes in UHT milk quality have been discussed in detail elsewhere (Datta, Elliott, Perkins, & Deeth, 2002; Tran, Datta, Lewis, & Deeth, 2008; Lewis & Deeth, 2009).

2.8 Changes to milk during UHT treatment

2.8.1 Chemical changes

2.8.1.1 Changes in pH and mineral balance

Both pH and ionic calcium (Ca^{2+}) concentration decrease with increase in the temperature of milk. Milk pH has been reported to decrease to 6.0 at 100 °C (Walstra et al., 1984) and may be as low as 5.6 at 140 °C (Deeth & Lewis, 2017a). Although decrease in pH is expected to increase

ionic calcium, there has been studies in the past and recently that reported the exact opposite (Tessier & Rose, 1958; Chandrapala, McKinnon, Augustin, & Udabage, 2010; On-Nom, Grandison, & Lewis, 2010). Deeth and Lewis (2017a) suggested that both the pH and Ca^{2+} at 140 $^{\circ}$C affect the heat stability at this temperature.

UHT processing has less effect on the pH of white milk and is rarely reported in the literature (Deeth & Lewis, 2017a). According to Gaucher et al. (2008), pasteurisation increased the pH of raw milk from 6.69-6.76 to 6.70-6.78 and after subsequent UHT treatment, it was decreased to 6.66-6.76. However, the pH of milk is reduced substantially (0.2-0.3 units) after in-container sterilisation (Deeth & Lewis, 2017a). In contrast to little effect on pH of milk, UHT treatment substantially reduces Ca^{2+} concentration, which recovers on further storage but not to its original value (Geerts, Bekhof, & Scherjon, 1983). The decrease in the solubility of calcium phosphate during UHT treatment might lead to its precipitate formation (fouling deposit) on the heat exchanger walls or association with casein micelle. Overall, UHT treatment has a minor effect on mineral partitioning (Deeth & Lewis, 2017a).

2.8.1.2 Whey protein denaturation and disulphide crosslinking

The most discussed change in milk proteins induced by UHT treatment (or any heat treatment) is the denaturation of whey proteins. The degree of denaturation of whey proteins is less in UHT milk as compared to 100 % in in-container sterilisation and depends on the type of processing (i.e. direct or indirect) and the temperature-time profile of the heating process. Among the whey proteins, Ig and BSA are completely denatured by sterilisation processes followed by β-Lg and α-La. Proteose peptones are not denatured by heat (Mulvihill & Donovan, 1987). Indirect UHT processing results in a greater extent of whey protein denaturation as compared to direct

processing (Datta et al., 2002; Tran et al., 2008). β-Lg is almost completely denatured by commercial indirect heating process compared to only 74-92 % denaturation in the direct one. However, the percentage denaturation of α-La was 25-90 % and 27-58 % for indirect and direct plants, respectively (Tran et al., 2008; Deeth & Lewis, 2016). Due to sufficient (non-zero) residual levels of α-La in UHT milk, its concentration has been suggested as an index of heat treatment (Dupont, Rolet-Repecaud, & Muller-Renaud, 2004; Tran et al., 2008).

Denaturation of whey proteins involves their unfolding and hence exposing reactive sulfhydryl groups and hydrophobic regions, which subsequently result in sulfhydryl-disulphide and hydrophobic protein-protein interactions. The most significant interaction involves crosslinking between β-Lg and κ-CN. Denaturation of β-Lg involves unfolding of the globular monomer exposing hydrophobic amino acids and a free sulfhydryl group, at Cys_{121}, which is normally buried inside the native globular structure. The native monomer undergoes intramolecular sulfhydryl-disulphide reactions with other exposed sulfhydryl groups resulting in the formation of reactive non-native monomers. These reactive monomers primarily react with κ-CN located on the surface of the micelle but may do so after reacting with α-La via both hydrophobic interactions and intermolecular sulfhydryl-disulphide interchange reactions. Thus, UHT treatment at normal pH 6.7 results in formation of the casein micelles with whey proteins attached. However, due to dissociation of some κ-CN from the micelle on heating, it also appears in the serum in associations with denatured whey proteins (Anema, 2008). The amount of these complexes in the serum phase depends on several factors such as the nature of the heat treatment and pH (Corredig & Dalgleish, 1996a; Corredig & Dalgleish, 1996b). Most of the denatured whey proteins are associated with the casein micelle in indirect heated UHT milk compared to only 50 % in direct with the remaining portion being in the serum phase. Indirect UHT treatments have

also more α-La attached to the casein micelle compared to β-Lg. This difference has significant practical implications because the micelle with increased amount of α-La attached becomes more hydrophobic, thus, increasing the water-holding capacity, an important consideration for some products. Other than type of heating process, the pH of heating also significantly affects the distribution of denatured whey proteins. At pH ~6.5, most of the denatured whey proteins attach to the casein micelle while at pH >6.8, most of them are in the serum with κ-CN (Deeth & Lewis, 2016).

2.8.1.3 Structural modifications of proteins and non-disulphide protein crosslinking

Dephosphorylation of the phosphoserine residues present in milk caseins occurs during sterilisation by either hydrolysis with a release of a phosphate group and serine (Eq. 1) or by β-elimination with formation of dehydroalanine and phosphate (Eq. 2) (Belec & Jenness).

$$\underset{\text{(phosphoserine)}}{R - CH_2 - O - PO_3^{2-}} + H_2O \rightarrow \underset{\text{(serine)}}{R - CH_2 - OH} + HPO_4^{2-} \qquad (1)$$

$$R - CH_2 - O - PO_3^{2-} \rightarrow R = CH_2 - OH + HPO_4^{2-} \qquad (2)$$

(phosphoserine) (dehydroalanine)

More phosphate and serine were reportedly formed during heating of caseinate solutions than dehydroalanine (van Boekel, 1999). Dehydroalanine is also formed from O -glycosylserine or cysteine residues by elimination of a sugar or H_2S, respectively. Once formed dehydroalanine reacts with the amino group of lysine residues, the imidazole group of histidine, or the thiol group of cysteine, resulting in intra- or intermolecular lysinoalanine, histidinoalanine, or lanthionine crosslinks, respectively (O'Connell & Fox, 2003). Proteins cross-linked via dehydroalanine unlike the disulphide-linked protein complexes cannot be dissociated with reducing agents such as

mercaptoethanol and on hydrolysis yield isodipeptides such as lysinoalanine, histidinoalanine and lanthionine (Deeth & Lewis, 2016). UHT milk contains very little lysinoalanine (0 to 50 μg/g protein) compared to autoclaved milk (110 to 710 μg/g protein) (Fritsch, Hoffmann, & Klostermeyer, 1983). Higher temperatures, higher pH and longer heating times increased lysinoalanine formation.

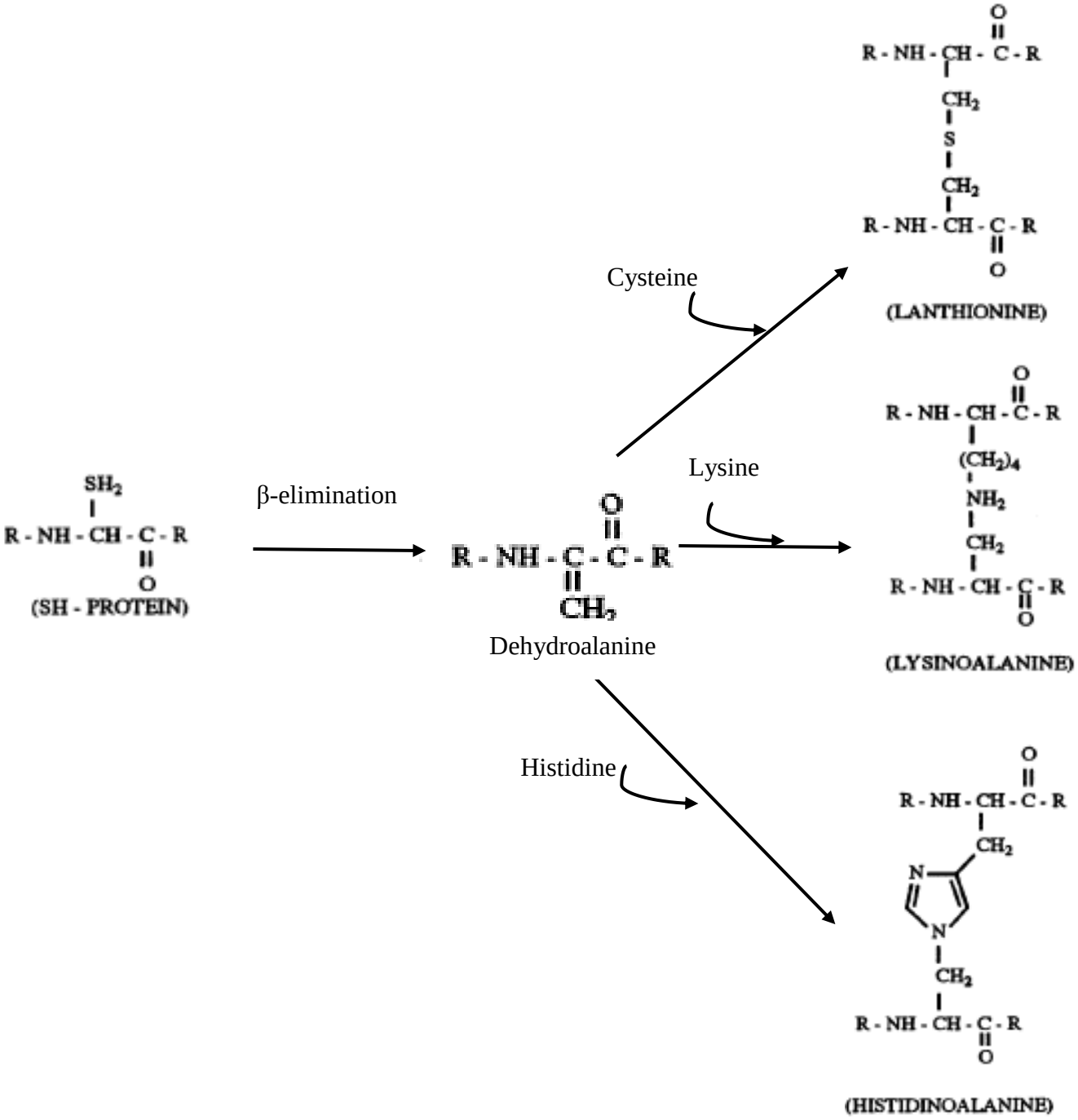

Figure 2.2. Formation of lanthionine, lysinoalanine and histidinoalanine from dehydroalanine

Lysine residues of milk proteins link with reducing sugar lactose to initiate Maillard reaction (Figure 2.2), the products of which such as glyoxal and methylglyoxal serve as another source of non-disulphide crosslinks in UHT milk (Andrews & Cheeseman, 1971; Andrews & Cheeseman, 1972; Andrews, 1975). Recently it has been shown that on incubating milk protein concentrate with methylglyoxal, polymerised proteins produced were similar to those formed in this product during storage (Le, Holland, Bhandari, Alewood, & Deeth, 2013). Protein crosslinking, whether via dehydroalanine or Maillard reaction products, reduces the nutritional availability of amino acids such as lysine and reduces the digestibility of the proteins (Deeth & Lewis, 2016). However, on a positive note, the non-disulphide crosslinking especially via Maillard reaction products may inhibit age-gelation (storage instability) of UHT milk during storage (McMahon, 1996).

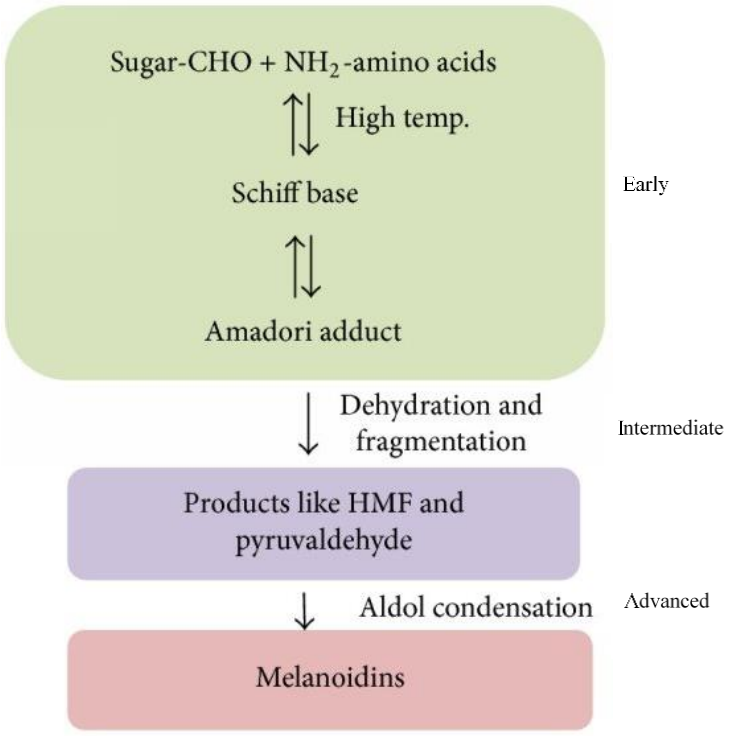

Figure 2.3. Overview of the early intermediated and advanced stages of Maillard reaction

2.8.1.4 Dissociation of proteins from the casein micelle

Considerable dissociation of individual caseins from the micelle takes place during heating of milk. Extent and nature of this dissociation depend on the heat intensity, pH and milk solids concentration. Dissociation of caseins is higher in in-container sterilised and concentrated milk products than unconcentrated UHT milk (Deeth & Lewis, 2017a). Most investigations have focused on the dissociation of κ-CN from the micelle before or after its interactions with whey proteins, especially β-Lg (Corredig & Dalgleish, 1996b; Anema, 2008; Anema, 2014). Dissociation of κ-CN from the surface of the micelle can make it more susceptible to calcium ion-mediated heat- induced aggregation, so this has a marked effect on the heat stability of the milk. Singh and Latham (1993) studied the aggregation and dissociation of protein in milk heated at UHT temperatures and found that initial heating gave rise to the formation of high molecular weight complexes composed of whey proteins and κ-CN. On extended heating, most of the whey proteins/κ-CN complexes remained associated with the micelles at the natural pH of milk (6.67) with little dissociation of monomeric proteins from the casein micelle. Increasing the pH under the same heating conditions resulted in increased quantities of whey proteins/κ-CN complexes and monomeric proteins in the serum phase. However recently, Anema (2017) proposed that dissociation of κ-CN occurs before interaction with the denatured whey protein and the complexes are formed in the serum phase.

2.8.1.5 Other changes

In addition to changes discussed above, another main UHT heat treatment induced changes are formation of lactulose, loss of thiamine, heat induced flavours and the effect on different enzymes. Lactulose, a disaccharide of glucose and galactose, is produced by epimerisation of lactose during heat treatment of milk. As lactulose is not present in raw milk and does not change

much during storage of UHT milk, it is a useful indicator of heat treatment intensity. Furthermore, the concentration of lactulose in freshly manufactured UHT milk is considerably correlated with the amount of furosine, which is a measure of lactosylation, another heat induced interaction of lactose, and intensity of cooked flavour (Cattaneo, Masotti, & Pellegrino, 2008). Indirect processed UHT milk as expected has higher lactulose content than direct UHT milk. An upper limit of 400 mg/l for lactulose content is suggested to avoid strong overcooked flavour in UHT milk (Deeth & Lewis, 2017a). The chemical index C*, a measure of chemical effect of heat treatment, is based on the destruction of vitamin thiamine. A C* value of 1 is equivalent to 3 % destruction of thiamine. Storage of UHT milk causes no further loss of thiamine if there is no exposure to light.

Three main flavours or off-flavours resulting mainly due to effect of UHT treatment are listed as cooked/cabbage/sulphurous, heated/rich and scorched/sterilized. Formation of heat induced off-flavours is not very relevant to this thesis and hence described in detail elsewhere (Deeth & Lewis, 2017a, Vazquez-Landaverde, Torres, & Qian, 2006; Al-Attabi, D'Arcy, & Deeth, 2014).

Native proteases of the milk (mainly plasmin) and bacterial proteases and lipases survive UHT treatment (Gaucher, Mollé, Gagnaire, & Gaucheron, 2008; Deeth & Lewis, 2017a). Plasmin exists in the raw milk as a complex system including its inactive precursor plasminogen, plasminogen activators and inhibitors. All these constituents determine its activity in the product. Milk with high somatic cell count, as an indication of udder health, have highest plasmin activity (Auldist et al., 1996). Somatic cells contain a plasminogen activator, which enhances the conversion of inactive plasminogen to plasmin (Kelly & Foley, 1997). Bacterial proteases are produced in raw milk at the end of the log phase of growth of psychrotrophic bacteria when the

count exceeds ~10^6 cfu/ml. Bacterial proteinases can also activate the plasminogen to plasmin in milk (Nielsen, 2002).

Inactivation of plasmin and bacterial proteinases can be achieved using higher sterilisation temperatures. Indirect UHT processes generally inactivate more plasmin (Manji, Kakuda, & Arnott, 1986) and bacterial proteinases (Corradini & Pecchini, 1981) than direct ones. However, significant plasminogen and plasminogen activators still remain in both direct and indirect UHT milk. UHT milk processed using an indirect heating process at 150 °C showed less proteolysis during storage than one at 140 °C (Topçu, Numanoğlu, & Saldamlı, 2006). However, high temperature treatment (150-180 °C for 0.2 s) using steam injection method was able to inactivate effectively highly heat-resistant bacterial spores although the product still developed bitter flavours in UHT milk due to plasmin action (Huijs, van Asselt, Verdurmen, & De Jong, 2004). Complete inactivation of plasmin could be achieved using preheating prior to high sterilisation temperature. A preheating of 80 °C for 300 s (Van Asselt, Sweere, Rollema, & De Jong, 2008) or of at least 90 °C for 30 s (Newstead, Paterson, Anema, Coker, & Wewala, 2006)) prior to UHT processing inactivated plasmin and thus prevented proteolysis during storage. Preheating led to inactivation of plasmin via its association with denatured β-Lg through sulfhydryl–disulphide interactions. Similarly, the use of low temperature inactivation (LTI) treatment (~55 °C for 15-60 min) with UHT sterilization has been shown to reduce proteolysis and increase the shelf life of UHT milk containing psychrotrophic bacterial proteases and lipases (Kocak & Zadow, 1985). Bacterial proteinases probably either autodigest at ~55 °C or undergo a conformational change and engage in interaction with caseins to form an enzymatically inactive proteinase-casein complex. Furthermore, different bacterial proteinases and lipases require different LTI conditions (Kocak &

Zadow, 1985). Moreover, LTI is most effective when applied a day after UHT processing which seems commercially inviable (Deeth & Lewis, 2016).

2.8.2 Physical changes

2.8.2.1 Fouling

Fouling of heat exchangers during heat treatment refers to deposit formation on heat exchanger surfaces. Fouling deposits reduce the efficiency of the heat transfer process and make it difficult to reach the product outlet temperature without raising the temperature of the heating medium to an undesirable extent. Excessive deposit formation particularly in indirect heating plants limits the run time of UHT plants. The major area where deposits occur is the preheating section. If these deposits detach, they may cause problems downstream of the holding tube or in the final product as sediment (Ramsey & Swartzel, 1984; Deeth & Lewis, 2016). More fouling has been reported in tubular heat exchangers than plate heat exchangers, and has been attributed to the higher shear rates and the total cross sectional area for flow in the latter (Bansal & Chen, 2006). Direct UHT plants require longer run times than indirect ones for a poorer quality milk due to comparably quick rise in temperature and the reduced heat transfer at the surface at high temperatures. However, the direct UHT milk may contain more sediment in comparison to indirect (Ramsey & Swartzel, 1984). In addition, deposits may still form in other sections of direct UHT plants namely the holding tube, the back-pressure valve and the beginning of the cooling section.

Two distinct types of fouling deposits, depending on the temperature at which these are formed, have been recognized in UHT milk. Type A deposit formed at comparatively low temperatures (80-105 °C) is a white voluminous deposit with a high protein content (50-70 %) and a significant mineral content (30-40 %) which tends to block flow passages. Type B deposits,

formed at higher temperatures, are finer, more granular and predominantly mineral in origin (70-80 %, probably β-tricalcium phosphate), with only small amounts of protein (10-20 %). β-Lg is the main denatured protein at lower temperatures, whereas casein predominates at the high temperature (Deeth & Lewis, 2016). Interestingly, fat despite being present in equal concentrations to protein and in greater concentration than minerals in whole milk does not feature significantly (usually less than 5 %) in any of the two types of deposits. Furthermore, even in creams with fat representing up to 75 % of the dry matter in some cases, fouling is reported to be predominantly caused by proteins and minerals. However, in recombined milk, higher levels of fat in the fouling deposits (up to 60 %) compared to fresh milk (10 % or less) were observed (Newstead, Groube, Smith, & Eiger, 1998). Likewise, higher proportions of fat (0-35 %) were found in deposits from direct steam injection plants, attributed to fat destabilisation during the injection process. High temperature (138 °C) homogenisation after sterilisation treatment also produces deposits with a higher proportion of fat (Deeth & Lewis, 2016).

Fouling can be reduced by aging raw milk at 4 °C for 12-24 h (without change of pH), addition of capric acid and preheating milk (70-80 °C for 40-70 s) prior to high-temperature sterilisation. Aging probably results in lipolysis and the production of fatty acids. Capric acid might associate with the casein micelle and hence prevent interactions leading to the build-up of the deposit. Preheating denatures β-Lg to a certain degree, decreases fouling and extends the processing time (Burton, 1988; Deeth & Lewis, 2016)

Fouling is mainly affected by pH and ionic calcium of milk. In general, fouling is inversely related to both pH and ionic calcium. For the same milk sample, the amount of deposit formed increased as the pH was reduced, whereas on increasing the pH by 0.7 units both processing times and product quality increased with slight increase in product viscosity. Deeth and Lewis (2016)

recommended that both pH and ionic calcium should be monitored to gain a better understanding of the fouling process. However, along with pH and ionic calcium, other factors like seasonal variations, κ-CN content, concentration of ammonia and presence of air bubbles affect fouling. There is still uncertainty whether protein denaturation or protein aggregation are the key reactions in fouling and whether it is denatured whey protein or minerals that deposit first on the heat exchange surface. Further details in fouling can be studied elsewhere (Burton, 1988; Deeth & Lewis, 2016; Deeth & Lewis, 2017a).

2.8.2.2 Sediment formation

Some amount of sediment is frequently present in most heat-treated milk and is usually not noticeable by the consumers (Burton, 1988). Sediment appears to become clearly noticeable upon tasting above about 1 % (dwb) (Deeth & Lewis, 2016). Similar mechanisms are suggested to be responsible for sedimentation and fouling (Burton, 1988). A good quality raw cow's milk with high heat stability results in a very low level of sediment in UHT milk. Sediment formation increases with severity of the heat treatment and thus direct UHT processes has higher sedimentation than indirect (Ramsey & Swartzel, 1984). Furthermore, like fouling, very little sediment is formed in UHT cow's milk at pH > 6.62 but extent of sedimentation is enhanced rapidly below this pH level. Addition of only 4.5 mM calcium chloride produced a voluminous sediment following UHT treatment and could be reduced by addition of disodium hydrogen phosphate (DSHP) and trisodium citrate (TSC) (Lewis, Grandison, Mei-Jen, & Tsioulpas, 2011). Therefore, experiments involving addition of calcium salts and reduction of pH need to be performed cautiously as these can block a UHT plant. Sediment formation was only slight for milk samples whose ethanol stability was greater than 80 % (Deeth & Lewis, 2016).

2.9 Storage changes

Considerable changes occur in the UHT milk system during storage that affect sensory and nutritional quality of UHT milk. These include changes in colour (browning-Maillard reaction), flavour (cooked, stale, rancid, bitter, chalky), texture (sedimentation or gelation) and fall in nutritional value due to changes in proteins, fats and lactose and loss of vitamins. The rate of these changes depends mainly on the storage temperature and to some extent on the UHT heating mode and conditions, milk composition (mainly fat content), dissolved oxygen content and concentration of heat-resistant enzymes (Deeth & Lewis, 2016; Deeth & Lewis, 2017a).

2.9.1 Chemical changes

Change of pH of milk during heat treatment appears to be minor, however pH is noticeable reduced during storage. This has been attributed to Maillard reaction intermediates, formation of formic acid and acetic acid and proteolysis (Van Boekel, 1998; Gaucher, Mollé, et al., 2008). In addition to heated and cooked flavours produced by heat treatment, which remain and are noticeable during the first few weeks of storage, some flavours like stale (due to lipid oxidation), bitter (due to proteolysis by indigenous or bacterial proteases) and rancid (due to lipolysis of the milk fat by bacterial lipases) arise during storage. The rate and extent of all flavour formation and dissipation depends strongly on storage temperature and especially for stale flavour on the level of dissolved oxygen content, which has been reported to decrease during storage in Tetra Brik cartons (Perkins, Elliott, D'Arcy, & Deeth, 2005). In addition to changes in flavours, storage might also result in a significant loss of vitamins and some light induced changes discussed in detail elsewhere (Deeth & Lewis, 2017b).

Considerable changes in conformation and interactions of milk proteins occur during storage of UHT milk. The change in milk proteins have been demonstrated by different methods such as 2-D electrophoresis (Holland et al., 2011), reversed-phase HPLC (Al-Saadi & Deeth, 2008) and by measurement of changes in non-protein nitrogen (NPN), non-casein nitrogen (NCN), content of high-molecular weight protein material, casein micelle size, hydration and zeta potential (Garcia-Risco et al., 1999; Gaucher, Mollé, et al., 2008; Gaucher et al., 2011). Although not all the changes have been elucidated, some of these changes have been characterised. These include protein crosslinking, Maillard reaction (glycosylation), deamidation and proteolysis.

2.9.1.1 Protein crosslinking

Crosslinking of proteins is initiated by heat treatment and progresses during storage. Crosslinking mainly involves caseins (Deeth & Lewis, 2016) with α_{S1}-CN being the major player (Andrews, 1975; Holland et al., 2011). Higher the storage temperature, the greater is the extent of crosslinking (Andrews, 1975; Al-Saadi & Deeth, 2008). In UHT milk stored at 37 °C, more than 50 % of the casein was reported to be polymerized compared to 23 % at 4 °C (Andrews, 1975). Increase in the amount of lysinoalanine was found to be correlated with rise in polymerised casein at higher storage temperatures (Al-Saadi & Deeth, 2008), and thus this compound was suggested as a measure of crosslinking and a sensitivity index of the storage conditions of UHT milk (Cattaneo et al., 2008). In addition to crosslinking of caseins through isopeptide linkages like lysinoalanine, caseins also reportedly crosslink through advanced Maillard reaction products (Henle, Schwarzenbolz, & Klostermeyer, 1996; Le et al., 2013). Furthermore, the extent of protein crosslinking during storage has been positively correlated with the amount of sediment formed in UHT milk (Andrews & Cheeseman, 1972). However, increase in crosslinking in UHT milk stored at temperatures >30 °C may retard age-gelation (McMahon, 1996). Crosslinking has been

demonstrated in UHT milk using size-exclusion chromatography (Andrews & Cheeseman, 1972) and one-dimensional electrophoresis (Al-Saadi & Deeth, 2008) and two-dimensional electrophoresis (Holland et al., 2011).

2.9.1.2 Maillard reactions (glycosylation/ lactosylation)

Maillard reaction is a series of reactions initiated during UHT processing with lactosylation of lysine residues in milk proteins and continues during storage. Maillard reaction products in addition to acting as protein crosslinks (as discussed above) also lead to brown discoloration, off-flavours and reduction in pH through production of acids such as formic acid. Furosine, an acid degradation product of the Amadori product lactulosyllysine, is used as an index of the severity of heat treatment. However due to its degradation during storage to other Maillard reaction products, its value in stored UHT milk is limited. In addition to furosine, lactosylation of whey proteins has been proposed as a measure of the thermal history of UHT milk (Losito, Stringano, Carulli, & Palmisano, 2010). Holland et al. (2011) demonstrated lactosylation of α-La and β-Lg during storage of UHT milk using 2-D electrophoresis. Both whey proteins appeared as stacked spots with up to five spots per stack corresponding to proteins with molecular weights differing by the molecular weight of lactose, i.e., the proteins contain multiple molecules of lactose. However, lactosylation of caseins was not observed on 2-D gels.

2.9.1.3 Deamidation

Non-enzymatic deamidation (amide hydrolysis) of the asparagine and glutamine residues of proteins into aspartic acid and glutamic acid, respectively, and ammonia occurs to only a small extent during UHT heating. However, significant deamidation occurs during storage of UHT-sterilised milk (Holland et al., 2011; Deeth & Lewis, 2016). The extent of deamidation increases with temperature and time of storage. The highest rates of deamidation are observed for asparagine

residues followed by glycine, although significant rates are also encountered with asparagine residues next to serine and histidine residues (Holland et al., 2011; Holland, Gupta, Deeth, & Alewood, 2012). The reaction occurs *via* formation of a cyclic imide (succinimide or glutarimide for asparagine and glutamine, respectively). The extent of deamidation can be estimated by measuring amount of ammonia released using an ammonia kit (Miwa, Yokoyama, Wakabayashi, & Nio, 2010), the increase in non-protein nitrogen (NPN) due to ammonia release (Metwalli & Van Boekel, 1998), or the appearance of new more negatively charged protein particularly α_{s1}-CN, α-La and β-La using isoelectric focusing in 2-D electrophoresis (Holland et al., 2011; Holland et al., 2012). Deamidation when induced intentionally using enzymes has been reported to improve some physical functional properties and the nutritional value of milk proteins probably due to reduction of blocked lysines (Miwa et al., 2010).

2.9.1.4 Proteolysis

Proteolysis is hydrolytic degradation of milk proteins into peptides caused by heat-resistant proteinases, mainly involving the indigenous milk proteinase - plasmin and heat resistant bacterial proteinases. The latter are produced by bacterial contaminants, mainly *Pseudomonas* species, in the raw milk prior to heat treatment. These enzymes can generally withstand UHT processing conditions and hence can cause proteolysis during storage. Proteolysis is the major destabilising process of milk proteins in sterilised milk. It results in bitter flavours due to release of hydrophobic peptides and physical destabilisation particularly gelation during storage.

UHT milk processed using an indirect heating process at 150 °C showed less proteolysis during storage than one at 140 °C (Topçu et al., 2006). However, complete inactivation of plasmin could be achieved only using preheating prior to high sterilisation temperature plasmin (Newstead et al., 2006; Van Asselt et al., 2008). Similarly, the use of low temperature inactivation (LTI)

treatment (~55 °C for 15-60 min) with UHT sterilization has been shown to reduce proteolysis and increase the shelf life of UHT milk containing psychrotrophic bacterial proteases and lipases (Kocak & Zadow, 1985). In addition to preheating and higher temperature of UHT processing, proteolysis is also affected by the fat content of milk. Greater proteolysis (by both plasmin and bacterial proteinases) has been observed during storage in UHT skim milk than in UHT whole milk subjected to the same UHT treatment (López-Fandiño et al., 1993). The finding suggests that UHT heating conditions should be more severe for skim milk than for whole milk, a practice followed by some processors. Table 2.5 highlights main differences between plasmin and bacterial induced proteolysis (adapted from (Deeth & Lewis, 2016).

2.9.2 Physical changes (visible storage instabilities/defects)

Two main visible storage defects in UHT milk which affect its shelf life are age-gelation and sedimentation.

2.9.2.1 Age gelation

Age gelation is a major storage defect in UHT milk limiting its shelf life. This is particularly an issue in countries where the expected shelf life is greater than 6 months. Typically, the viscosity of the milk increases gradually during storage and immediately before gelation rises sharply upto approximately 10 mPas. It is not always clear whether sedimentation in sterilised milk is the same as or different from gelation. Nieuwenhuijse and van Boekel (2003) identified four different types of gels formed in sterilised milk depending upon the storage temperature and the type of proteinase. These were particle gels, fine-stranded gels, gels created by bridging flocculation and gelled sediment caused by bacterial proteolysis, plasmin proteolysis, low temperature storage and high-temperature storage, respectively. Age-gelation is governed by several factors, which mainly

include proteolysis by native plasmin or bacterial proteinases, severity and nature of the heat treatment, storage temperature and various additives. These factors have been discussed in detail in exclusive reviews on gelation in UHT milk (Datta & Deeth, 2001; Nieuwenhuijse & van Boekel, 2003).

Table 2.6 Main differences between action of plasmin and bacterial proteinases

	Plasmin	**Bacterial proteinases**
Preferred milk protein	β- and α_{s2}-CN	β- > α_{s1}- > κ- > α_{s2}-CN (depends on the bacterial species/strain and/or different experimental conditions)
Peptides produced	γ-casein and proteose peptones	*para*-κ-CN, fragment 1-105 and related peptides 1-103, 1-104, 1-106 and1-107
Nature of peptides produced	Larger and more hydrophobic which precipitate in 4 % trichloroacetic acid (TCA) and are soluble at pH 4.6	Smaller and less hydrophobic which are soluble in both 4 % TCA and at pH 4.6.
Gel formed	A creamy surface layer which thickens into a curd-like layer	Custard-like gel with a tighter protein network of thicker strands and contains more intact casein micelles and micelle aggregates than plasmin-initiated gels

In brief, the proteolysis has been shown by many researchers to be highly significant during age gelation of UHT milk. Plasmin has been identified as the main cause of gelation in milk free of bacterial enzymes. However, when both proteinases are present, it is difficult to identify which one is responsible for the gelation. Gelation occurs earlier in directly processed UHT milk than in indirectly processed due to greater content and activity of plasminogen/plasmin in the former (Deeth & Lewis, 2016). Very low concentrations of proteinase can cause sufficient proteolysis to

cause gelation during storage at room temperature (Button, Roginski, Deeth, & Craven, 2011). However, the time to gelation and the extent of proteolysis does not always correlate well (Manji et al., 1986). The more severe the sterilisation heating, the less is the risk of gelation or the longer time required for gelation to occur, and is mainly attributed to the inactivation of proteinases. As discussed above, direct UHT milk is more susceptible to gelation than indirect UHT milk (Tran et al., 2008). Storage at low temperature, i.e., ~4 °C, and high temperature (> ~30 °C) has been consistently reported to retard gelation compared to the intermediate temperatures (Kocak & Zadow, 1985). Retardation of gel formation at the higher temperatures has been attributed to fast proteolysis (Manji et al., 1986) and the crosslinking of proteins. The latter could stabilise the micelles and prevent release of proteins or protein complexes such as the β-Lg–κ-CN-complex from casein micelles into the milk serum, which could initiate gel formation (McMahon, 1996). Moreover protein crosslinking via dehydroalanine and advanced Maillard products block any further protein-protein interactions via lysine (Samel, Weaver, & Gammack, 1971).

The mechanism of age gelation in UHT milk have been mostly based around a central role of proteolysis together with physicochemical effects (Nieuwenhuijse & van Boekel, 2003). Most cited or accepted mechanism was proposed by McMahon (1996) and states that gelation takes place in two stages. The first stage involves release of the β-Lg–κ-CN-complex from the casein micelle due to proteolytic action and is followed by the second stage including formation of a gel network. After it reaches a certain critical concentration in the serum, this network starts incorporating casein micelles. At higher storage temperatures, intramicellar covalent crosslinking prevents release of the β-Lg-κ-CN complex. Recently, Anema (2017), based on his observations, has proposed a modified hypothesis for non-enzymatic age gelation. According to him, κ-CN-

depleted casein micelles, formed during UHT treatment, slowly sediment due to gravity and cross-link to form a gel once a critical concentration is attained.

2.9.2.2 Sedimentation

Sediment formation during storage above a certain level can be a major problem for UHT milk (Vesconsi, Valduga, & Cichoski, 2012). It is initiated during sterilisation of milk (section 2.7.2.2) and is affected by the extent and nature of the heat treatment as well as milk compositional factors such as pH and ionic calcium (Deeth & Lewis, 2016).

Direct UHT process is more prone to sediment formation than indirect UHT. Recently, Gaur, Schalk, and Anema (2018) reported that sediment in UHT milk was composed of κ-CN depleted casein micelles, with low levels of denatured whey proteins. In indirect UHT milk samples, higher levels of denatured whey proteins associated with the casein micelles reduce their propensity to aggregate and sediment.

Decreasing the pH by addition of acids or increasing the ionic calcium levels by fortification with calcium salts markedly increased sedimentation during storage. At low pH (<∼pH 6.65) and/or high ionic calcium levels (>∼1.5 mM), high sedimentation has been reported in direct UHT milk samples and has been attributed to calcium-mediated aggregation of the unstable κ-CN-depleted casein micelles (Gaur et al., 2018). Sedimentation in direct UHT milk samples could be reduced by increasing the pH with alkali or reducing the ionic calcium with chelators like tri-sodium citrate (Gaur et al., 2018).

In addition to pH and ionic calcium, the level of fat in the milk has been reported to have no effect on sediment formation (Hawran, Jones, & Swartzel, 1985). Furthermore, sedimentation increases with both storage time and temperature (Ramsey & Swartzel, 1984). However, regular disturbance of UHT milk packages decreases sediment formation.

2.10 Shelf life testing

Shelf life is the length of time within which the characteristics of a packaged product are kept at acceptable levels (Pedro & Ferreira, 2006). In determining the shelf life of shelf stable foods and commercially sterilised product like UHT milk, the characteristics primarily include quality changes, rather than microbial safety (Corrigan, Hedderley, & Harvey, 2012). UHT milk has a long shelf-life of 9 months at room temperature (Holland et al., 2011). End of shelf life and the acceptability of UHT milk is determined by deterioration in its sensory properties like visual appearance and flavour. The change in these sensory quality parameters and hence the shelf life of UHT milk depends on the progression of various physico-chemical and biochemical changes during storage as discussed in previous sections. Mainly, proteolytic, lipolytic, oxidative and Maillard type reactions reportedly affect the visual appearance and flavour the most (Datta & Deeth, 2003).

Proteolytic activity in UHT milk, due to presence of heat-stable native and bacterial enzymes, affect its appearance by formation of a gel and flavour by development of off-flavours and bitter flavour due to release of tyrosine and hydrophobic peptides in the milk, respectively (Deeth & Lewis, 2017b). The gel formation is probably initiated with the release of β-Lg-κ-CN complexes, formed during heat treatment, from the micelle and subsequent aggregation of these complexes (McMahon, 1996).

Lipolysis by lipases involves hydrolysis of triacylglycerols into medium and short-chain fatty acids resulting in soapy and tangy flavours, respectively. Additionally, lipolysis also releases free fatty acids, which act as precursors for other flavour compounds responsible for the formation of off-flavours such as oxidised, cardboard, bitter, rancid, soapy, unclean and metallic (Richards

et al., 2014). Oxidative and Maillard reactions result in browning of the milk and development of off-flavours (Burton, 1988; Van Boekel, 1998; Hedegaard et al., 2006).

Shelf life testing of long life products such as UHT milk can be very resource and time consuming. In practice, the UHT products are incubated at 55 °C for 7 days and at 30 °C for 15 days to check for sterility/ bacterial growth, which might happen due to a faulty heat treatment or some sort of post-heat treatment contamination (Deeth & Lewis, 2016; Deeth & Lewis, 2017b). These accelerated storage temperatures can also be used for assessing progress of sensory or other changes during storage, and is usually termed as accelerated shelf life testing. The assumption is that most of the degradation reactions are Arrhenius-like, and thus higher the temperature, the faster is the rate of achieving high degradation levels (Pedro & Ferreira, 2006). The results obtained from accelerated tests can be extrapolated to estimate the shelf-life at the normal storage conditions. Recently, Richards et al. (2014) employed a multivariate accelerated shelf life test (MASLT) to predict the shelf life of the low fat UHT milk stored in High-density polyethylene (HDPE) bottles by evaluating degradation in sensory attributers. They concluded that similar levels of degradation marking the end of shelf life can be achieved in only 27 days at 45 °C compared to 211 days at 25 °C. Same authors also conclude that accelerated shelf life testing could be safely used in UHT milk and the results obtained at accelerated storage temperatures can be converted to actual market conditions. However, when it comes to storage defects like gelation, it might not happen at accelerated temperatures. Furthermore, the extent of Maillard browning at temperatures >40 °C could be exponential and cannot be related to those taking place at 20 °C.

Storage defects like sedimentation can be tested using centrifugation as accelerated tests. Deeth and Lewis (2017b) mentioned use of 3000 g, room temperature, 20-30 min and 1147 g, 3.5 hours simulating six-month storage (Tobin, Fitzsimons, Kelly, & Fenelon, 2011) to test for

sedimentation. However, the efficacy of above discussed tests as a rapid tool to predict shelf life of UHT milk under a set of storage conditions is still questionable. To avoid any delay into product distribution after manufacturing and into the market and also to steer clear of any recalls, the UHT milk industry in recent years has emphasised the need of a rapid technique for predicting shelf life of UHT milk. The use of Fourier-Transform Infrared (FTIR) spectroscopy in combination with chemometrics appears as a suitable rapid tool that could predict the shelf life of UHT milk.

2.11 Fourier-Transform Infrared (FTIR) Spectroscopy

Infrared (IR) spectroscopy is based on the principle that any molecule possessing or experiencing a change a dipole moment will absorb particular frequencies of infrared radiation depending upon the frequency, at which the bonds within the molecule are vibrating. Vibrational frequency of a chemical bond is further determined by the mass of its constituent atoms, bond strength, geometrical arrangement and the periods of the associated vibrational coupling (Karoui, Downey, & Blecker, 2010). Every compound has thus a unique IR spectrum. This has enabled IR spectroscopy to identify and even quantitate components of a food system or distinguish between different foods or different types of same food. Furthermore, with the advent of FTIR instruments, improvements in laser design, higher signal to noise ratio, advances in detector technology coupled with significant advances in computing power and the utilization of chemometric analysis (discussed in next section), infrared spectroscopy technique has become very rapid (once calibrated), simple, inexpensive and non-destructive, and these benefits hold great importance when a large number of samples must be analysed. However, the major advantage which has increased its acceptance in industry and academic research is no sample preparation and reagent-less analysis.

Infrared spectral regions used for food analysis include near-infrared (NIR) (700–2,500 nm; 12,500-4000 cm^{-1}) and mid infrared (MIR) regions (2,500–15,000 nm; 4000-600 cm^{-1}). NIR region is characterized by harmonics and combination bands and is widely used for composition analysis of food products. However, due to the superposition of many different overtone and combination bands, NIR spectra has a very low structural selectivity as compared to MIR spectra containing many fundamentals usually observed in isolated positions (Karoui et al., 2010). MIR region thus can elucidate structure and conformation of organic molecules like proteins and lipids. In addition, the band position in the FTIR spectrum is also sensitive to its environment; this providing added information about the structure and intra- and intermolecular bonding. This ability has made FTIR spectroscopy a valuable technique for the study of the changes in structure and interaction of food components especially protein, lipids and lactose caused by varying physiochemical conditions during processing and subsequent storage, and that too without introducing perturbing probe molecules (Kher, Udabage, McKinnon, McNaughton, & Augustin, 2007; Carbonaro & Nucara, 2010). These changes are important from quality perspective for the dairy industry because they determine quality and shelf life of the product.

Characteristic absorption bands in MIR spectra of milk are associated with major components of milk. However, water is a significant absorber in the MIR region with major bands at 3920, 3490, 3280, and 1645 cm^{-1}. The exact location and shape of these bands may be affected by the presence of solutes, hydrogen-bonding, and temperature can interfere with the determination of other components present in milk system. Precise subtractions of the H_2O bands, which was earlier difficult using dispersive infrared spectrometers, are now possible because of the frequency precision achievable with FTIR (Powell, Wasacz, & Jakobsen, 1986; Dong, Huang, & Caughey, 1990). In addition, due to strong absorption band of water at 1640 cm^{-1} overlapping

amide I and II protein bands, the path length of the cuvette for transmission FTIR has to be in the 10 mm range to comply with the Beer-Lambert law. However, the development of the attenuated total reflectance (ATR) sampling accessory has overcome the sampling problems encountered while collecting spectra from opaque and viscous samples. This has made FTIR spectral acquisition even more simple and reproducible.

2.11.1 Spectral regions attributed to different milk components

After successful water subtraction, regions of the MIR spectra of milk attributed to different milk components are: 3000-2800 cm^{-1} (milk lipids (fat B)), 1800-1700 cm^{-1} (lipids (fat A)), 1700-1500 cm^{-1} (milk proteins amide I and II), 1500-1200 cm^{-1} (milk proteins-amide III, carbohydrates and interactions between different milk components) and 1200-900 cm^{-1} (milk minerals, milk fat, lactose, fingerprint region) (Figure 2.4) (Iñón, Garrigues, & de la Guardia, 2004; Zhou et al., 2006; Murphy, Fenelon, Roos, & Hogan, 2014).

Absorption observed between 3000-2800 cm^{-1} and at 1750 and 1175 cm^{-1} corresponds to the acyl chain, triacylglycerol ester linkage C=O and C–O, respectively, and is commonly used to determine milk fat. Additionally, the infrared bands appearing in the 3000–2800 cm^{-1} region are sensitive to the conformation and the packing of the phospholipid acyl chains (Karoui, Mazerolles, & Dufour, 2003) and hence particularly useful to study the phase transition of phospholipids (sol to gel state transition) on increasing temperature (Dufour et al., 2000).

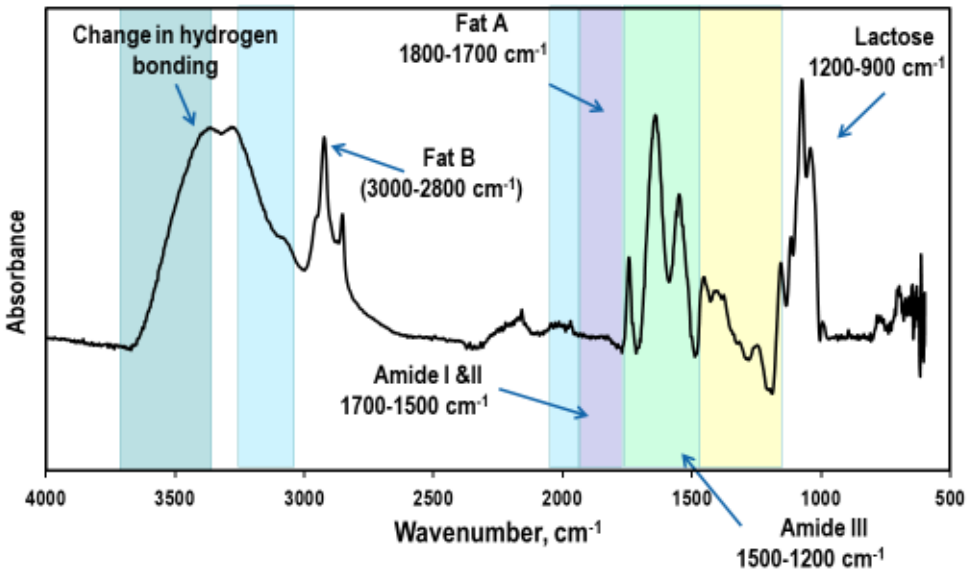

Figure 2.4 Typical FTIR spectra of milk

The absorption between 1700 and 1500 cm^{-1} has two main parts, namely amide I (1700-1600 cm^{-1}) corresponding to C=O stretching vibrations of the peptide bonds and amide II (1600-1500 cm^{-1}) attributed to C-N stretching vibrations in combination with N-H bending (Kher et al., 2007). The amide I and II bands (1700–1500 cm^{-1}) are known to be sensitive to the conformation adopted by the protein backbone. Amide I band has been particularly used for the estimation of protein secondary structure since it has good correlations with the levels of α-helix, β-sheet and unordered structure in proteins (Dong et al., 1990). Although the peptide bonds are essentially responsible for the absorbance of proteins in the amide II region, the side chains of several amino acids (glutamic acid, aspartic acid, glutamine, asparagine, lysine, arginine and tyrosine) also contribute to the signal. The carboxylate groups of the side chains of aspartic and glutamic acids absorb between 1580 and 1520 cm^{-1}, the nature of anion interacting with carboxylate group determining the exact location of the band within this interval. The O–C–O stretching vibrations

of glutamate and aspartate residues shifted from 1575 to1565 cm^{-1} when potassium ions bound to the proteins are replaced by calcium ions (Mazerolles et al., 2001; Karoui et al., 2003).

The peaks in amide III spectral region correspond to N-H bending and C-N stretching vibrations (Jaiswal et al., 2015) and also to CH_2 scissoring of acyl chains of lipids (Mendelsohn, Mao, & Flach, 2010). Although, having relatively weak signals in contrast to most commonly used amide I region (1700–1600 cm^{-1}), amide III does not suffer from strong interference of vibrational band of water, relatively unstructured spectral contour and overlap of revolved bands corresponding to various secondary structures (Fu, Deoliveira, Trumble, Sarkar, & Singh, 1994). Differernt frequency windows in amide III corresponding to secondary structures include α -helix 1328-1289 cm^{-1}; β-sheets, 1255-1224 cm^{-1}; unordered, 1288-1256 cm^{-1}.

Absorptions in the fingerprint region are mainly caused by bending and skeletal vibrations, which are particularly sensitive to large wavenumber shifts (Karoui et al., 2010). In this region, a peak around 1159 cm^{-1} has been previously associated with C-O vibrations of milk fat (Zhou et al., 2006). The area between 1250 and 800 cm^{-1} embodies characteristic peaks of various C–O vibrations in carbohydrates, mainly lactose (Zhou et al., 2006). Bands around 995 and 987 cm^{-1} suggested changes in stretching vibrations of $-PO_3^{2-}$ moiety of the serine-phosphate residue in milk (Gebhardt, Takeda, Kulozik, & Doster, 2011).

2.11.2 Major applications in dairy

FTIR has been successfully used to study thermal denaturation of whey proteins in milk (Parris, Purcell, & Ptashkin, 1991), the structure of β-Lg (Boye, Ismail, & Alli, 1996), aggregation and gelation kinetics of β-Lg at a molecular level (Dufour, Robert, Renard, & Llamas, 1998) and

detection (Nicolaou, Xu, & Goodacre, 2010) and quantification in milk adulteration. Spectra of casein and whey hydrolysates have been shown to be useful in predicting their physical parameters such as bitterness, solubility, emulsifying and foaming properties (van der Ven et al., 2002). ATR-FTIR spectroscopy was successfully used to determine the plasminogen concentration in various protein solutions and to differentiate between plasmin and plasminogen (Ozen, Hayes, & Mauer, 2003). As discussed earlier, plasmin and plasminogen are enzymes, which cleave milk proteins and could contribute to age gelation of milk, thus ATR FTIR shows great promise as a technique to investigate factors which accelerate age-gelation. Additionally, Kher et al. (2007) investigated the use of ATR-FTIR spectroscopy for predicting solubility of spray-dried samples of MPC. Although it was not possible to predict solubility of MPC powders after processing and storage, the changes in solubility during storage correlated well with ATR-FTIR spectra. ATR-FTIR was found useful in tracking changes in conformation of the milk protein concentrate. Second derivative spectra and PCA (principal component analysis) were the most useful spectral analysis tools. Other applications of FTIR in dairy have been reviewed in detail by Karoui et al. (2003); Karoui and De Baerdemaeker (2007); Karoui et al. (2010).

2.11.3 Chemometrics/multivariate analysis (MVA)

Multivariate analysis methods also known as chemometrics in case of chemical data analysis, developed in 1970, is the combination of mathematical and statistical tools applied to analyse complex datasets such as FTIR spectra with multiple variables (Granato & Ares, 2014). Moreover, FTIR spectra contains chemical information in form of different band positions, intensities and shapes. Band positions give information about the molecular structure of chemical compounds in a mixture, whereas the intensities of the bands are related to the concentration of

these compounds as described by the Beer-Lambert law (Karoui et al., 2010). In a pure component system, the content of a chemical compound can be easily determined by measuring the change in the intensity of a well-resolved band attributed only to it. However, foods contain numerous components and hence has a complex spectrum with overlapping bands. By far the most successful approach to extract quantitative, qualitative, or structural information from such spectra is to use multivariate mathematical analysis (Karoui et al., 2010).

In addition, a spectral dataset usually contains large number of variables and some with significant degree of collinearity, which renders the classical multiple linear regression unsuitable. Chemometric tools reduce the dimensionality of the dataset as well as overcome the collinearity between variables by converting them into a few orthogonal 'latent' non-measurable variables. The new latent variables provide an overview of the main variations in the data and also facilitate the recognition of otherwise hidden structures. Additionally, the methods allow identification of outliers, 'missing values' and separation of the noise from the signal (Bruun, 2006). A broad range of powerful chemometric tools including data reduction tools, regression techniques and classification methods is now available. Furthermore, accompanied with the appropriate computer technology, which is readily available in recent years, the use of these chemometric tools has become a significant feature of IR spectroscopy. Two basic chemometric tools used in this study are principal component analysis (PCA) and partial least square regression (PLSR).

2.11.3.1 Principal component analysis (PCA)

PCA is a non-supervised classification technique used to explore patterns and clustering in a data set. It is a bilinear modeling method that provides an overview of the main information contained in a multidimensional dataset. Hence, it is a commonly used data compression and visualization tool for large and complex data tables like FTIR /spectral data, in which the

information may be partly hidden and thus hard to interpret. It reduces dimensionality by projecting information carried by a large number of original variables on a smaller number of latent orthogonal (i.e., non-correlated) variables called Principal Components (PC) (Karoui et al., 2010). It can identify spectral variables, which contribute most to an observed difference between samples. It can also reveal the correlation between variables, and more importantly detect gross or subtle outliers. Not only a very useful method, it also forms the basis for many of the other methods like Principal Component Regression (PCR), Partial Least Squares (PLS) Regression, and Multivariate Curve Resolution (MCR), canonical correlation analysis (CCA) and common components and specific weights analysis (CCSWA) (Karoui et al., 2010). Thus, PCA is considered the basic workhorse of multivariate data analysis techniques.

The working of PCA is aimed to find the directions in space, along which the distance between (i.e. the dispersion of) the data points is the largest. This can be interpreted as finding the linear combinations of the initial variables that contribute most to making the samples different from each other. To explain the working, the objects/samples (described by n variables) are first visualized as points in the n-dimensional space with each axis represented by one variable. PCA replaces the original variable axes with new PC axes, which are orthogonal and determined sequentially in such a way that PC1 describes as much as possible of the variance in the original data, and each successive PC accounts for as much as possible of the remaining variance. The last PCs only describe the noise in the data. Only the PCs that make up the structured part and have the noise part separated out are subject for further interpretation.

In the PCA model, often the mean-centred data matrix X, is composed of score matrix (T), loading matrix P and the residual unmodelled variance (noise) E.

$$X = T \cdot P' + E = \Sigma PC_i + E \qquad (3)$$

Each of the PCs is composed of a loading- (p) and a score vector (t) as expressed in equation below.

$$X= t_1p_1=t_2p_2+\ldots t_Ap_A \quad (4)$$

The score vectors t_1, t_2 …t_A hold the score values for the objects obtained by projection onto the new PC axes, and the 2D score plots are usually represented as plot of one PC against another. Each sample has a score on each PC, which reflects the sample location along that PC and is the coordinate of the sample on the PC. The score describes the major features of the sample, relative to the variables with high loadings on the same PC. Therefore, the samples with close scores along the same PC are similar (they have close values for the corresponding variables). Conversely, samples for which the scores differ greatly are quite different from each other with respect to those variables. The loading vectors: p_1, p_2 …p_A express the relation between the original variables and the new PC variables. Like scores for samples, every variable analyzed has a loading on each PC (geometrically, cosine of the angle between the variable and the current PC), which reflects the individual variable contribution to that PC, and how well the PC takes into account the variation contained in a variable. A high loading value (positive or negative) signifies a variable with a high contribution to the PC, while a loading value close to zero signifies a variable without much contribution. Variables that lie close together are highly correlated. If both loadings have the same sign, the correlation is positive (when one variable increases, so does the other). If the loadings have opposite signs, the correlation is negative (when one variable increases, the other decreases). Loadings cannot be interpreted without scores, and vice versa. To summarize, if the score of a sample and the loading of a variable on a particular PC have the same sign, the sample has higher than average value for that variable and vice-versa. The larger the scores and loadings, the stronger that relation (Figure.2.5).

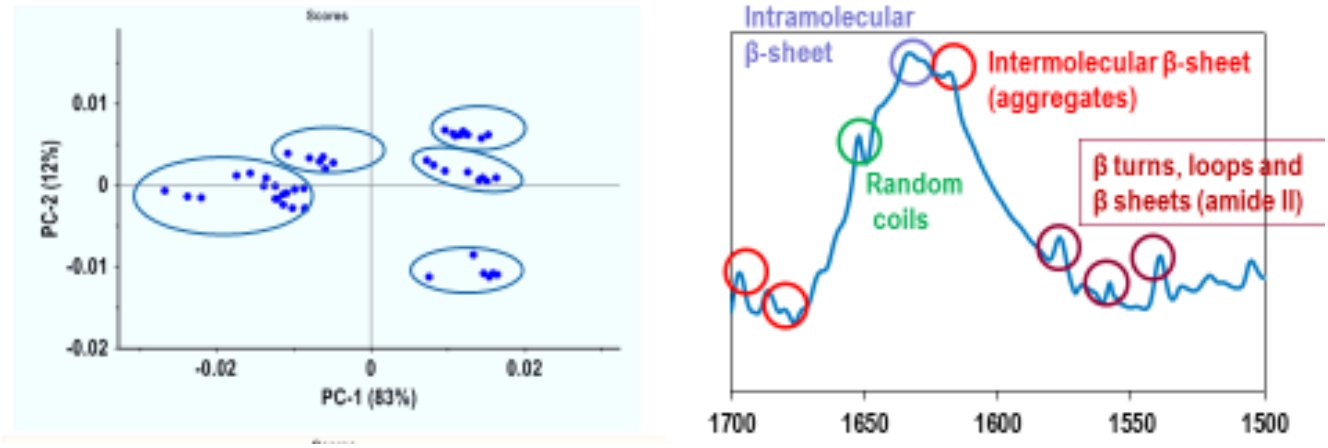

Figure 2.5 Typical score and loading plot of PCA

The combination of scores and loadings is the structured and hence informative part of the data. The part remaining is called error or residual, and represents the fraction of variation that cannot be modeled well. Explained variance is an error measure and often expressed as a percentage of the total variance in the data explained by the different PCs. The relative importance of each principal component is expressed in terms of explained variance. The variance which is not explained is residual variance. Models with small total residual variance (close to 0) or large total explained variance (close to 100 %) explain most of the variation in the data. Ideally, one should strive to have simple models, i.e. models where the residual variance goes down to zero with as few components as possible. If this is not the case, it means that there may be a large amount of noise in the data or, alternatively, that the data structure may be too complex to be accounted for by only a small number of components.

PCA works as a kind of curve resolution technique, which have the purpose to find the pure chemical spectra and their concentrations in a mixture. However, even though the loading vectors can be subject to interpretation to explain the chemical/physical meaning of the PC, the loading vectors from spectroscopic analyses seldom have a pure chemical meaning, due to the

constraints of orthogonality (Bruun, 2006). In addition, a PC does not necessarily result from a single source of variation. However, the PCA results may be used as initial estimates for the pure chemical spectra, which can then be found by adding constraints such as non-negativity, unimodality etc. and optimizing by alternating least squares. Further detailed description of PCA can be found elsewhere (Martens & Martens, 2001; Esbensen, Guyot, Westad, & Houmoller, 2002).

2.11.3.2 Partial least squares regression (PLSR)

The use of IR spectra for quantification purposes maybe achieved by regression techniques such as PLS regression. Partial Least Squares Regression (PLSR), also referred as Projection to Latent Structures or just PLS, models both the X- and Y-matrices simultaneously to find the latent (or hidden) variables in X that will best predict the latent variables in Y. These PLS components are similar to principal components, but are referred as 'factors'. In addition, PLS regression like PCA is based on the construction of new and uncorrelated factors from the original spectral data. However, a major difference between PCA and PLS regression is that, while PCA reduces the quantity of spectral data independent of any associated chemical information, PLS calculates new variables by selecting those dimensions that explain the maximum variance in both the spectral and the associated reference data sets. Therefore, PLS regression incorporates variables in the data that are relevant for describing the variation in associated reference data. PLSR may be carried out with multiple Y responses.

In multivariate calibration, first the relationship between the independent variables X and the dependent variables Y is established by use of a calibration set with known Y-values. The obtained model can then be used for prediction of Y for a data set of unknown Y-values. The model can be summarised as

$$Y=bX+F \quad (5)$$

The inspection of regression coefficients b-vectors can help draw attention to the spectral regions of high correlation to Y, thus enabling band assignment in spectroscopic analyses (Bruun, 2006). The b-vectors may be found by regression of latent variables (e.g. the score matrix from a PCA) against the Y-variables. However in PLSR, both X and Y are modelled by latent variables and the Y-variance is used as a guide for decomposition of X, on order to increase the covariance of the X- and Y scores (Bruun, 2006). This ensures that the first PLS-components, termed factors, are relevant to Y.

In addition to the calibration purposes, PLSR may also be applied for an explorative analysis of identifying relationship between different variables (hypothesis-generating method) and/or determination of the influence of the design factors on some response values (hypothesis-testing method) (Bruun, 2006).

Relationships between several X- and Y-variables can be inspected from the two-dimensional correlation loading plots. These plots show the correlations of each original variable to the two latent variables that are plotted against each other. If the main variation is explained by two factors, the correlation between variables can be inspected from the plot: The positively correlated variables are placed close, whereas negatively correlated variables are opposite. Variables close to the origin are poorly explained by the PLS-components and contain no useful information (Martens & Martens, 2001) (Figure. 2.6).

Validation of a PLSR model is important in order to prevent overfitting and wrong conclusions to be drawn. The external validity of the model is checked by employing prior knowledge. The internal validation considers the reliability of the results and is usually done by test set validation and/or cross validation (CV). The validation methods assess the stabilities of the

model parameters and estimate the prediction errors expected in the future predictions (Martens & Martens, 2001). CV simulates test set validation by consecutively taking out subsets from the calibration set and using these as temporary test sets in several predictions. The stability of the model parameters against the perturbations in CV reflects the reliabilities of the parameters. Thus, reliability ranges for e.g. the b-coefficients can be estimated on the basis of CV results, and hence the X-variables with a significant influence on Y may be identified in this way (Martens & Martens, 2001). The predictive ability of the PLSR model is assessed from the root mean square error of Y (RMSE(Y)), which sum up all Y-residuals and is a measure of both precision and accuracy. The future prediction result can be reported as Y±2*RMSE(Y), which is an empirical interval (Martens & Martens, 2001). A specific ratio of RMSE(Y) to the original Y-variance has also been suggested as a criterion for a successful calibration (Oberg, Ruysschaert, & Goormaghtigh, 2004). PLSR is described in more details in Martens and Martens (2001); Esbensen et al. (2002).

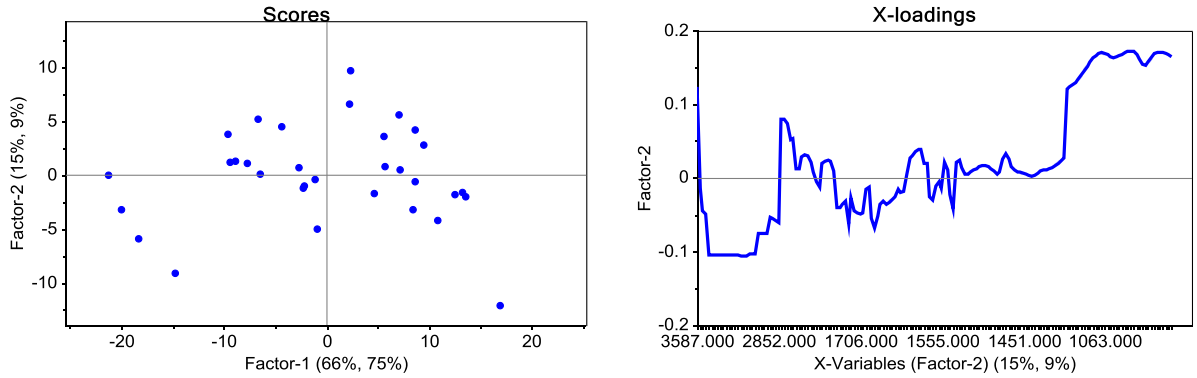

Figure 2.6 Typical PLS scores and loading plot

CHAPTER 3

Electrophoretic characterization of protein interactions suggesting limited feasibility of accelerated shelf-life testing of ultra-high temperature milk

This chapter has been published as a research paper entitled "Electrophoretic characterization of protein interactions suggesting limited feasibility of accelerated shelf-life testing of ultra-high temperature milk" by Manpreet Kaur Grewal, Jayani Chandrapala, Osaana Donkor, Vasso Apostolopoulos and Todor Vasiljevic. In the peer reviewed journal, Journal of Dairy Science, 100, 1–13 (2016).

VICTORIA UNIVERSITY
MELBOURNE AUSTRALIA

GRADUATE RESEARCH CENTRE

DECLARATION OF CO-AUTHORSHIP AND CO-CONTRIBUTION: PAPERS INCORPORATED IN THESIS BY PUBLICATION

This declaration is to be completed for each conjointly authored publication and placed at the beginning of the thesis chapter in which the publication appears.

1. PUBLICATION DETAILS (to be completed by the candidate)

Title of Paper/Journal/Book:	Electrophoretic characterization of protein interactions suggesting limited feasibility of accelerated shelf-life testing of ultra-high temperature milk
Surname:	Grewal
First name:	Manpreet Kaur
College:	College of Health & Biomedicine
Candidate's Contribution (%):	80

Status:

Accepted and in press:	☐	Date:	
Published:	☑	Date:	17 11 2016

2. CANDIDATE DECLARATION

I declare that the publication above meets the requirements to be included in the thesis as outlined in the HDR Policy and related Procedures – policy.vu.edu.au.

Manpreet Kaur Grewal Digitally signed by Manpreet Kaur Grewal Date: 2018.02.18 10:50:38 +11'00'	18.02.2018
Signature	**Date**

3. CO-AUTHOR(S) DECLARATION

In the case of the above publication, the following authors contributed to the work as follows:

The undersigned certify that:

1. They meet criteria for authorship in that they have participated in the conception, execution or interpretation of at least that part of the publication in their field of expertise;
2. They take public responsibility for their part of the publication, except for the responsible author who accepts overall responsibility for the publication;
3. There are no other authors of the publication according to these criteria;
4. Potential conflicts of interest have been disclosed to a) granting bodies, b) the editor or publisher of journals or other publications, and c) the head of the responsible academic unit; and

VICTORIA UNIVERSITY
MELBOURNE AUSTRALIA

5. The original data will be held for at least five years from the date indicated below and is stored at the following **location(s)**:

College of Health & Biomedicine
Institute of Sustainable Industries and Liveable cities
Victoria University
Australia

Name(s) of Co-Author(s)	Contribution (%)	Nature of Contribution	Signature	Date
Manpreet Kaur Grewal	80	Concept development, research design, experiment execution, interpretation, drafting manuscript and its revision	Manpreet Kaur Grewal Digitally signed by Manpreet Kaur Grewal Date: 2018.02.22 15:54:28 +11'00'	22 02 2018
Jayani Chandrapala	8	Concept development, support and technical expertise, manuscript revision	Jayani Chandrapala Digitally signed by Jayani Chandrapala DN: cn=Jayani Chandrapala, o=RMIT University, ou=School of Science, email=jayani.chandrapala@rmit.edu.au, c=AU Date: 2018.02.26 08:23:46 +11'00'	26022018
Osaana Donkor	2	Concept development, manuscript revision	Osaana Donkor Digitally signed by Osaana Donkor DN: cn=Osaana Donkor, o=Victoria University, ou, email=osaana.donkor@vu.edu.au, c=AU Date: 2018.02.26 10:32:22 +11'00'	26.02.2018
Vasso Apostolopoulos	2	Concept development, manuscript revision	[redacted] Digitally signed by Vasso DN: cn=Vasso, o, ou, email=vasso.apostolopoulos@vu.edu.au, c=AU Date: 2018.02.26 10:50:06 +10'00'	26/02/2018
Todor Vasiljevic	7	Concept development, experimental design, statistical analysis, manuscript revision	Todor Vasiljevic Digitally signed by Todor Vasiljevic DN: cn=Todor Vasiljevic, o, ou, email=todor.vasiljevic@vu.edu.au, c=AU Date: 2018.02.23 13:57:59 +11'00'	23.02.2018

J. Dairy Sci. 100:1–13
https://doi.org/10.3168/jds.2016-11278

Electrophoretic characterization of protein interactions suggesting limited feasibility of accelerated shelf-life testing of ultra-high temperature milk

Manpreet Kaur Grewal,* Jayani Chandrapala,* Osaana Donkor,* Vasso Apostolopoulos,† and Todor Vasiljevic*[1]
*Advanced Food Systems Research Unit, and
†Immunology in Chronic Diseases Program, Centre for Chronic Disease, College of Health and Biomedicine, Victoria University, Melbourne, VIC 8001, Australia

ABSTRACT

Accelerated shelf-life testing is applied to a variety of products to estimate keeping quality over a short period of time. The industry has not been successful in applying this approach to ultra-high temperature (UHT) milk because of chemical and physical changes in the milk proteins that take place during processing and storage. We investigated these protein changes, applying accelerated shelf-life principles to UHT milk samples with different fat levels and using native- and sodium dodecyl sulfate-PAGE. Samples of UHT skim and whole milk were stored at 20, 30, 40, and 50°C for 28 d. Irrespective of fat content, UHT treatment had a similar effect on the electrophoretic patterns of milk proteins. At the start of testing, proteins were bonded mainly through disulfide and noncovalent interactions. However, storage at and above 30°C enhanced protein aggregation via covalent interactions. The extent of aggregation appeared to be influenced by fat content; whole milk contained more fat than skim milk, implying aggregation via melted or oxidized fat, or both. Based on reduction in loss in absolute quantity of individual proteins, covalent crosslinking in whole milk was facilitated mainly by products of lipid oxidation and increased access to caseins for crosslinking reactions. Maillard and dehydroalanine products were the main contributors involved in protein changes in skim milk. Protein crosslinking appeared to follow a different pathway at higher temperatures (≥40°C) than at lower temperatures, making it very difficult to extrapolate these changes to protein interactions at lower temperatures.

Key words: storage, aggregation, protein interactions, ultra-high temperature, whole and skim milk

INTRODUCTION

Production of UHT milk involves heating the milk to a high temperature (usually 130 to 140°C) for 3 to 5 s, followed by aseptic packaging to produce a commercially sterile product with minimal changes in quality (Holland et al., 2011). Thermal treatment enables storage of UHT milk at room temperature for up to 9 mo, eliminating the need for refrigeration in the distribution chain. Its long shelf life at room temperature has made UHT milk an important food product from nutritional, technological, and economic points of view. However, high temperature treatment induces changes such as whey protein denaturation, Maillard reaction, and mineral imbalances, which may lead to changes in protein–protein interactions and result in physical storage instabilities, including sedimentation of proteinaceous material at the bottom of the storage container, gel formation (age gelation), or both (Andrews and Cheeseman, 1972; McMahon, 1996; Deeth and Lewis, 2016). Proteolysis, another underlining mechanism of gelation, also involves protein network formation (i.e., interaction or linking between proteins or their fragments; Deeth and Lewis, 2016). Irrespective of mechanism, gelation or sedimentation appears to be governed and preceded by changes in the extent and nature of interactions among milk proteins.

Changes in protein interactions primarily involve noncovalent interactions, via either weak bonding (such as hydrophobic, van der Waals, or electrostatic interactions) or covalent crosslinking with other proteins through formation of disulfide bonds, advanced Maillard products (**AMP**), and dehydroalanine (Singh, 1991; Friedman, 1999; Wang et al., 2010; Holland et al., 2011). In addition to protein–protein linking, the role of protein–lipid interactions in the initiation and buildup of sediment or gel has not been studied extensively. However, several reports have reported on the lower extent of proteolysis (López-Fandiño et al., 1993; Garcia-Risco et al., 1999), and the creation of products of Maillard reaction (AMP; Valero et al., 2001) in stored

Received April 5, 2016.
Accepted September 17, 2016.
[1]Corresponding author: todor.vasiljevic@vu.edu.au

UHT milk with higher fat content indicates that fat may play some role in the extent of protein interactions during storage.

Exploring the progression and extent of changes in protein interactions by applying full-length shelf-life tests would be time- and resource-intensive. Accelerated shelf-life tests could be a suitable alternative for predicting storage changes in products such as UHT milk. In fact, by accelerating the rate of deterioration of sensory attributes by exposing the product to elevated storage temperatures, shelf life has been predicted in a comparably short time (Richards et al., 2014). Besides deterioration in sensory attributes, protein–protein interactions are also enhanced at higher storage temperatures (Al-Saadi and Deeth, 2008). Therefore, using elevated storage temperatures, protein interactions could also be accelerated, and the results could then be extrapolated to predict aggregation mechanisms at lower storage temperatures using a rapid method of determination such as Fourier transform infrared spectroscopy, avoiding lengthy real-time analysis. However, as has been previously reported, higher storage temperatures ($\geq$40°C) inhibit age gelation (Kocak and Zadow, 1985; McMahon, 1996; Deeth and Lewis, 2016). The reasons for this are not known, but a few suggestions have been postulated. First, an increased rate of proteolysis at higher temperatures results in extensively degraded proteins, which are no longer able to form a stable gel matrix (Datta and Deeth, 2001). The second hypothesis is that accelerated Maillard browning reactions at higher temperatures block lysine residues, which would likely participate in protein–protein interactions leading to gelation (Samel et al., 1971; Gaucher et al., 2008). Third, higher rates of chemical crosslinking via Maillard and other reactions prevents the release of βκ complex from the micelle, which is the starting point for the onset of age gelation (McMahon, 1996). Furthermore, high storage temperatures slow gelation but result in increased nondispersible sediment (Nieuwenhuise and van Boekel, 2003). Thus, accelerated shelf-life testing in UHT milk could only be used to predict sedimentation at room temperature.

The present study was aimed at establishing the feasibility of using elevated temperatures during storage of UHT milk with different fat contents to predict changes in the interactions of milk proteins that may lead to sedimentation at room temperature.

MATERIALS AND METHODS

Materials

Commercial UHT whole (full cream) milk (**WM**) and skim milk (**SM**) were provided by a local manufacturer (Murray Goulburn Co-operative Co. Ltd., Victoria, Australia). All milk packs originated from the same batches. Both SM and WM packs were produced on the same day using an established process on an indirect tubular processor (SPX Flow Technology, Mulgrave, Australia) with a 9,000 L/h capacity at 138°C for 6 s. The composition of the WM as reported by the manufacturer was 33 g/L protein, 34 g/L fat, 53 g/L sugars, 0.55 g/L sodium, and 1.2 g/L calcium. The composition of the SM was 34 g/L protein, 1 g/L fat, 53 g/L sugars, 0.55 g/L sodium, and 1.2 g/L calcium.

The electrophoresis chemicals were obtained from Bio-Rad Laboratories (Richmond, CA). The reducing agent 2-mercaptoethanol, bovine milk standards α-LA, β-LG, and BSA were purchased from Sigma (Castle Hill, NSW, Australia). Prestained SDS-PAGE standard (SeeBlue Plus2) was procured from Thermo Fisher Scientific (Scoresby, Victoria, Australia).

Storage of UHT Milk

The UHT milk packs were stored at room temperature (20°C) and 3 elevated temperatures (30, 40, and 50°C) for 28 d in incubators (Thermoline Scientific Pty Ltd., Wetherill Park, NSW, Australia). The elevated storage temperature served to accelerate the development of storage instabilities. Milk packs were analyzed on the first day of delivery (d 0), and then at two 2-wk intervals (14 and 28 d) during storage for change in the interactions of milk proteins.

Electrophoretic Analysis of Changes in Protein Interactions

We investigated changes in the interactions of milk proteins during storage of UHT milk using gel electrophoresis—native- and SDS-PAGE under reducing and nonreducing conditions, as previously described (Dissanayake et al., 2013), with some minor modifications. For native-PAGE, milk from each pack was diluted with the native sample buffer [0.11 *M* Tris-HCl buffer (pH 6.8), 8.8% (vol/vol) glycerol, 2.22% (vol/vol) of 0.4% (wt/vol) bromophenol blue solution]. A working volume of 10 μL was then loaded on 12.5% gels and run for 85 min at 210 V and 70 mA in a Protean II xi cell (Bio-Rad Laboratories), filled with tank buffer solution (0.025 *M* Tris, 0.19 *M* glycine, pH 8.3). Gels were rinsed in MilliQ water for 15 min and stained using staining solution (0.15% Coomassie Brilliant Blue R250 dye, 72% isopropanol, and 3% acetic acid) by slowly shaking for 1 h. The stain was completely removed, and the gel was destained by shaking it slowly in destaining solution (10% isopropanol, 10% acetic acid) overnight on a shaking platform.

The same protocol used for native-PAGE was followed for SDS-PAGE, except that we used an SDS sample buffer [0.0625 *M* Tris-HCl buffer (pH 6.8), 10% (vol/vol) glycerol, 2.5% (vol/vol) of 0.4% (wt/vol) bromophenol blue solution, 20% (vol/vol) of 10% (wt/vol) SDS]. In reducing SDS-PAGE, 20 μL of 2-mercaptoethanol was added per 1 mL of milk and SDS buffer mix, vortexed, heated in a boiling water bath for 5 min, and cooled before running on SDS-PAGE gels in SDS running buffer (0.1% SDS, 0.025 *M* Tris, and 0.191 *M* glycine, pH 8.6). We used prestained SDS-PAGE standard (3–200 kDa) to compare molecular weights. Milk samples from different packs were analyzed in duplicate. Representative gel patterns are shown in Figures 1 to 3. Native-PAGE and SDS-PAGE gels were scanned using a ChemiDoc imager (Chemidoc MP; Bio-Rad Laboratories).

Quantitation and Kinetics of Changes in Protein Interactions

We determined the intensities of the major protein bands in reducing SDS-PAGE using the Image Lab 5.2.1 software associated with the densitometer (Bio-Rad Chemidoc MP imaging system). We calculated the absolute quantity of reduced proteins from their respective band intensity, and because the gels were run in duplicate, the absolute quantity was averaged. The average loss in absolute quantity of reduced milk pro-

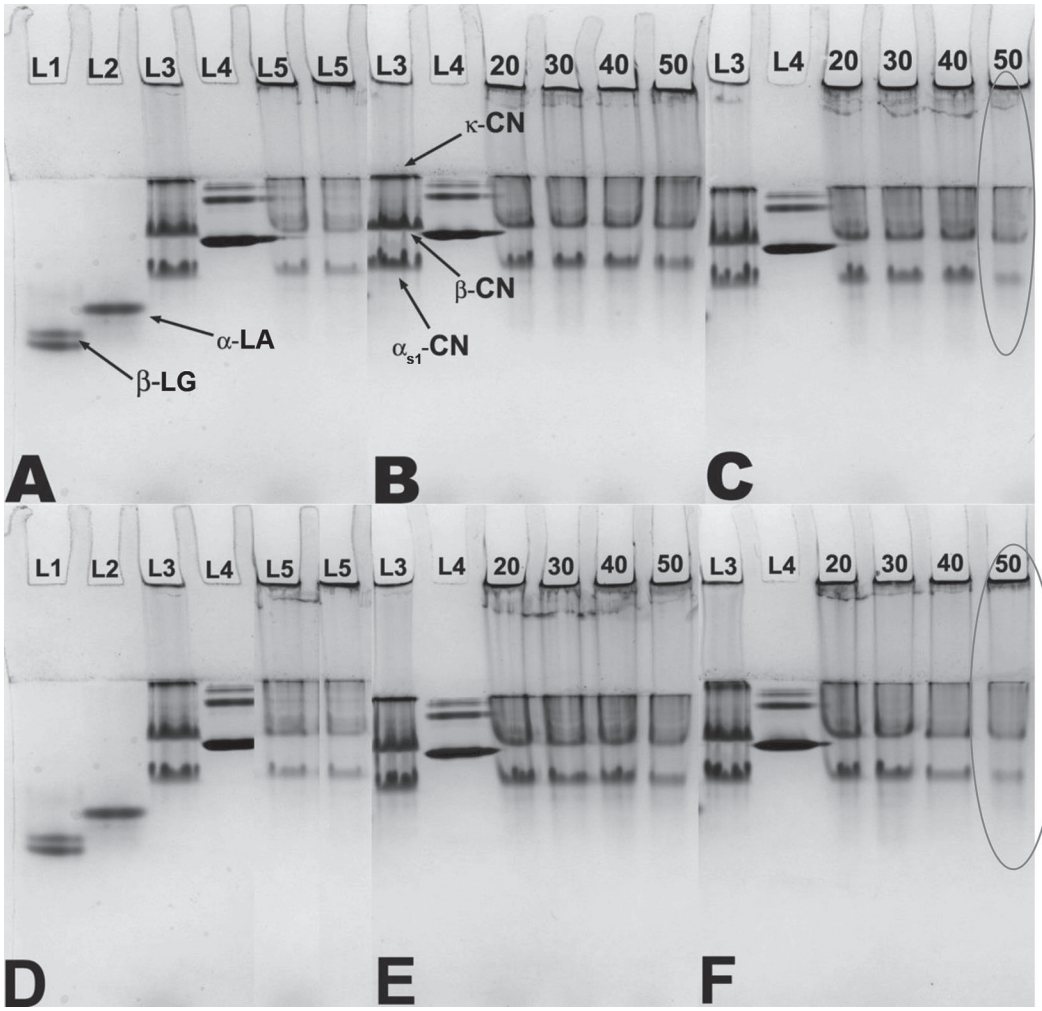

Figure 1. Native-PAGE patterns of UHT skim milk and whole milk on d 0, 14, and 28 of storage. Lanes labeled L1, L2, L3, and L4 represent protein standards of β-LG, α-LA, calcium caseinate, and BSA on d 0, respectively. L5 represents controls: skim milk (A) and whole milk (D). The numbers 20, 30, 40, and 50 indicate samples stored at 20, 30, 40, and 50°C at a given storage time for skim milk (A, B, and C) and whole milk (D, E, and F). Circled lanes indicate accelerated band fading. Color version available online.

teins and increase in amount of aggregates obtained at different storage temperature was plotted versus time.

Statistical Analysis

The experiments were arranged in a block, split plot in time design, with fat content as the main factor and time as a subplot. The design was replicated on a separate occasion, which served as a block. All samples were also subsampled at least twice, giving at least 4 independent observations. The data were analyzed using the GLM procedure of SAS (version 9.1, SAS Institute Inc., Cary, NC). The level of significance was preset at $P < 0.05$.

RESULTS AND DISCUSSION

Changes in protein interactions during the storage of UHT milk under different conditions were demonstrated by alterations in electrophoretic mobility. We explored the type and extent of the interactions at room temperature and at elevated temperatures using native, nonreducing, and reducing SDS-PAGE assays. We identified different bands in patterns by concurrent electrophoresis of standards and by comparing the results with similar reported patterns in the literature (Patel et al., 2007).

Effect of Storage Conditions on Loss of Native Proteins

The effect of storage time and temperature on native-PAGE patterns in SM and WM is presented in Figure 1. The patterns show thick bands at the entry of stacking gel, corresponding to high-molecular-mass protein aggregates, which were not able to penetrate the gel. Aggregates probably corresponded to denatured whey proteins associated with themselves and with caseins via thiol-disulfide exchange (Guyomarc'h et al., 2003; Anema, 2008), noncovalent interactions (Donato and Guyomarc'h, 2009), or covalent interactions (Al-Saadi et al., 2013). Faint bands corresponding to native-like

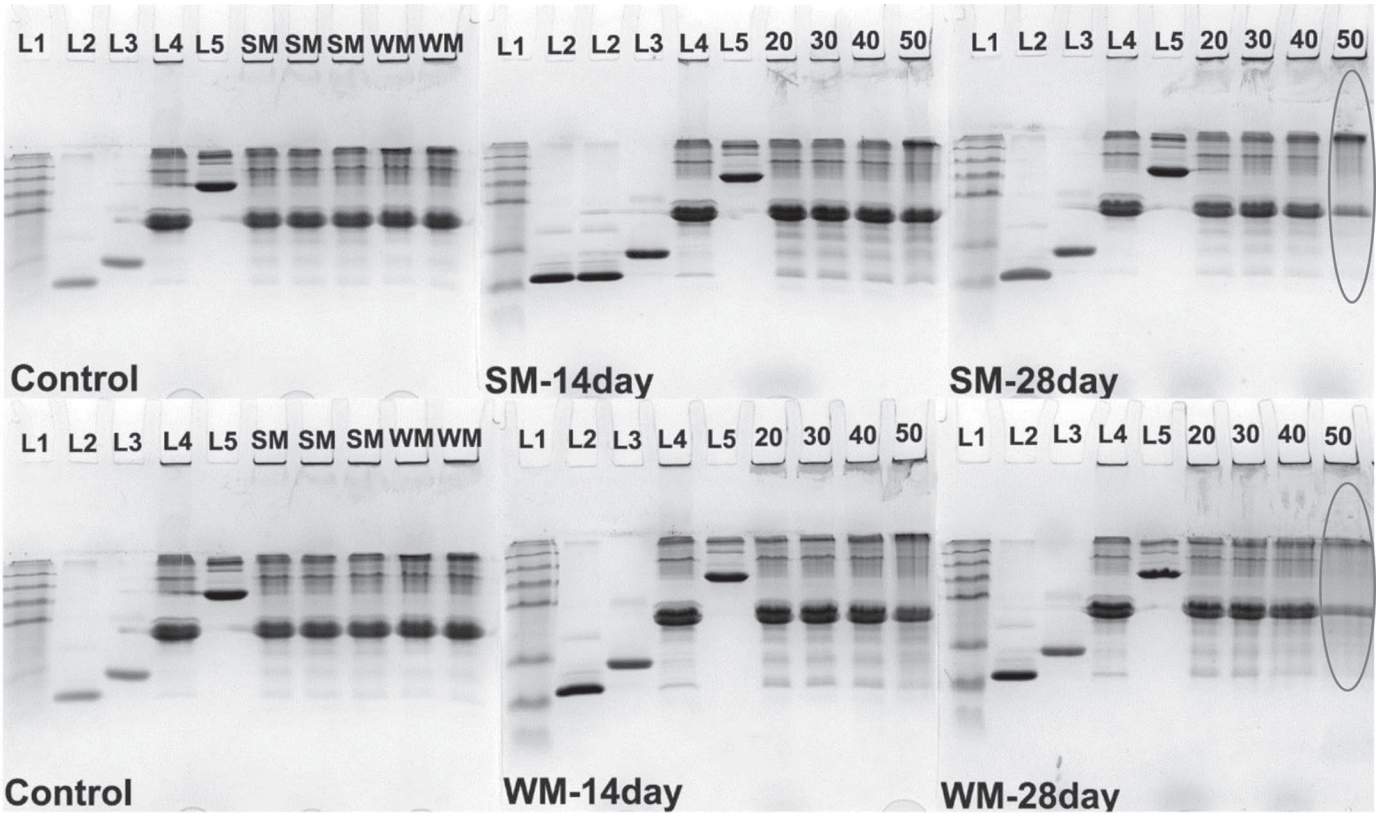

Figure 2. Nonreducing SDS-PAGE patterns of UHT skim milk (SM) and whole milk (WM) on d 0 (control), 14, and 28 of storage. Lanes labeled L1, L2, L3, L4, and L5 represent a molecular weight marker and protein standards for α-LA, β-LG, calcium caseinate, and BSA, respectively. Skim milk and whole milk samples were stored at d 0, and 20, 30, 40, and 50 denote samples stored at 20, 30, 40, and 50°C at a given storage time. Circled lanes indicate accelerated fading and aggregation. Color version available online.

whey proteins—namely, α-LA and β-LG, further supported this suggestion. Patterns also exhibited bands corresponding to native κ-CN, β-CN, and α_{S1}-CN. We observed a diffusely stained region between κ-CN and β-CN bands, which has been attributed previously to crosslinked milk proteins (Patel et al., 2007). Native-PAGE patterns in both SM and WM at the start of storage (d 0) appeared to be similar (Figures 1A and D). However, we observed more prominent changes between these samples during storage, depending on the storage temperature.

Storage of SM and WM at 20, 30, or 40°C for 14 d did not alter the intensity of the bands corresponding to individual native-like caseins (Figures 1B and 1E). However, after 28 d of storage at the same temperatures, the intensity of all native protein bands appeared to decrease for both SM and WM (Figures 1C and F). Notably, loss in "native-like" band intensities of individual milk proteins appeared to be higher in WM at 40°C after 28 d than in SM. This could be due to liquefaction of milk fat around 40°C (MacGibbon and Taylor, 2006). Fat globules are surrounded by caseins and whey proteins upon homogenization, and when melted, they may act as a "glue" between adjacent proteins, increasing the proteins' chance of interaction. A similar observation has been made for the lower heat stability of homogenized milk (Huppertz, 2016) because of the predominant presence of a casein fraction on homogenized fat globules, increasing a volume fraction of casein micelles and enhancing casein particles' rate of encounter, leading to enhanced heat-induced coagulation. Another proposed mechanism driving these changes is oxidation of lipids at elevated storage temperatures. The intermediates (e.g., free radicals and hydroperoxides) and end products (e.g., malondialdedyde) from lipid peroxidation interact with AA residues such as cysteine, lysine, histidine, valine, methionine, and phenylalanine, resulting in protein

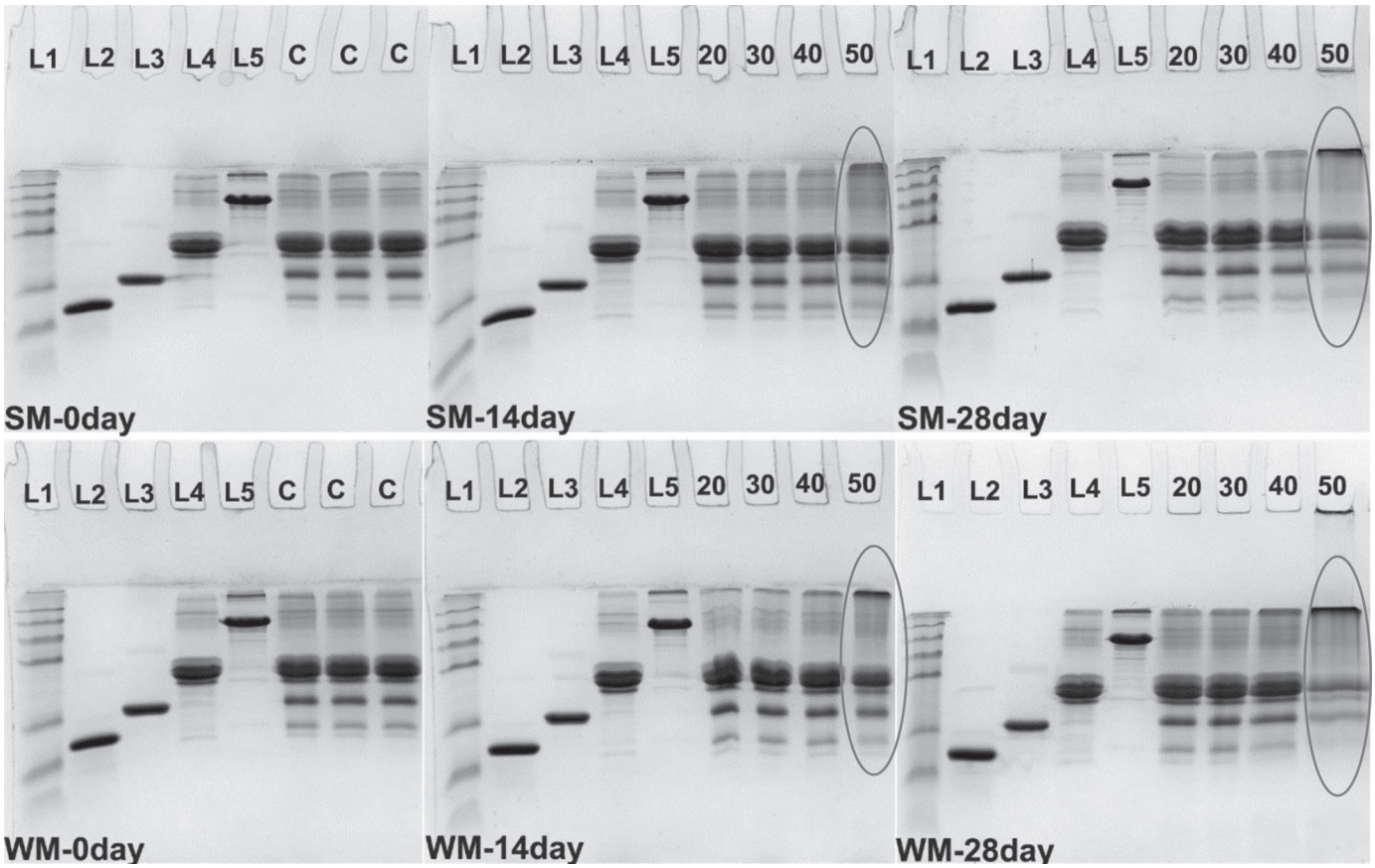

Figure 3. Reducing SDS-PAGE patterns of UHT skim milk (SM) and whole milk (WM) on d 0, 14, and 28 of storage. Storage samples were reduced with β-mercaptoethanol and electrophoresed on SDS gels (4–12.5%). Lanes labeled L1, L2, L3, L4, L5, and C represent a molecular weight marker and protein standards for α-LA, β-LG, calcium caseinate, BSA, and SM and WM samples stored at 0 d, respectively. The SM and WM samples were stored at d 0, and 20, 30, 40, and 50 denote samples stored at 20, 30, 40, and 50°C at a given storage time. Circled lanes indicate accelerated fading and aggregation. Color version available online.

crosslinks (Singh, 1991; Le et al., 2011). In addition to changes in the physical state of lipids and greater generation of the products of lipid oxidation, promoting protein aggregation at higher temperatures, other bulk physiochemical changes (including decline in pH and increase in ionic calcium activity) could also have contributed to the observed differences in native-PAGE patterns for SM and WM (Boumpa et al., 2008). The effect of fat content on ionic calcium activity and its subsequent effect on protein interactions during storage is not known at present and requires further elaboration.

Although only WM indicated accelerated aggregation of milk proteins at 40°C, native-PAGE patterns for both SM and WM samples stored at 50°C were substantially different from those at other temperatures. After 14 d of storage at 50°C in both SM and WM, bands corresponding to β-LG and α-LA completely disappeared, with a concomitant decrease in intensity of α_{S1}-CN, κ-CN, and β-CN bands (Figures 1B and E). The intensity of the diffuse region between κ-CN and β-CN bands also diminished. The complete disappearance of bands corresponding to β-LG and α-LA indicated greater reactivity of whey proteins in the formation of aggregates. This was likely caused by denaturation of β-LG and α-LA and exposure of lysine residues to a high level in these proteins. These characteristics render them a preferable reactant for lactosylation over caseins (Le et al., 2011). Lactosylated whey proteins may further be converted to AMP at higher storage temperatures, which then also crosslink caseins and result in loss of native-like caseins (Le et al., 2011). Further fading out of bands occurred after 28 d of storage, indicating even greater crosslinking of proteins and at a far higher rate than at other storage temperatures in both SM and WM (Figure 1C and F). As well as increasing concentrations of AMP, higher storage temperatures also accelerate other protein crosslinks through intermediates and end products of lipid oxidation (predominantly in WM), dehydroalanine and hydrophobic or other noncovalent interactions (Singh, 1991; Holland et al., 2011). Dehydroalanine is produced by heat-induced elimination of phosphate from phosphoserine residues in caseins. It then reacts with the amino group of lysine residues, the imidazole group of histidine, or the thiol group of cysteine, resulting in intra- or intermolecular lysinoalanine, histidinoalanine, or lanthionine crosslinks, respectively (O'Connell and Fox, 2003). Higher storage temperature also induces changes in the secondary structure of milk proteins (Mahler et al., 2009). This results in the exposure of hydrophobic regions, which may associate via noncovalent interactions (Andrews, 1975; Henle et al., 1996; Donato and Guyomarc'h, 2009; Holland et al., 2011).

Effect of Storage Temperature on Loss of SDS Monomeric Proteins

To obtain information regarding the type of aggregation (covalent and noncovalent) and the involvement of particular milk proteins, we further analyzed milk samples using the dissociating agent SDS without the reducing agent. We know that SDS dissociates intermolecular and intramolecular aggregates that are noncovalently linked. Thus, nonreducing SDS-PAGE could reveal the involvement of hydrophobic interactions in the formation of the high-molecular-mass aggregates observed in native-PAGE patterns.

Figure 2 shows SDS-PAGE nonreducing patterns for both SM and WM. These patterns showed intense bands corresponding to monomeric α_{S1}-CN, κ-CN, and β-CN, α_{S2}-CN dimer and BSA. Bands corresponding to SDS monomeric α-LA and β-LG were faint but had a higher intensity than native bands, implying that these proteins were linked via noncovalent interactions in addition to disulfide or other covalent bonds (Havea et al., 1998; Donato and Guyomarc'h, 2009). Reduction in the intensity of high-molecular-mass aggregates at the top of the stacking gel further supported this suggestion (Figures 1 and 2). However, noticeable bands corresponding to high-molecular-mass aggregates and diffuse regions at the top of the stacking gel and resolving gel, respectively (Figure 2), indicated that these aggregates were either disulfide-linked or covalently bonded. Furthermore, SDS-PAGE patterns of SM and WM at the start of storage were similar (Figure 2), suggesting that the effect of UHT treatment was independent of fat content. This finding contradicted the theory that milk fat protects other components of milk from heat-induced changes (Pellegrino, 1994). However, the effect of fat content appeared to be more relevant during storage at different temperatures.

At and below 40°C, storage for the first 14 d did not change the intensity of protein bands in SM (Figure 2). However, in WM, the intensity of bands corresponding to whey proteins decreased, with a concomitant increase in the intensity of aggregate bands at the top of the resolving gel. This was in line with similar observations made in native-PAGE patterns of WM after 14 d of storage at 40°C, implying the likely involvement of fat. After 28 d of storage for SM and WM at 20, 30, and 40°C, we observed a decrease in the intensity of different SDS monomeric bands (Figure 2). Thus, covalent crosslinking of proteins progressed at a slower rate, even at lower storage temperatures (Gaucher et al., 2008). However, in WM, the bands corresponding to whey proteins were diffuse and faint compared with SM at the same temperature. The decrease in band intensity of whey proteins was further exacerbated in

WM at 50°C. After 28 d of storage at this temperature, whey protein bands disappeared, and we were able to observe only a diffuse region (smear) with very faint bands corresponding to high-molecular-mass protein aggregates α_{S1}-CN and β-CN in WM (Figure 2). This diffuse region has been attributed to nondisulfide covalent crosslinking of proteins (Singh, 1991). Skim milk also exhibited an intense aggregate band at the top of the resolving gel and faint bands corresponding to β-CN, α_{S1}-CN, and whey proteins at 50°C. The faster and more complete disappearance of whey proteins in WM at and above 40°C could be due partly to enhanced covalent crosslinking stemming from changes in the physical state of fat and the oxidation of lipids. Also, other unexplored mechanisms involving changes in pH or mineral balance differing affected by the presence of fat might have resulted in the different electrophoretic patterns observed for WM.

Only α_{S1}-CN and β-CN were present in both SM and WM in SDS-PAGE nonreduced at 50°C after 28 d; this could be due to their comparatively higher amounts in milk (Huppertz, 2013). Furthermore, because of their more hydrophobic nature and lack of cysteine residues, α_{S1}-CN and β-CN may be more prone to involvement in noncovalent interactions than other caseins.

Effect of Storage Conditions on Loss of Reduced Proteins

We further explored the nature of the aggregates and smear (disulfide or other type of covalently bonded) produced at higher temperatures in SDS-PAGE nonreducing patterns by using SDS-PAGE under reducing conditions. The SDS dissociated hydrophobic interactions and, with the addition of β-mercaptoethanol, it reduced disulfide bonds. Hence, the bands corresponding to aggregates in SDS-PAGE reducing patterns would be entirely due to nondisulfide covalent interactions.

Skim milk and WM had similar patterns on d 0 for native-PAGE and SDS-PAGE nonreducing patterns (Figures 1 to 3). This finding reconfirmed previous observations that the effect of UHT treatment on the electrophoretic mobility of milk proteins was independent of fat content. At the beginning of storage, high-molecular-mass aggregates were not present on top of the stacking gel (Figure 3). Only a faint band demonstrative of nonreducible protein aggregates were present at the top of the resolving gel, as shown earlier for nonreducing SDS-PAGE. Furthermore, patterns on d 0 had intense bands corresponding to caseins, β-LG and α-LA, suggesting that thiol-disulfide exchange and hydrophobic interactions were major aggregation pathways at the beginning of storage (Pizzano et al., 2012). We also observed a diffuse region between the nonreducible aggregate band and the α_{S2}-CN dimer, and between BSA and the α_{S2}-CN dimer. This region probably also had nondisulfide, covalently linked caseins and whey proteins, because it was present in native-PAGE and in nonreducing SDS-PAGE patterns. It appeared that at the beginning of storage, the order of interactions in both SM and WM was disulfide > noncovalent > covalent (nondisulfide). Although SM and WM had similar patterns on d 0, storage conditions affected them differently in the context of extent of aggregation and loss of different individual milk proteins.

Kinetics of Aggregate Formation

Skim milk did not exhibit an increase in the amount of nonreducible and high-molecular-mass aggregates after 28 d of storage at 20°C (Figures 3 and 4). However, after 28 d of storage at 30 and 40°C, we did note an increase in nonreducible aggregates, although not in high-molecular-mass aggregates. In WM, the trend was slightly different: the nonreducible aggregates started to build up only after 14 d of storage at 20, 30, or 40°C. However, like SM, WM showed no apparent increase in the concentration of high-molecular-mass aggregates, even after 28 d of storage (Figures 3 and 6). At 50°C, the amount of nonreducible and high-molecular-mass aggregates increased to a great extent in both SM and WM (Figure 4). The proteins were most likely aggregated by covalent interactions to form high-molecular-mass aggregates, and rate of these interactions was enhanced sharply above 40°C. Furthermore, the extent of formation of high-molecular-mass aggregates was greater in WM than in SM following 28 d of storage (Figure 4), suggesting enhanced protein aggregation at higher temperatures in the presence of fat.

Besides the difference in the amounts of aggregates formed, SM and WM also differed by how individual caseins and whey proteins participated in the formation of covalently bound aggregates. In SM at 20°C, we observed no change in the quantity of whey proteins and caseins (Figure 5A), supporting our earlier observation that there was no change in reducible and high-molecular-mass aggregates (Figures 3, 4A). In SM at 30 and 40°C, α_{S2}-CN, β-CN, and β-LG decreased during the first 14 d of storage, followed by α_{S2}-CN and α-LA during the next 14 d of storage (Figures 5B and C). However, in WM, the reduction in the quantity of proteins started at 20°C (Figures 6A to C). At 20, 30, and 40°C, β-LG was one of the first proteins to initiate nondisulfide aggregation in WM, as evidenced by its decrease in concentration after the first 14 d of storage (Figures 6A to C). A reduction in the quantity

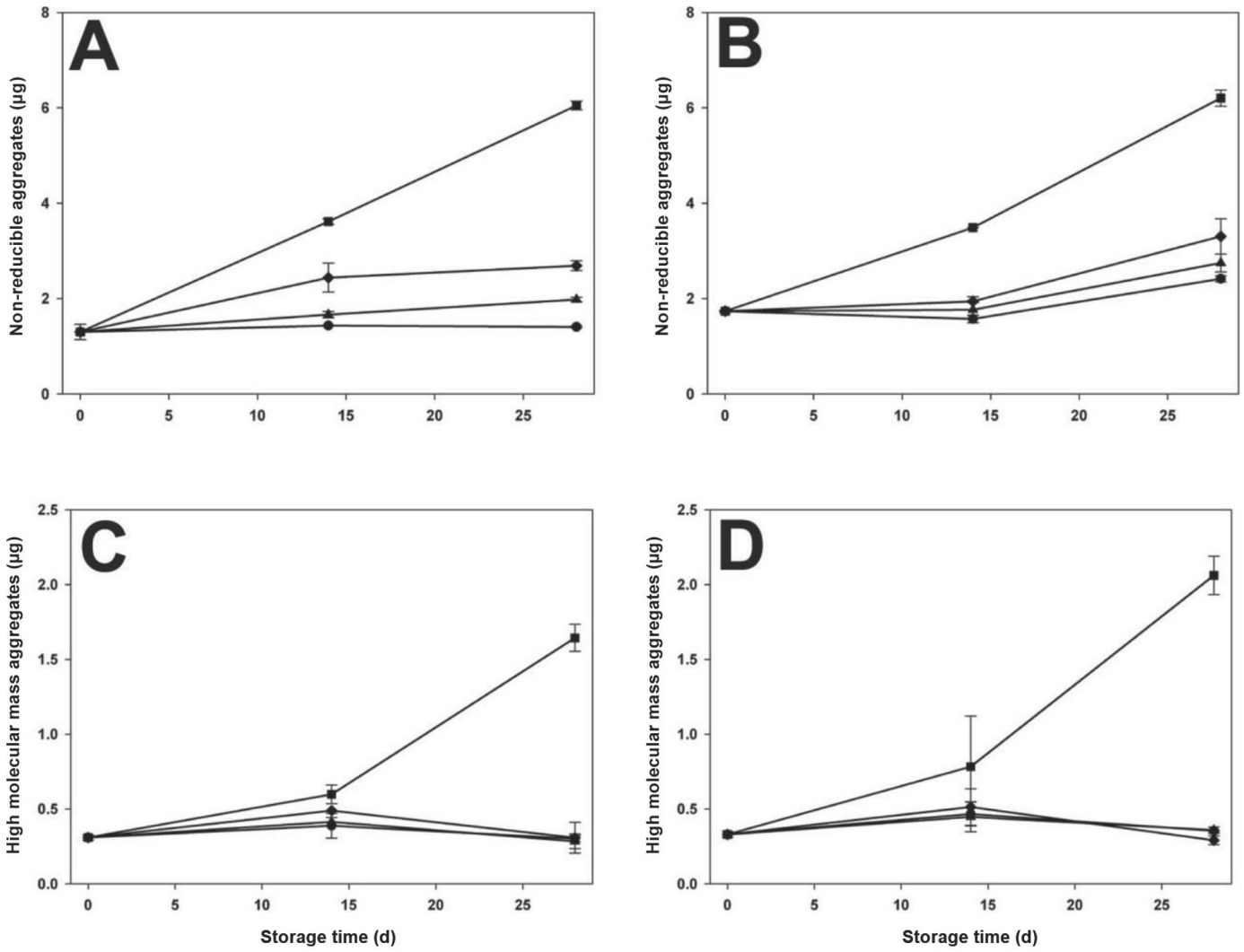

Figure 4. Change in absolute quantity of nonreducible (A and B) and high-molecular-mass (C and D) aggregates during storage of UHT skim milk (A, C) and whole milk (B, D) at storage temperatures of 20°C (●), 30°C (▲), 40°C (◆), and 50°C (■), as obtained from image analysis of reducing SDS-PAGE. Error bars represent SD.

of α_{S1}-CN, α_{S2}-CN, and βLG in WM was evident over the next 14 d at 20 and 30°C (Figures 6 A and B). At 40°C, α-LA also participated in aggregation through nondisulfide covalent interactions in WM, similar to SM. Loss in the quantity of proteins was much higher at 50°C than at 20, 30, or 40°C in both SM and WM. In addition, κ-CN participated in covalent aggregation only in the latter half of storage at 50°C in both WM and SM, overruling proteolysis by bacterial proteinases. All the proteins in milk seemed to be actively involved in crosslinking at 50°C. Higher storage temperatures increase intra-micellar crosslinking, which might result in increased electrostatic repulsion inside the micelle and lead to dissociation and sedimentation of crosslinked proteins (Nieuwenhuise and van Boekel, 2003). However, β-CN and α_{S2}-CN were main players in SM, whereas α_{S1}-CN, α_{S2}-CN, and α-LA were central to protein–protein interactions in WM (Figures 5 and 6). The difference in type of caseins involved in WM and SM at different temperatures suggested preferences for specific pathways of covalent (nondisulfide) crosslinking.

Nondisulfide covalent crosslinking in UHT milk during storage occurs via AMP, dehydroalanine, and lipid oxidation products (in WM) (Singh, 1991; Le et al., 2011). Crosslinking via AMP involves lactosylation of lysine residues as the first step (Van Boekel, 1998), implying that proteins with a higher number of lysine residues would be preferentially involved in this reaction. The lysine content of different milk proteins vary, following this order: α_{S2}-CN > βLG > α_{S1}-CN > α-LA > β-CN > κ-CN (Huppertz, 2013). Involvement of α_{S2}-CN as one of the major players in covalent aggrega-

tion in SM (Figure 5) indicates higher levels of AMP-mediated crosslinking. Additionally, disappearance of α-LA in SM even at 30°C also suggests a higher rate of Maillard reaction in the former. The preference of α-LA for reaction with lactose was demonstrated earlier by lactosylation of almost all its lysine residues during storage of UHT milk (Holland et al., 2011). Moreover, α-LA may also preferentially engage in this reaction (Le et al., 2011) because of conformational changes and denaturation that take place during UHT treatment (Losito et al., 2010). The greater extent of Maillard reaction in SM is also supported by the comparatively higher increase in the "b" value of color in SM than WM at temperatures above 30°C (data not shown). Valero et al. (2001) had also reported higher levels of Maillard products in SM than WM during storage. Greater AMP-mediated crosslinking in SM also explained the reduction in quantity of β-CN in SM. Lactosylation results in increased hydrophilicity of the casein micelle interior, which might have weakened hydrophobic associations (Rauh et al., 2015) and released β-CN to the solution (Figure 7A). In addition to lactosylation, α_{S2}-CN also appears to be most reactive candidate for dehydroalanine-linked proteins, because of a high number of phosphoserine residues and the presence of 2 cysteine residues (O'Mahony and Fox, 2013). Skim milk with greater involvement of α_{S2}-CN and β-CN implied a higher rate of AMP and dehydroalanine-mediated crosslinking (Figure 7A).

In WM, α_{S1}-CN, α_{S2}-CN, and α-LA were the main proteins involved in nondisulfide covalent crosslinking (Figure 6). Previous reports have shown α_{S1}-CN

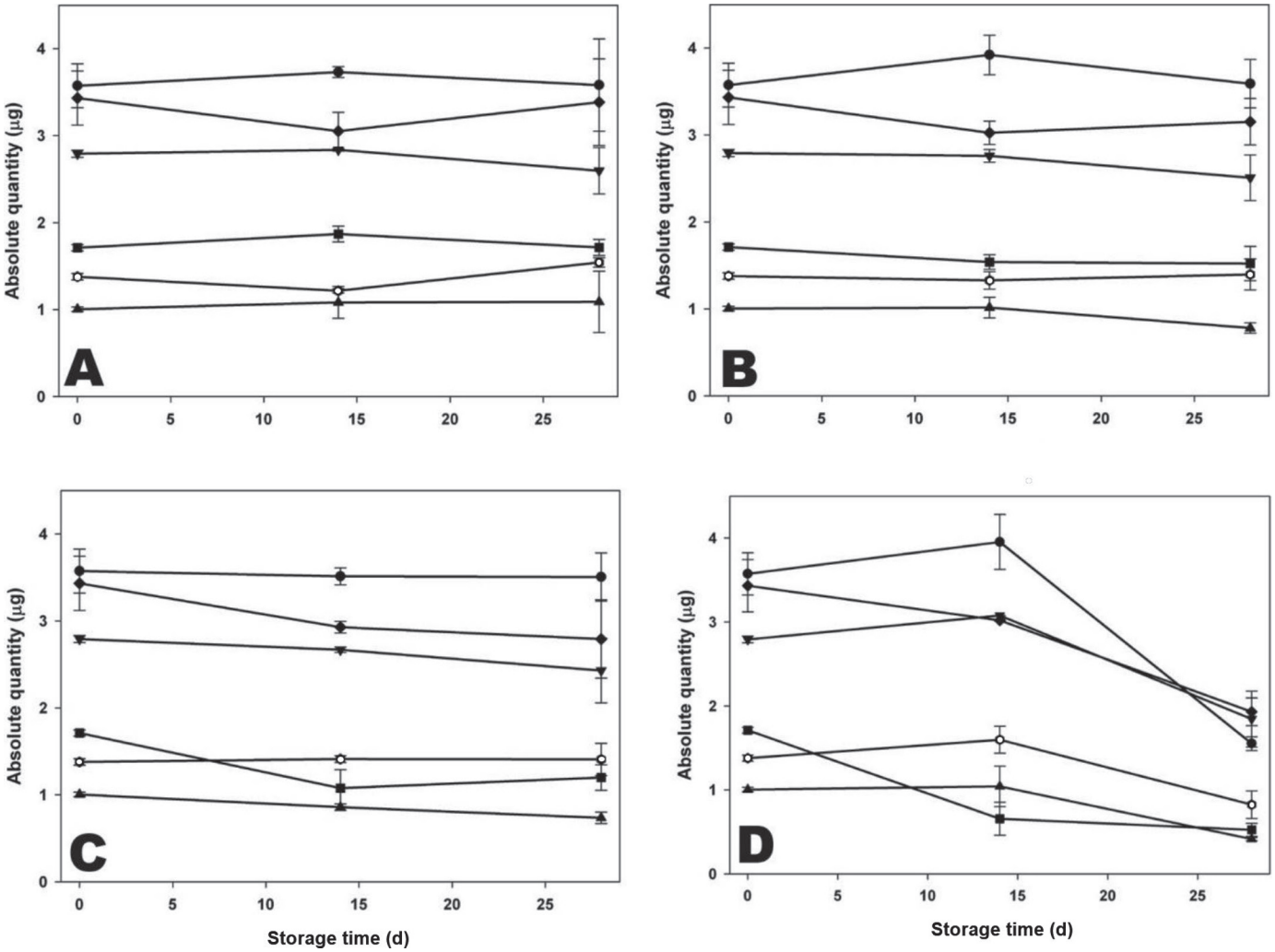

Figure 5. Change in absolute quantity of caseins (α_{S1}-CN, ●; α_{S2}-CN, ■; β-CN, ◆; κ-CN, ○) and whey proteins (β-LG, ▼; α-LA, ▲) during storage of UHT skim milk at storage temperatures of 20°C (A), 30°C (B), 40°C (C), and 50°C (D), as obtained from image analysis of reducing SDS-PAGE. Error bars represent SD.

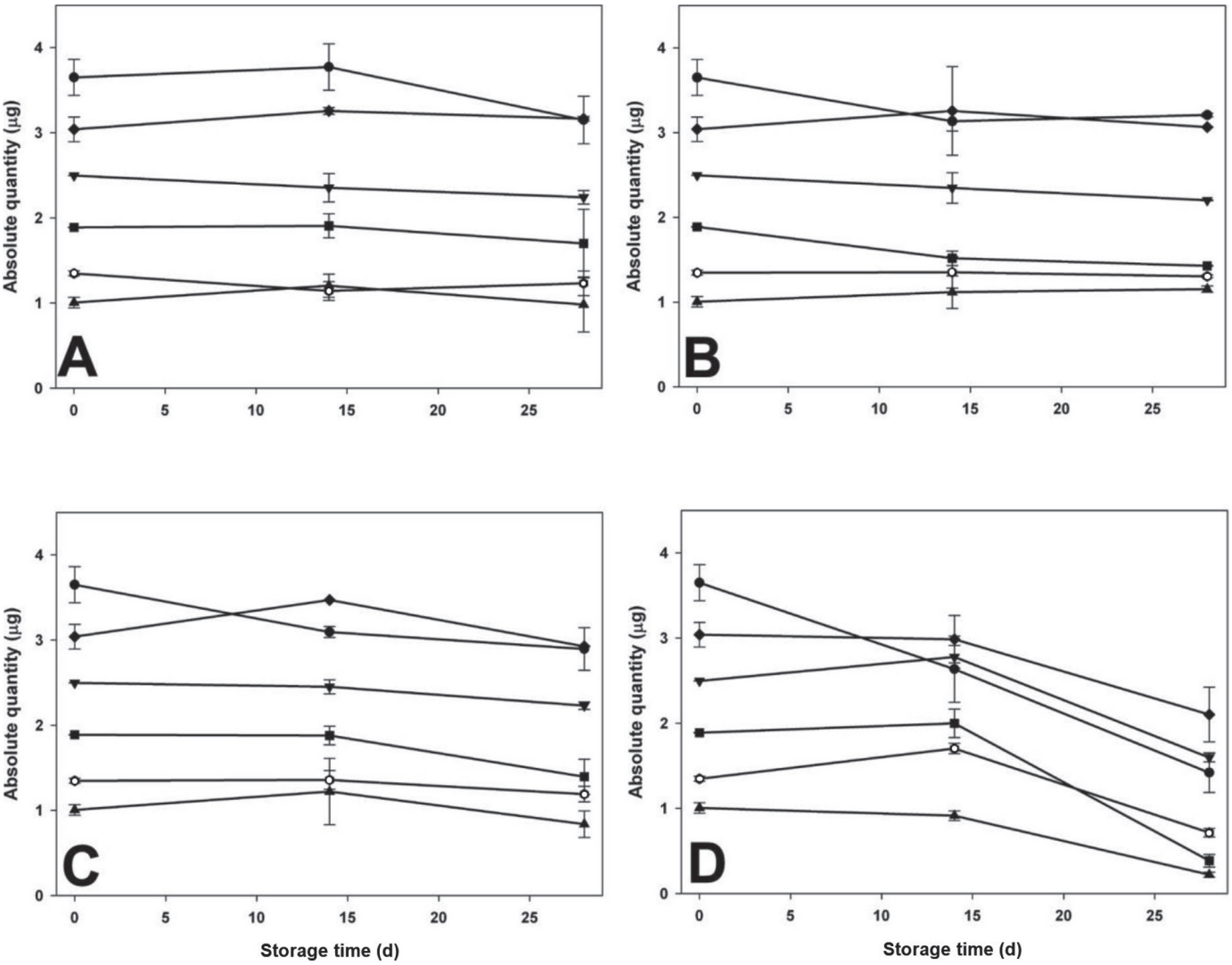

Figure 6. Change in absolute quantity of caseins (α_{S1}-CN, ●; α_{S2}-CN, ■; β-CN, ◆; κ-CN, ○) and whey proteins (β-LG, ▼; α-LA, ▲) during storage of UHT whole milk at storage temperatures of 20°C (A), 30°C (B), 40°C (C), and 50°C (D), as obtained from image analysis of reducing SDS-PAGE. Error bars represent SD.

to be the most abundant protein in aggregates (Holland et al., 2011). Furthermore, the higher amount of aggregates in WM than in SM can be attributed to crosslinking via lipid oxidation products and melted fat globules, at and above 40°C in WM. The modified fat globule membrane also consists of whey proteins and predominantly caseins besides its native components (Huppertz, 2016). In addition to change in state and oxidation of milk fat, high storage temperatures lower pH and increase ionic calcium activity during storage of UHT milk (data not shown). Homogenized fat globules are stabilized by casein micelles on their surface, which may not contain enough κ-casein molecules on the outside due to distorted and randomized spreading (Huppertz, 2016). As all other caseins are calcium-sensitive, protein coagulation and thus aggregation in WM would be enhanced due to the increase in ionic calcium activity (Huppertz, 2016). Therefore, the difference in involvement of different proteins in SM and WM might be due to differences in their access and availability. Thus, it appeared that covalent crosslinking in UHT WM was facilitated via products of lipid oxidation and increased access to caseins for crosslinking reactions, and that Maillard and dehydroalanine products were the main contributors for the observed changes in UHT SM (Figure 7B). However, these suggestions would require further elaboration.

In conclusion, protein interactions—especially covalent crosslinking—were accelerated at higher storage temperatures. However, at temperatures above 30°C in

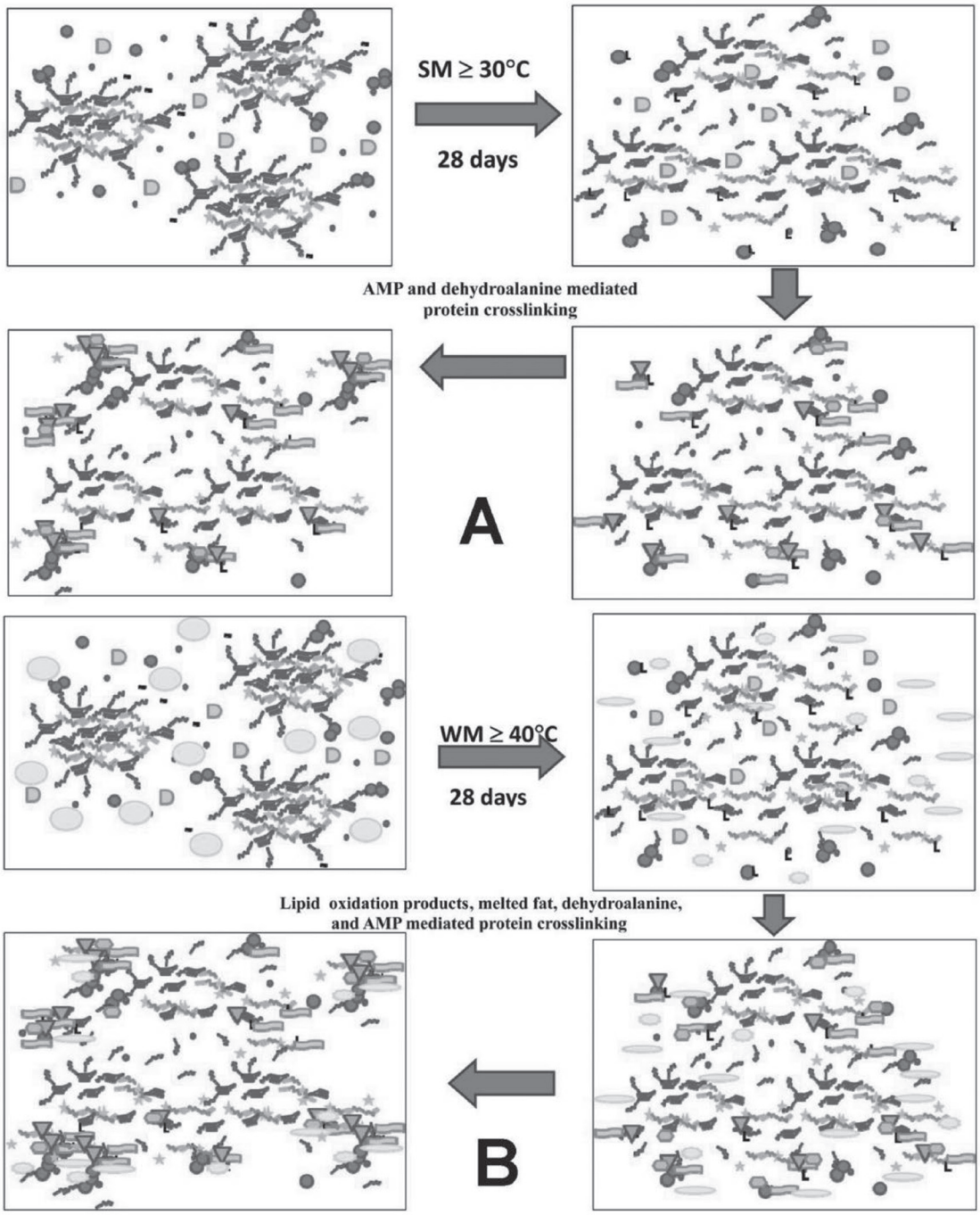

	α_{s1}-CN		α_{s2}-CN		β-CN		κ-CN
	α-LA		β-LG		CCP		Lactose
L	L-lysine		AMP		DHA		AWP
	fat globules		oxidized fat globules		melted fat globules		
	crosslinked aggregates				crosslinked aggregates plus melted and oxidized fat		

Figure 7. Advanced Maillard products (AMP), dehydroalanine (DHA), and lipid oxidation products mediated protein crosslinking in (A) skim milk (SM) at and above 30°C and (B) whole milk (WM) at and above 40°C. AWP = aggregated whey proteins; CCP = colloidal calcium phosphate. Color version available online.

WM and above 40°C in SM, the rate and type of these reactions were very different from those at 20°C. Especially in case of WM, protein crosslinking appeared to follow a different pathway that may not occur in storage at lower temperatures. In addition, the pathways discussed above that enhance protein interactions were only the major ones and did not include all possible factors, which are numerous because of the complex nature of milk. Extrapolating these reactions to predict changes in protein interactions at lower temperatures is very difficult and emphasizes the need for long-term study. However, acquired knowledge of the involvement of individual proteins and the kinetics of these changes may assist in identifying structural changes that can be determined by a spectral analysis, such as Fourier transform infrared spectroscopy. A detailed long-term study would also need to be undertaken to confirm these changes and establish them as markers for prediction of the shelf life of UHT milk using spectral analysis.

ACKNOWLEDGMENTS

This work is supported by the Department of Business and Innovation of the Victorian Government, through its Victoria India Doctoral Scholarship Program (managed by the Australia India Institute). The first author also acknowledges her employer, the Indian Council of Agricultural Research, for granting study leave to pursue a PhD.

REFERENCES

Al-Saadi, J. M., and H. C. Deeth. 2008. Cross-linking of proteins and other changes in UHT milk during storage at different temperatures. Aust. J. Dairy Technol. 63:93–99.

Al-Saadi, J. M. S., A. M. Easa, and H. C. Deeth. 2013. Effect of lactose on cross-linking of milk proteins during heat treatments. Int. Dairy J. 66:1–6.

Andrews, A. 1975. Properties of aseptically packed ultra-high-temperature milk: III. Formation of polymerized protein during storage at various temperatures. J. Dairy Res. 42:89–99.

Andrews, A., and G. Cheeseman. 1972. Properties of aseptically packed ultra-high-temperature milk: II. Molecular weight changes of the casein components during storage. J. Dairy Res. 39:395–408.

Anema, S. G. 2008. The whey proteins in milk: Thermal denaturation, physical interactions and effects on the functional properties of milk. Pages 239–281 in Milk Proteins: From Expression to Food. A. Thompson, M. Boland, and H. Singh, ed. Academic Press, San Diego, CA.

Boumpa, T., A. Tsioulpas, A. S. Grandison, and M. J. Lewis. 2008. Effects of phosphates and citrates on sediment formation in UHT goats' milk. J. Dairy Res. 75:160–166.

Datta, N., and H. C. Deeth. 2001. Age gelation of UHT Milk—A review. Food Bioprod. Process. 79:197–210.

Deeth, H., and M. Lewis. 2016. Protein stability in sterilised milk and milk products. Pages 247–286 in Advanced Dairy Chemistry, Vol. 1B: Proteins, Applied Aspects. 4th ed. P. L. H. McSweeney, S. A. O'Mahony, ed. Springer Sci. Business Media, New York, NY.

Dissanayake, M., L. Ramchandran, C. Piyadasa, and T. Vasiljevic. 2013. Influence of heat and pH on structure and conformation of whey proteins. Int. Dairy J. 28:56–61.

Donato, L., and F. Guyomarc'h. 2009. Formation and properties of the whey protein/κ-casein complexes in heated skim milk—A review. Dairy Sci. Technol. 89:3–29.

Friedman, M. 1999. Chemistry, biochemistry, nutrition, and microbiology of lysinoalanine, lanthionine, and histidinoalanine in food and other proteins. J. Agric. Food Chem. 47:1295–1319.

Garcia-Risco, M. R., M. Ramos, and R. Lopez-Fandino. 1999. Proteolysis, protein distribution and stability of UHT milk during storage at room temperature. J. Sci. Food Agric. 79:1171–1178.

Gaucher, I., D. Mollé, V. Gagnaire, and F. Gaucheron. 2008. Effects of storage temperature on physico-chemical characteristics of semi-skimmed UHT milk. Food Hydrocoll. 22:130–143.

Guyomarc'h, F., A. J. Law, and D. G. Dalgleish. 2003. Formation of soluble and micelle-bound protein aggregates in heated milk. J. Agric. Food Chem. 51:4652–4660.

Havea, P., H. Singh, L. K. Creamer, and O. H. Campanella. 1998. Electrophoretic characterization of the protein products formed during heat treatment of whey protein concentrate solutions. J. Dairy Res. 65:79–91.

Henle, T., U. Schwarzenbolz, and H. Klostermeyer. 1996. Irreversibles crosslinking of casein during storage of UHT-treated skim milk. In Proc. Heat Treatments and Alternative Methods, Vienna, Austria. Int. Dairy Fed., Brussels, Belgium.

Holland, J. W., R. Gupta, H. C. Deeth, and P. F. Alewood. 2011. Proteomic analysis of temperature-dependent changes in stored UHT milk. J. Agric. Food Chem. 59:1837–1846.

Huppertz, T. 2013. Chemistry of the caseins. Pages 135–160 in Advanced Dairy Chemistry, Vol. 1A: Proteins, Basic Aspects. P. L. H. McSweeney and P. F. Fox, ed. Springer, New York, NY.

Huppertz, T. 2016. Heat stability of milk. Pages 179–196 in Advanced Dairy Chemistry, Volume 1B: Proteins, Applied Aspects. H. P. L. McSweeney and A. J. O'Mahony, ed. Springer New York, New York, NY.

Kocak, H. R., and J. G. Zadow. 1985. Age gelation of UHT whole milk as influenced by storage temperature. Aust. J. Dairy Technol. 40:14–21.

Le, T. T., B. Bhandari, J. W. Holland, and H. C. Deeth. 2011. Maillard reaction and protein cross-linking in relation to the solubility of milk powders. J. Agric. Food Chem. 59:12473–12479.

López-Fandiño, R., A. Olano, N. Corzo, and M. Ramos. 1993. Proteolysis during storage of UHT milk: differences between whole and skim milk. J. Dairy Res. 60:339–347.

Losito, I., E. Stringano, S. Carulli, and F. Palmisano. 2010. Correlation between lactosylation and denaturation of major whey proteins: An investigation by liquid chromatography–electrospray ionization mass spectrometry. Anal. Bioanal. Chem. 396:2293–2306.

MacGibbon, A. K. H., and M. W. Taylor. 2006. Composition and structure of bovine milk lipids. Pages 1–42 in Advanced Dairy Chemistry, Vol. 2: Lipids. 3rd ed. P. F. Fox and P. L. H. McSweeney, ed. Springer, New York, NY.

Mahler, H.-C., W. Friess, U. Grauschopf, and S. Kiese. 2009. Protein aggregation: Pathways, induction factors and analysis. J. Pharm. Sci. 98:2909–2934.

McMahon, D. J. 1996. Age gelation of UHT milk: Changes that occur during storage, their effect on shelf life and the mechanism by which age gelation occurs. Pages 315–326 in Heat Treatments and Alternative Methods. Int. Dairy Fed., Brussels, Belgium.

Nieuwenhuise, J. A., and M. A. J. S. van Boekel. 2003. Protein stability in sterilised milk and milk products. Pages 947–974 in Advanced Dairy Chemistry, Vol. 1: Proteins. 3rd ed. P. F. Fox and P. L. H. McSweeney, ed. Kluwer Academic/Plenum Publishers, New York, NY.

O'Connell, J. E., and P. F. Fox. 2003. Heat-induced coagulation of milk. Pages 879–945 in Advanced Dairy Chemistry, Vol. 1: Proteins. 3rd ed. P. F. Fox and P. L. H. McSweeney, ed. Kluwer Academic/Plenum Publishers, New York, NY.

O'Mahony, J. A., and P. F. Fox. 2013. Milk proteins: Introduction and historical aspects. Pages 43–85 in Advanced Dairy Chemistry, Vol. 1A: Proteins, Basic Aspects. 4th ed. P. L. H. McSweeney and P. F. Fox, ed. Springer Science, New York, NY.

Patel, H. A., S. G. Anema, S. E. Holroyd, H. Singh, and L. K. Creamer. 2007. Methods to determine denaturation and aggregation of proteins in low-, medium- and high-heat skim milk powders. Lait 87:251–268.

Pellegrino, L. 1994. Influence of fat content on some heat-induced changes in milk and cream. Nederlands melk en Zuivel Tijdschrift 48:71–80.

Pizzano, R., C. Manzo, M. Adalgisa Nicolai, and F. Addeo. 2012. Occurrence of major whey proteins in the pH 4.6 insoluble protein fraction from UHT-treated milk. J. Agric. Food Chem. 60:8044–8050.

Rauh, V. M., L. B. Johansen, M. Bakman, R. Ipsen, M. Paulsson, L. B. Larsen, and M. Hammershøj. 2015. Protein lactosylation in UHT milk during storage measured by liquid chromatography–mass spectrometry and quantification of furosine. Int. J. Dairy Technol. 68:486–494.

Richards, M., H. L. De Kock, and E. M. Buys. 2014. Multivariate accelerated shelf-life test of low fat UHT milk. Int. Dairy J. 36:38–45.

Samel, R., R. W. V. Weaver, and D. B. Gammack. 1971. Changes on storage in milk processed by ultra-high-temperature sterilization. J. Dairy Res. 38:323–332.

Singh, H. 1991. Modification of food proteins by covalent crosslinking. Trends Food Sci. Technol. 2:196–200.

Valero, E., M. Villamiel, B. Miralles, J. Sanz, and I. Martínez-Castro. 2001. Changes in flavour and volatile components during storage of whole and skimmed UHT milk. Food Chem. 72:51–58.

Van Boekel, M. 1998. Effect of heating on Maillard reactions in milk. Food Chem. 62:403–414.

Wang, W., S. Nema, and D. Teagarden. 2010. Protein aggregation—Pathways and influencing factors. Int. J. Pharm. 390:89–99.

CHAPTER 4

Fourier transform infrared spectroscopy analysis of physicochemical changes in UHT milk during accelerated storage

This chapter has been published as a research paper entitled "Fourier transform infrared spectroscopy analysis of physicochemical changes in UHT milk during accelerated storage" by Manpreet Kaur Grewal, Jayani Chandrapala, Osaana Donkor, Vasso Apostolopoulos, Lily Stojanovska and Todor Vasiljevic in the peer reviewed International Dairy Journal, 66, 99-107 (2017).

VICTORIA UNIVERSITY
MELBOURNE AUSTRALIA

GRADUATE RESEARCH CENTRE

DECLARATION OF CO-AUTHORSHIP AND CO-CONTRIBUTION: PAPERS INCORPORATED IN THESIS BY PUBLICATION

This declaration is to be completed for each conjointly authored publication and placed at the beginning of the thesis chapter in which the publication appears.

1. PUBLICATION DETAILS (to be completed by the candidate)

Title of Paper/Journal/Book:	Fourier transform infrared spectroscopy analysis of physicochemical changes in UHT milk during accelerated storage
Surname:	Grewal
First name:	Manpreet Kaur
College:	College of Health & Biomedicine
Candidate's Contribution (%):	80

Status:

Accepted and in press:	☐	Date:	
Published:	☑	Date:	2 12 2016

2. CANDIDATE DECLARATION

I declare that the publication above meets the requirements to be included in the thesis as outlined in the HDR Policy and related Procedures – policy.vu.edu.au.

Manpreet Kaur Grewal	Digitally signed by Manpreet Kaur Grewal Date: 2018.02.18 10:50:38 +11'00'	18.02.2018
Signature		**Date**

3. CO-AUTHOR(S) DECLARATION

In the case of the above publication, the following authors contributed to the work as follows:

The undersigned certify that:

1. They meet criteria for authorship in that they have participated in the conception, execution or interpretation of at least that part of the publication in their field of expertise;
2. They take public responsibility for their part of the publication, except for the responsible author who accepts overall responsibility for the publication;
3. There are no other authors of the publication according to these criteria;
4. Potential conflicts of interest have been disclosed to a) granting bodies, b) the editor or publisher of journals or other publications, and c) the head of the responsible academic unit; and

VICTORIA UNIVERSITY
MELBOURNE AUSTRALIA

5. The original data will be held for at least five years from the date indicated below and is stored at the following **location**(s):

College of Health & Biomedicine
Institute of Sustainable Industries and Liveable cities
Victoria University
Australia

Name(s) of Co-Author(s)	Contribution (%)	Nature of Contribution	Signature	Date
Manpreet Kaur Grewal	80	Concept development, research design, experiment execution, statistical analysis interpretation, drafting manuscript and its revision	Manpreet Kaur Grewal Digitally signed by Manpreet Kaur Grewal Date: 2018.02.22 15:56:18 +11'00'	22 02 2018
Jayani Chandrapala	5	Concept development, support and technical expertise, manuscript revision	Jayani Chandrapala Digitally signed by Jayani Chandrapala DN: cn=Jayani Chandrapala, o=RMIT University, ou=School of Science, email=jayani.chandrapala@rmit.edu.au, c=AU Date: 2018.02.26 08:25:06 +11'00'	26.02. 2018
Osaana Donkor	2	Concept development, manuscript revision	Osaana Donkor Digitally signed by Osaana Donkor DN: cn=Osaana Donkor, o=Victoria University, ou, email=osaana.donkor@vu.edu.au, c=AU Date: 2018.02.26 10:35:54 +11'00'	26.02.2018
Vasso Apostolopoulos	2	Concept development, manuscript revision	[redacted] Digitally signed by Vasso DN: cn=Vasso, o, ou, email=vasso.apostolopoulos@vu.edu.au, c=AU Date: 2018.02.26 10:51:04 +10'00'	26/02/2018
Todor Vasiljevic	9	Concept development, experimental design, manuscript revision	Todor Vasiljevic Digitally signed by Todor Vasiljevic DN: cn=Todor Vasiljevic, o=Victoria University, ou=Advanced Food Systems Research Unit, College of Health and Biomedicine, email=todor.vasiljevic@vu.edu.au, c=AU Date: 2018.03.01 15:47:41 +11'00'	23.02.2018
Lily Stojanovska	2	Concept development, manuscript revision	Lily Digitally signed by Lily Date: 2018.03.01 11:41:20 +11'00'	28.02.2018

International Dairy Journal 66 (2017) 99–107

Contents lists available at ScienceDirect

International Dairy Journal

journal homepage: www.elsevier.com/locate/idairyj

Fourier transform infrared spectroscopy analysis of physicochemical changes in UHT milk during accelerated storage

Manpreet Kaur Grewal [a], Jayani Chandrapala [a], Osaana Donkor [a], Vasso Apostolopoulos [b], Lily Stojanovska [b], Todor Vasiljevic [a, *]

[a] Advanced Food Systems Research Unit, Centre for Chronic Disease, College of Health and Biomedicine, Victoria University, Melbourne, VIC 8001, Australia
[b] Immunology in Chronic Diseases Program, Centre for Chronic Disease, College of Health and Biomedicine, Victoria University, Melbourne, VIC 8001, Australia

ARTICLE INFO

Article history:
Received 25 September 2016
Received in revised form
25 November 2016
Accepted 25 November 2016
Available online 2 December 2016

ABSTRACT

The feasibility of using Fourier transform infrared spectroscopy (FTIR) to detect heat induced conformational rearrangements of proteins, protein–protein and protein–lipid interactions was studied with accelerated shelf-life protocols. Ultra-high temperature treated whole (WM) and skim milk (SM) were stored at 20, 30, 40 and 50 °C for 28 days. The changes leading to increased sedimentation in SM and WM at higher temperatures (≥40 °C) were observed during first 14 days of the storage period. Milk samples stored at 40 and 50 °C showed marked changes in the bands corresponding to conformations of milk lipids and formation of intermolecular β sheet of proteins, indicating protein–lipid interactions and aggregation. Dried sediment contained fat confirming protein–lipid participation in the sedimentation. FTIR was also able to detect changes that led to increased sedimentation in SM at temperatures lower than 40 °C, but only after 28 days.

1. Introduction

UHT treatment of milk (130–140 °C for 3–5 s) followed by aseptic packaging enables its storage at room temperature for up to 9 months (Holland, Gupta, Deeth, & Alewood, 2011). Long shelf life at room temperature has made UHT milk an important food product from nutritional, technological and economical points of view. However, high temperature treatment of milk induces certain chemical and physical changes, which may lead to storage instabilities involving formation of proteinaceous sediment at the bottom of the storage container (sedimentation) or a gel throughout the milk (age gelation) (Dalgleish, 1992; McMahon, 1996; Ramsey & Swartzel, 1984). Sedimentation or gelation limits the shelf life and market potential of UHT milk. Thus, the changes resulting in these instabilities are of concern for the dairy industry.

Physico-chemical changes leading to sedimentation or gelation during storage in UHT milk primarily involve aggregation of milk proteins, which follows different pathways. The most assessed pathway is mediated by denaturation of whey proteins as a result of UHT treatment (Singh, 1991). Denaturation exposes a free sulphydryl group of β-lactoglobulin (β-Lg), which is involved in intramolecular and intermolecular thiol-disulphide exchange reactions with other whey proteins and caseins [κ-casein (κ-CN) and α_{S2}-casein (α_{S2}-CN)] present on the surface of the casein micelles and homogenised fat globules (Sharma & Dalgleish, 1993). Additional crosslinking can also occur via dehydroalanine and advanced Maillard products (AMPs) (Holland et al., 2011).

The aggregation of milk proteins progresses at a slow rate during storage at room temperatures. Studying these changes at this temperature would thus be resource and time consuming. The accelerated shelf life testing methods may be used as an alternative to long realtime analysis as storage temperatures accelerate aggregation of milk proteins. However, in our previous study (Grewal, Chandrapala, Donkor, Apostolopoulos, & Vasiljevic, 2016), protein interactions and especially covalent crosslinking were accelerated at higher storage temperatures but the rate and type of these reactions were different from those at lower temperatures, which was presumably affected by numerous factors due to complex nature of milk. This emphasises detection and prediction under more appropriate and temperate storage conditions more valuable than using elevated storage temperatures. However, acquired knowledge of involvement of individual proteins and kinetics of these

* Corresponding author. Tel.: +61 3 9919 8062.
E-mail address: todor.vasiljevic@vu.edu.au (T. Vasiljevic).

http://dx.doi.org/10.1016/j.idairyj.2016.11.014
0958-6946/

changes determined at high storage temperatures may assist in identifying structural alterations that could be determined by spectral analysis with FTIR.

The development and use of proteomic analysis have added information about different types of prospective crosslinking during storage of UHT milk, but these techniques are still limited in elucidating about the related changes in structure and interactions of proteins (Holland et al., 2011). Furthermore, the sample preparation is fairly laborious accompanied with a complex analysis, all of which require highly trained experts, limiting the application. FTIR spectroscopy could prove to be a simple and fast alternative with minimum sample preparation. FTIR is sensitive to changes in covalent bonding and non-covalent electrostatic and hydrophobic interactions, which are hallmarks of thermal treatment and subsequent storage. This method has been successfully used to study ageing of pharmaceuticals (Masmoudi, Dréau, Piccerelle, & Kister, 2005) and oil in water emulsions (Whittinghill, Norton, & Proctor, 1999) by determination of changes in molecular structure and interactions, but has not been used in UHT milk. Hence, for the first time in the current study, we studied feasibility of the FTIR technique to detect physico-chemical changes leading to sedimentation under accelerated storage temperatures in UHT milk. The focus was only on build-up of sediment and not on gelation because higher storage temperatures ($\geq$40 °C) inhibit age-gelation (Deeth & Lewis, 2016; Kocak & Zadow, 1985; McMahon, 1996) and result in increased non-dispersible sediment (Nieuwenhuijse & van Boekel, 2003).

In addition to storage temperature, fat content of milk also influences certain heat-induced modifications in UHT milk (De Koning, Badings, Van der Pol, Kaper, & Vos-Klompmaker, 1990; Pellegrino, 1994) and the extent of proteolysis during storage (López-Fandiño, Olano, Corzo, & Ramos, 1993). Moreover, milk fat may undergo a phase change and oxidation when stored at elevated temperatures. This necessitated need to study the effect of presence of milk fat in UHT milk on changes leading to development of sediment during storage at elevated storage temperatures.

2. Materials and methods

2.1. Materials

Commercial UHT full cream whole milk (WM) and skim milk (SM) were kindly provided by a local manufacturer (Murray Goulburn Co-operative Co. Ltd., Victoria, Australia). All milk packs were processed as described previously (Grewal et al., 2016). Briefly, both SM and WM packs were produced on the same day using an indirect tubular processor (SPX Flow Technology, Mulgrave, Australia) with a 9000 L h^{-1} capacity at 138 °C for 6 s. The milk was homogenised prior to the heat treatment. The composition of WM as reported by the manufacturer per litre of milk was 33 g protein, 34 g fat and 53 g carbohydrates, 0.55 g Na and 1.2 g Ca. The SM samples contained on average 34 g protein, 1 g fat and 53 g of carbohydrates, 0.55 g Na and 1.2 g Ca per litre of milk. The UHT milk packs were stored at room temperature (20 °C) and 3 elevated temperatures (30, 40 and 50 °C) for 28 d in incubators (Thermoline Scientific Pty Ltd, Wetherill Park, NSW, Australia). The elevated storage temperature served to accelerate the development of storage instabilities. Milk packs were analysed on the first day of delivery (day 0), and then at two fortnightly intervals (14 and 28 days) during storage.

2.2. Measurement of sediment

Sedimentation was measured by a centrifugation method as previously described (Boumpa, Tsioulpas, Grandison, & Lewis, 2008) with slight modifications. Briefly, the milk packs were manually shaken to mix the contents and approximately 40 g was centrifuged at 2760× *g* for 15 min at 20 °C (Beckman Coulter Avanti J-26S XP Centrifuge, CA, USA). The sediment was then oven-dried at 50 °C for 48 h to a constant weight and expressed as the amount of sediment (mg 100 g^{-1} milk).

2.3. Fourier transform infrared spectroscopy

Three milk packs corresponding to each storage time and temperature were placed at room temperature (20 °C) and equilibrated for 6 h. After mixing the content, exactly 0.5 mL of sample was pipetted from each pack separately onto attenuated total reflectance (ATR) cell. Sample spectra were acquired using PerkinElmer Frontier Fourier transform infrared spectroscopy (FTIR) spectrometer (PerkinElmer, MA, USA) in the range 4000–600 cm^{-1} with a resolution of 4 cm^{-1} and by averaging 16 scans of each spectrum. Background spectrum was scanned at the beginning of the measurements with a blank Diamond ATR cell using same instrumental conditions as for sample spectra acquisition. The spectra of three sub samples of each sample were taken by refilling the ATR cell. Spectra of dried SM and WM sediments were also acquired to estimate composition of sediment.

2.4. Data analysis with statistics

The FTIR spectra of all samples were exported to the Unscrambler software (version 9.8; CAMO AS, Trondheim, Norway). The quality of the spectra was confirmed using their descriptive statistics (Jaiswal et al., 2015) and visual inspection. This allowed for selection of appropriate pre-processing treatments to account for variations due to baseline shifts, sample concentration on the cell or any factor other than intrinsic variations in the sample. A multivariate analysis technique, principal component analysis (PCA), was then employed to ascertain classifications in UHT milk samples as function of storage time and temperature. The principal component analysis (PCA) technique gives an overview of all the information in the data set by generating a new set of fewer coordinate axes called principal components (PCs) with minimum loss of information. Score plots obtained following PCA demonstrate groupings whereas loading plots help to identify wavenumbers which have high loadings or contributed the most in classification of samples into different groups.

The sediment dry weight data corresponding to all determinations was analysed using a GLM (Generalized Linear Model) procedure of SAS software (SAS Institute, 1996). The effects of main factors (type of milk, storage time and temperature) and interactions were analysed in a split plot in time design at pre-set level of significance $P < 0.05$. The design was replicated 3 times.

3. Results and discussion

3.1. Sediment formation

Fat content along with storage temperature influenced the extent of sedimentation. In WM, the amount of formed sediment did not increase substantially at 20 and 30 °C during storage, whereas after 28 d storage at 40 and 50 °C sediment surged by 28.6% and 41.3%, respectively. On the other hand, sedimentation increased significantly in SM during storage irrespective of storage temperature. SM had lower ($P < 0.05$) amount of sediment on day 0 than WM; however, when stored at 20 and 30 °C, no significant difference in sedimentation was observed between two types of milk after 28 d storage. However, at

temperatures ≥40 °C, the amount of sediment formed in WM after 28 days of storage was significantly ($P < 0.05$) higher than that in SM (Table 1).

The substantial increase in the amount of sediment in WM at elevated temperatures (40 and 50 °C) was accompanied by an increase in appearance of high molecular mass aggregates (Grewal et al., 2016). This was attributed primarily to change in protein–lipid interactions as a result of melting of milk fat at 40 °C. Change of physical state of milk lipids results in changed conformation and packing of constituent phospholipid and triglyceride acyl chains (Boubellouta & Dufour, 2012; Karoui, Mazerolles, & Dufour, 2003), which might have enhanced protein–lipid associations in milk at higher storage temperatures resulting in aggregate formation. Presence of lipid absorbance regions in FTIR spectra (3000–2800 cm^{-1}, 1800–1700 cm^{-1}, Fig. 1B, insert b) of the sediment in WM evidenced that protein–lipid interactions participated in the sediment formation as the fat precipitated along with the proteins. Furthermore, increased intensity of lipid region in dried sediments of WM samples stored at 50 °C compared with those at 20 °C indicated that protein–lipid associations were enhanced by elevated storage temperature resulting in a greater complexation and consequently precipitation. In addition to enhanced protein–lipid interactions, the increase in the amount of aggregates in WM at higher temperatures (Grewal et al., 2016) was also attributed to protein crosslinking via lipid oxidation products, advanced Maillard products and dephosphorylated residues. Additionally, elevated absorbance of the fat region in the sediment of WM obtained at 20 °C (Fig. 1B) could also encounter for a higher amount of sediment on day 0 compared with that in SM. Upstream homogenisation results in dispersion of fat globules, which would be covered primarily with caseins, thus increasing the density of fat globules (Lee & Sherbon, 2002). UHT heating on the other hand enhances association of denatured whey proteins with caseins and phospholipids and lipoproteins on the fat globule surface (Sharma & Dalgleish, 1994), which consequently further increases the density of fat globules (Nieuwenhuijse & van Boekel, 2003). Inclusion of these modified fat globules with greater density into aggregates leads to enlargement of the particles and subsequently enhanced sedimentation, which is in accordance with the Stokes' law (Walstra, Jenness, & Badings, 1984).

Similarly, the rise in the amount of sediment in SM at higher temperature could also be associated with protein–lipid association as evidenced by absorbance regions of fat in FTIR spectra of the sediment (Fig. 1A). However, the noticeable changes in the amount of sediment at temperatures below 40 °C in SM point out at pronounced protein–protein interactions in comparison with those in WM. Comparably diminished association of denatured β-Lg to κ-casein on the surface of the casein micelle in SM in comparison with that in WM (Garcia-Risco, Ramos, & Lopez-Fandino, 1999) enhances availability of β-Lg for crosslinking reactions. This protein exhibits greater reactivity than caseins for formation of links via non-covalent, disulphide and non-disulphide covalent bonding (Grewal et al., 2016) likely due to their denaturation as a consequence of heat treatment. Denaturation results in exposure of hydrophobic regions, free thiol groups and preferable amino acid residues like lysine, asparagine, and glutamine, which subsequently participate in lactosylation and linking via dehydroalanine to caseins (Andrews, 1975; Donato & Guyomarc'h, 2009; Henle, Schwarzenbolz, & Klostermeyer, 1996; Holland et al., 2011). In addition, a high proportion of β-Lg present at the surface of the casein micelles and fat globule in WM also reduces access of proteinases and hence the degree of proteolysis. Fat in WM appears to have a protective effect against enzymatic attack in UHT milk (Datta, Elliott, Perkins, & Deeth, 2002).

From the observations above, it appears that changes in protein–lipid and protein–protein interactions during storage govern sediment formation in the SM and WM samples. Precise identification and prediction of these changes in a shorter time under accelerated conditions could save substantial waiting time to establish sediment formation visually. Therefore, feasibility of FTIR to detect these changes was assessed.

3.2. Fourier transform infrared spectroscopy

The spectra of SM and WM were predominated by absorption bands of water in regions 3500–3000 cm^{-1} (H–O stretching) and 1730–1600 cm^{-1} (H–O–H bending vibration) (Iñón, Garrigues, & de la Guardia, 2004). This was overcome by subtraction of water spectra from milk spectra after correcting for baseline offsets. Important spectral regions of milk spectra were 3700–2800 cm^{-1} (Region I), 1800–1700 cm^{-1} (Region II), 1700–1500 cm^{-1} (Region III), 1500–1200 cm^{-1} (Region IV) and 1200–900 cm^{-1} (Region V) (Fig. 2). These regions have been previously attributed to different milk components (Table 2). Multivariate analysis (PCA) was then employed to establish whether FTIR spectra could detect changes that lead to formation of sediment at different temperatures during storage of SM and WM.

3.3. Principal component analysis

PCA was performed in the regions 4000–600 cm^{-1} (full range) separately for SM and WM samples. In SM, PC 1 and PC 2 explained 78% and 20% of the variance, respectively (Fig. 3a). In WM (Fig. 4a), first two principal components explained 81% and 17% of the variance respectively. In both SM and WM first two PCs classified samples into three separate groups, named A, B and C. In skim milk, group A comprised day 28 samples stored at 20, 30, 40 and 50 °C, group B included day 14 samples stored at 40 and 50 °C and group C constituted samples of day 0 (stored at 20 °C) and day 14 samples stored at 20 and 30 °C. Grouping of SM samples stored for 28 days at 20 and 30 °C with those stored above 40 °C implied that FTIR was also able to detect changes that lead to increased sedimentation in SM even at temperatures below 40 °C. However, in WM, group A was comprised only of day 28 samples stored at and above 40 °C,

Table 1
Effect of milk type (skim or whole milk), time and temperature on amount of sediment (insoluble precipitates) formed in UHT.[a]

Temperature (°C)	Storage time (d)							
	Skim milk				Whole milk			
	0	7	21	28	0	7	21	28
20	52.5[a]	68.8^{bA}	90.1^{cA}	96.8^{deA}	93.6^{ecd}	105.4^{deA}	99.9^{cdeA}	105.6^{cdeA}
30	–	63.1^{bA}	95.0^{cA}	99.4^{dA}	–	99.4^{ecdA}	92.0^{ecdA}	104.3^{ecdA}
40	–	67.1^{bA}	93.1^{cA}	92.4^{dA}	–	108.9^{eA}	101.2^{ecdA}	120.4^{fB}
50	–	69.4^{bA}	106.4^{cB}	101.7^{cA}	–	122.5^{dB}	119.7^{dB}	132.3^{eB}

[a] Values (mg 100 g^{-1} milk; SEM 4.32) are means; means in the same row and in the same column that do not share the same lowercase and uppercase letters, respectively, differ ($P < 0.05$).

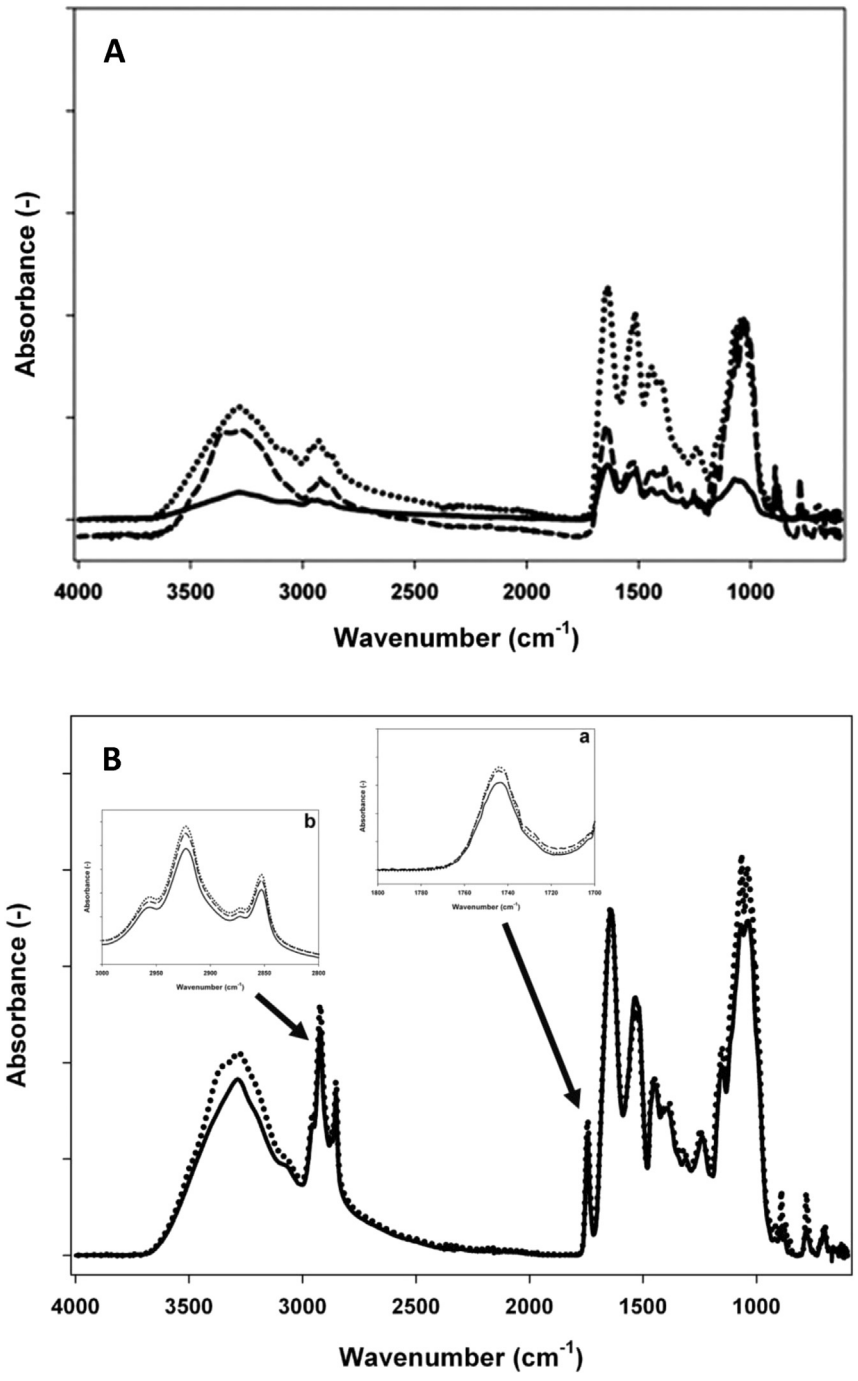

Fig. 1. FTIR of dried sediment on day 0 and day 28 of UHT (A) skim milk and (B) whole milk samples stored at 20 °C and 50 °C. The solid, dashed and dotted line indicate the initial absorbance (day 0), absorbance after 28 d storage at 20 °C and absorbance after 28 d storage at 50 °C, respectively. The inserts (a) and (b) in panel B illustrate differences in the fat A (1800–1700 cm^{-1}) and the fat B region (3000–2800 cm^{-1}) in UHT whole milk, respectively.

group B included day 14 samples stored at 40 and 50 °C and group C constituted samples of day 0 (stored at 20 °C), day 14 and day 28 stored at 20 and 30 °C. Hence, the changes in FTIR spectra were in accord with changes observed in the sediment in both SM and WM.

All prominent regions observed in milk spectra (Fig. 2) contributed to the classification of samples into three groups in both SM and WM according to the loading plot (Figs. 3b & 4b). To further investigate changes in which specific wavenumbers in these regions mainly contributed to different classification in SM and WM, PCA was performed independently for regions I–V.

3.3.1. Region I: 3700–2800 cm^{-1}

This region registered substantial changes and was able to classify samples into three different groups in both SM (Fig. 3c) and WM (Fig. 4c). According to the loading plots (Figs. 3d & 4d), milk samples were separated along PC 1 with high loading for 3594 cm^{-1} and 3193–3194 cm^{-1} (hydrogen bonded O–H stretching), 2926 cm^{-1} (asymmetric stretching modes of CH_2 groups of acyl chains of milk lipids) and 2857 cm^{-1} (symmetric stretching modes of CH_2 groups of acyl chains of triglycerides and phospholipids). The presence of group B (day 14, 40 and 50 °C samples) in-

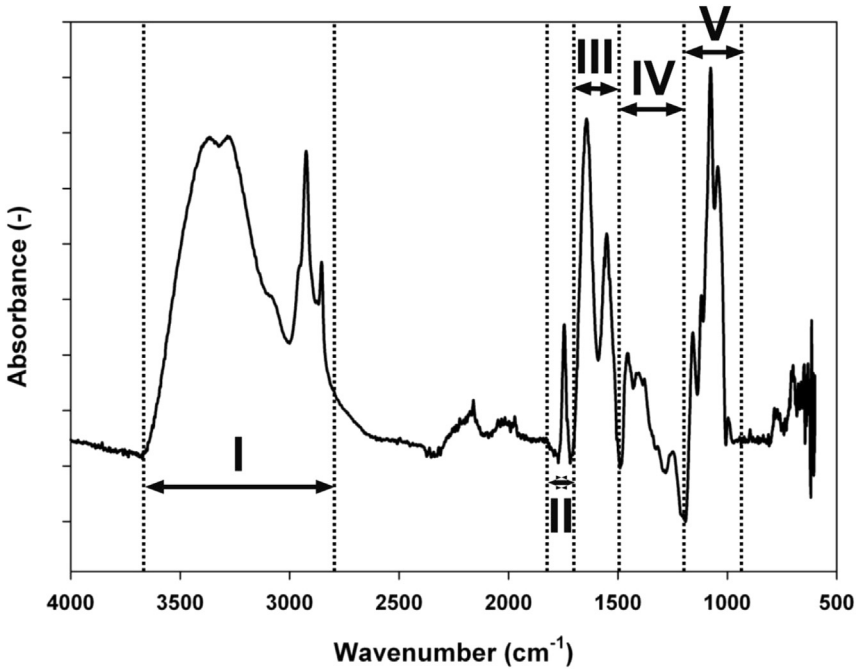

Fig. 2. FTIR spectra of UHT whole milk on day 0 of storage in the range 4000–600 cm^{-1} with annotated regions of interest (I–V).

Table 2
Milk components attributed to different regions of FTIR spectra.

IR region (cm^{-1})	Milk component	Reference
3000–2800	Milk lipids (Fat B)	Iñón et al. (2004)
1800–1700	Milk lipids (Fat A)	Iñón et al. (2004)
1700–1600	Milk proteins-amide I	Karoui et al. (2003); Murphy et al. (2014)
1600–1500	Milk proteins-amide II	Karoui et al. (2003)
1500–1200	Milk proteins-amide III, interactions between different milk components (Fingerprint region)	Anderle and Mendelsohn (1987); Kher et al. (2007)
1200–900	Milk minerals; milk fat, lactose (Fingerprint region)	Zhou et al. (2006); Gebhardt et al. (2011); Kher et al. (2007)

between group C and group A indicated progression of intensity changes of above wavenumbers with storage time.

After 28 d, WM samples stored at and above 40 °C and SM samples at all temperatures, a shift was observed in a band corresponding to a O–H stretch to higher wavenumbers resulting in depression around 3194 cm^{-1} in spectra upon water subtraction (Fig. 5A). Extent of hydrogen bonding (water related) decreases with increase in storage temperature, which shifts the O–H stretching frequency to higher wavenumbers (Choperena & Painter, 2009). On the same note, higher negative loading for 3594 cm^{-1} was concomitant with less positive loading at 3194 cm^{-1} in group A samples compared with group C. However, this did not explain the change in hydrogen bonding in SM even at 20 °C.

In WM, group A also experienced decrease in loadings for 2926 and 2857 cm^{-1} with storage time (Fig. 4d). The shift in these wavenumbers has been used previously to study phase transition of phospholipids (sol to gel state transition) with increase in temperature (Dufour et al., 2000). Milk fat melts around 40 °C which in turn results in prominent structural changes and interactions of milk lipids (Dufour et al., 2000). These changes led to protein–lipid interactions indicated by reduction in the absorbance intensities (Fig. 5A) and lower loading for group A as compared to group C samples (Fig. 4d). Even though, the peaks corresponding to wavenumbers 2926 and 2857 cm^{-1} were not visible in a loading plot of region I in SM (Fig. 3d), the fat B region (3000–2800 cm^{-1}) was independently able to classify samples into three groups A, B and C. Therefore, enhanced protein–lipid associations accounted for greater sedimentation observed at all storage temperatures in SM (Table 1). Increase in intensity of fat B region in sediment of SM samples stored at 20 °C (Fig. 1A) further supported this suggestion.

3.3.2. Region II: 1800–1700 cm^{-1}

Region II, attributed to milk fat A, classified storage samples into three groups in both SM (Fig. 3e) and WM (Fig. 4e). In WM, according to the loading plot (Fig. 4f), PC 2 separated group B samples from group C whereas group A samples were further separated from group B samples by PC 1. Samples stored above 40 °C after 14 days (group B) had higher loading mainly for 1701–1708, 1728 and 1747–1757 cm^{-1}. Loading plot of PC 1 revealed further increase in 1749–1755, 1786–1789, 1774 and 1796–1798 cm^{-1} for samples stored above 40 °C after 28 d (group A). In SM, group A (day 28 samples corresponding to all storage temperatures), B (day 14 samples at ≥40 °C) and C (day 0 and day 14 (20 and 30 °C) samples) were separated along PC 2. The loading plot of PC 2 in SM (Fig. 3f) indicated higher loading for group A samples for 1718 and 1734–1736 cm^{-1} in addition to wavenumbers mentioned in WM.

The flattening of peak around 1754 cm^{-1} (Fig. 5B) corresponds to changes in C=O stretching vibrations of ester linkage pertaining to triacylglycerols (Karoui et al., 2003). Changes in physical state of lipids at and above 40 °C also affected carbonyl stretching vibrations of ester linkage of triacylglycerols. Changes in stretching of ester linkage might be also due to protein–lipid association via

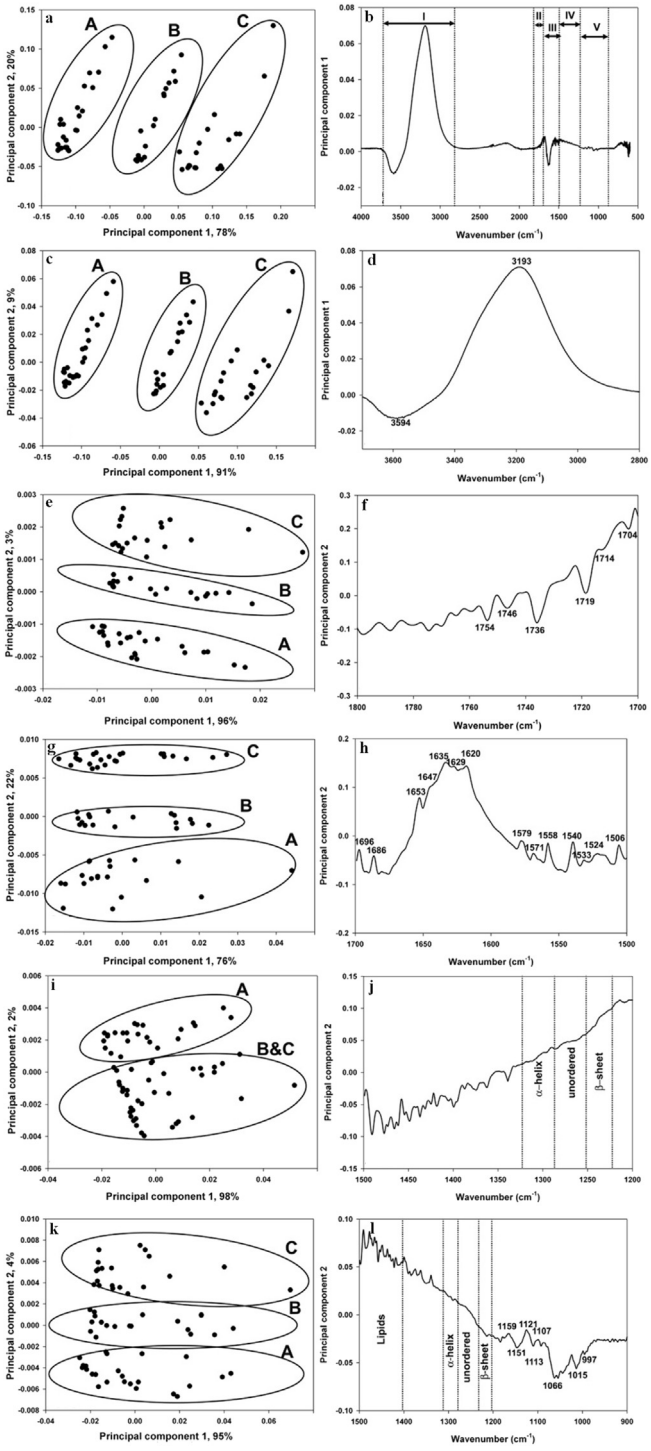

Fig. 3. Principal component scores and loading plots of spectra of UHT skim milk samples acquired at 0, 14 or 28 days storage at different temperatures for: spectral range 4000–600 cm^{-1} (a, b); region I, 3700–2800 cm^{-1} (c, d); region II, 1800–1700 cm^{-1} (e, f); region III, 1700–1500 cm^{-1} (g, h); region IV, 1500–1200 cm^{-1} (i, j); region V, 1500–900 cm^{-1} (k, l). Group A, day 28 samples stored at 20 °C, 30 °C, 40 °C and 50 °C; group B, day 14 samples stored at 40 and 50 °C; group C, day 0, day14 (20 °C and 30 °C) and day 28 (20 °C and 30 °C) samples.

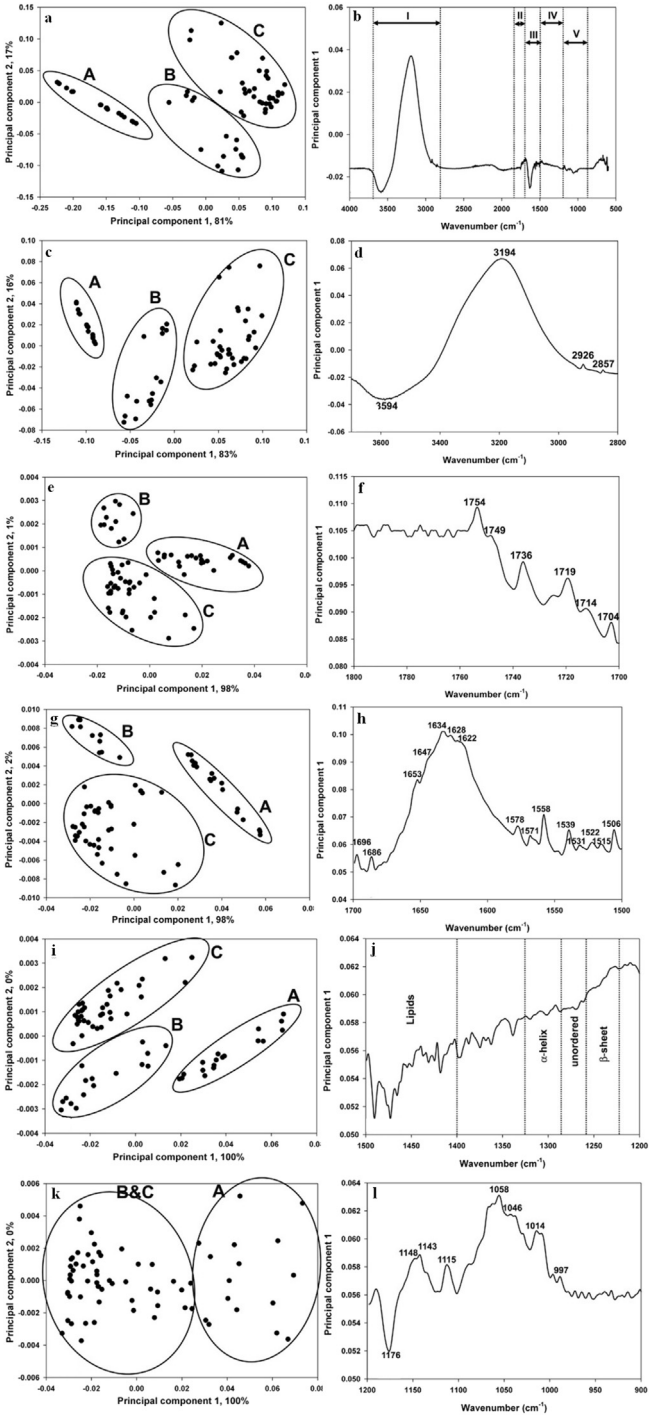

Fig. 4. Principal component scores and loading plots of spectra of UHT whole milk packs acquired at 0, 14 and 28 days storage at different temperatures for: spectral range 4000–600 cm^{-1} (a, b); region I, 3700–2800 cm^{-1} (c, d); region II, 1800–1700 cm^{-1} (e, f); region III, 1700–1500 cm^{-1} (g, h); region IV, 1500–1200 cm^{-1} (i, j); region V, 1200–900 cm^{-1} (k, l). Group A, day 28 samples stored at 40 °C and 50 °C; group B, day 14 samples stored at 40 °C and 50 °C; group C, day 0, 14 and 28 (20 °C and 30 °C) samples.

carbonyl groups (Surewicz, Moscarello, & Mantsch, 1987). Higher loading around 1720 cm^{-1} (Fig. 5B) has been associated previously with presence of hydrogen bonded carbonyl groups of esters (Dufour & Riaublanc, 1997). In addition, wavenumbers 1720 and 1715 cm^{-1} has also been assigned to C═O stretching vibration of aldehydes and ketones, respectively. AMPs and lipid oxidation products participate in crosslinking of proteins at higher temperatures due to presence of aldehyde and ketone functional groups (Harty-Major, 1997). Thus, higher loading for 1720 and 1715 cm^{-1} for group A and B (Fig. 5B) implies an elevated content of AMP and oxidation products in SM and WM samples stored at higher

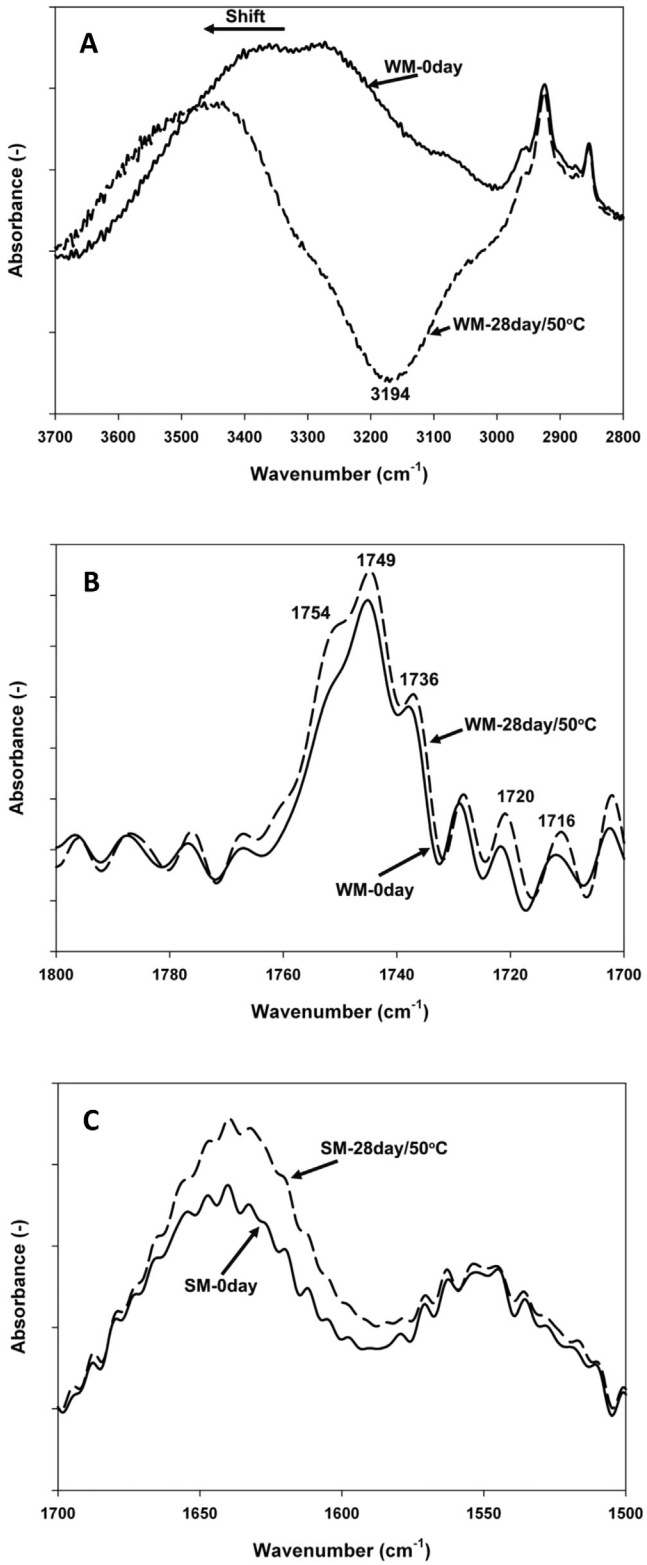

Fig. 5. FTIR spectra of UHT whole milk in the region 3700–2800 cm^{-1} (A) and 1800–1700 cm^{-1} (B) and UHT skim milk in the region 1700–1500 cm^{-1} (C).

temperatures with storage time, which in addition to enhanced lipid–protein associations, could further influence the rate of sedimentation at higher temperatures. However, this explanation could not address higher sedimentation in SM at ≤40 °C and hence requires further study.

3.3.3. Region III: protein (amide I and amide II) 1700–1500 cm^{-1}

Classification of storage samples into groups A, B and C by this region in a similar way as discussed above in SM (Fig. 3g) and WM (Fig. 4g) implies changes in the protein secondary structure, protein–protein and protein–lipid interactions at elevated storage temperature in WM and at all storage temperatures in SM (Karoui et al., 2003; Mendelsohn, Mao, & Flach, 2010; Sankaram & Marsh, 1993). The region III has two main parts, namely amide I (1700–1600 cm^{-1}) corresponding to C=O stretching vibrations of the peptide bonds and amide II (1600–1500 cm^{-1}) attributed to C–N stretching vibrations in combination with N–H bending (Kher, Udabage, McKinnon, McNaughton, & Augustin, 2007).

In WM, group A and B samples separated from group C samples due to increase in loading principally for 1696, 1686, 1653, 1647, 1634, 1628 and 1622 cm^{-1} (amide I); 1578, 1571, 1558, 1539, 1531, 1522, and 1515 cm^{-1} (amide II) (Fig. 4h). However in SM, sample group A and B separated due to rise in almost identical wavenumbers apart from a shift in 1628 cm^{-1} and amide II wavenumbers (Fig. 3h). The shift was also observed in spectra of this region for SM (Fig. 5C).

The increase in loading at 1697, 1686 and 1618 cm^{-1} suggested formation of aggregates consisting of intermolecular β sheets (Mendelsohn & Flach, 2002; Mendelsohn et al., 2010; Ngarize, Herman, Adams, & Howell, 2004). In addition, surge in loading around 1620–1618 cm^{-1} had also been attributed to disruption of intramolecular hydrogen bonds within a secondary structure, leading to formation of new stronger intermolecular hydrogen bonds (Ngarize et al., 2004). However, unlike previously reported (Murphy, Fenelon, Roos, & Hogan, 2014), increase in intermolecular β sheets (1686 and 1618 cm^{-1}) in the current study was not concomitant with decline in α-helix (1653 cm^{-1}) and intramolecular β sheet structure (1630–1627 cm^{-1}). It appeared that though there was an enhancement in intermolecular interactions leading to the aggregation, it was not at expense of intramolecular interactions. It can also be argued that amide I vibration could not distinguish clearly between α-helical and random-coil structures (Anderle & Mendelsohn, 1987), and thus, increase at 1653 cm^{-1} might also correspond to increase in random coil structure. Moreover, increase in random coil (1645 cm^{-1}) and turns (1676 cm^{-1}) could also be associated with increased participation of caseins in formation of aggregates. In addition to increase in protein–protein interactions, protein–lipid interactions initiated by change in physical state of milk fat at higher storage temperature in WM, induce formation of intermolecular hydrogen bonded β sheets resulting in protein aggregation (Sankaram & Marsh, 1993).

Schiff base intermediates formed during the course of Maillard browning have been reported to absorb at 1647 cm^{-1} (Murphy et al., 2014). Increase in intensity at 1647 cm^{-1} in both SM and WM in Group A and B samples suggests that lactosylation could be one of the confounding factors (Figs. 3h & 4h). Interestingly, absorbance at 1647 cm^{-1} was higher for SM than WM supporting higher rate of Maillard reaction in former as suggested in our previous study (Grewal et al., 2016). However, it would be interesting to explore reasons for lactosylation rates to be higher in SM samples even at 20 °C.

In amide II region, a band around 1575 cm^{-1} (Figs. 3h & 4h) has been used previously as a marker for start of acidification in cheese ripening process with formation of lactates (Mazerolles et al., 2001). In the current study, a band appearing at 1577 cm^{-1} may be caused by a slight pH decline during storage (data not shown). Peaks at 1571 cm^{-1} arose from the $-COO^{-}$ asymmetric stretching vibration of Asp and Glu residues, and an increase in its loading might be due to deamidation of amino acid residues observed during storage at elevated temperatures in UHT milk (Holland et al., 2011). Higher loading for 1571 cm^{-1} in group A samples in WM

compared to those in SM (Figs. 3h & 4h) indicated that the former had experienced a greater extent of deamidation than the later. Loading peak at 1515 cm^{-1} indicates changes in ring-stretching vibration of the tyrosine residues which could be further related to their oxidation and crosslinking. Loadings for wavenumbers in 1578–1555, 1555–1543 and 1542–1525 cm^{-1} region had also been attributed to changes in amount of β turns, alpha helices/loops and β sheets, respectively (Curley, Kumosinski, Unruh, & Farrell, 1998).

3.3.4. Region IV: protein (amide III) 1500–1200 cm^{-1}

Amide III spectral region also corresponds to secondary structure of proteins. Although having relatively weak signals in contrast to most commonly used amide I region (1700–1600 cm^{-1}), amide III does not suffer from several limitations including a strong interference from water vibrational band, relatively unstructured spectral contour and overlap of revolved bands correspondingly to various secondary structures (Fu, Deoliveira, Trumble, Sarkar, & Singh, 1994). The peaks in this region correspond to N–H bending and C–N stretching vibrations (Jaiswal et al., 2015) and also to CH_2 scissoring of acyl chains of lipids (Mendelsohn et al., 2010).

The region classified samples into three groups A, B and C only in WM samples (Fig. 4i). In SM, only group A was separated from the combined cluster consisting of group B and C (Fig. 3i). Lower amount of fat in SM may be one of the major factors explaining the classification of SM samples into 2 groups only by this region unlike 3 distinctively different groups in WM. Furthermore, lower loadings for CH_2 scissoring of acyl chains of lipids (1500–1400 cm^{-1}) (Figs. 3j & 4j) in group A samples could also be assigned to enhanced associations between proteins and lipids with increase in storage time and storage temperature in SM and WM, respectively. This could imply that milk fat and its content play a role in storage stability of UHT milk.

Highest loading for the secondary structure frequency windows (unordered, 1288–1256 cm^{-1} and β-sheets, 1255–1224 cm^{-1}) for group A samples in both SM and WM (Figs. 3j & 4j) further stressed on formation of β sheet and greater participation of caseins in protein aggregation and consequently sedimentation. Lower loading for group A samples for α-helix (1328–1289 cm^{-1}) still could not fully support concomitance of increase in β-sheet conformation related to protein aggregation with decline in α-helical structure as reported previously (Murphy et al., 2014; Qi et al., 1997). Furthermore, presence of a large number of observed bands in the loading plot obscured finding a particular difference between SM and WM. In addition, the slight variations in helical geometry, symmetry or interactions result in changed amide III frequencies, so, simple correlations between narrow frequency ranges and secondary structures may not be applicable for this mode (Anderle & Mendelsohn, 1987).

3.3.5. Region V: 1200–900 cm^{-1}

This region was able to classify samples into two groups (A and combined B & C) only in WM (Fig. 4k). The SM samples were not able to be separated into different groups. However, when PCA was applied for combined Region IV and V in SM, it clearly separated samples into three groups A, B and C as defined previously (Fig. 3k).

Loading plot in WM indicated high loading for 1176, 1148, 1143, 1115, 1058, 1046, 1014 and 997 cm^{-1}, which separated group A samples from the remaining two groups (Fig. 4l). In this region, a peak around 1159 cm^{-1} has been previously associated with C–O vibrations of milk fat (Zhou et al., 2006). As discussed earlier, the milk fat was sensitive to high storage temperatures governing the extent of protein–lipid associations, which resulted in greater sedimentation in WM. Low fat content might have reduced the signal which could have resulted in no separation in SM when only region between 1200 and 900 cm^{-1} was considered.

The area between 1250 and 800 cm^{-1} embodies characteristic peaks of various C–O vibrations in carbohydrates, mainly lactose (Zhou et al., 2006). It was expected from earlier observations that due to higher amount of AMP in SM, the chemical changes accompanying the Maillard reaction would lead to several changes in its mid-infrared spectrum. However, the inability of the region to classify samples in SM implied that changes as a result of Maillard reactions were not intense enough to be detected by FTIR. Maillard reactions principally involve the consumption of NH_2 functional groups typically from lysine with the appearance of other new functional groups such as the Amadori compound (C=O), Schiff base (C=N), and pyrazines (C–N). Even though lactose is present in a high concentration, it is only depleted by a small margin via the Maillard reactions due to absence of sufficient reactive amino groups. Lysine, one of the predominant reacting amino acid in proteins and because of the reactivity and availability of its amino group, comprises less than 0.25% by mass of SM. Subsequently, the concentration of the reaction products would be relatively low. In addition, reactants and products would share many functional groups, thus any changes may not be detectable (Turner et al., 2002).

Bands around 995 and 987 cm^{-1} suggested changes in stretching vibrations of $-PO_3^{2-}$ moiety of the serine-phosphate residue. The appearance of the two bands had been earlier related to release of colloidal calcium phosphate (CCP) from the phosphate residues by pressure and its dissociation into Ca^{2+} and HPO_4^{2-}, resulting in an increased negative charge of the casein molecules (Gebhardt, Takeda, Kulozik, & Doster, 2011). In our study, this may be related to heat-induced elimination of phosphate from phosphoserine residues in caseins producing dehydroalanine, which subsequently reacts with amino group of lysine residues, imidazole group of histidine or thiol group of cysteine resulting in intra- or intermolecular lysinoalanine, histidinoalanine or lanthionine crosslinks, respectively (Holland et al., 2011). It may also imply dissociation of CCP expressed as increase in ionic calcium observed during storage (data not shown). However, this aspect requires further investigation.

4. Conclusions

FTIR detected changes in samples stored at and above 40 °C within 14 days. This suggested that it may take even less than 14 days to detect significant changes using FTIR spectroscopy when applying accelerated storage stability testing. In addition, it appeared that changes in structure and interactions of milk lipids propelled the separation of samples according to storage temperatures and time in both SM and WM. Next major contribution to the classification of storage samples was from changes in the protein structure and associated interactions. Increase in sediment was correlated with increase in intermolecular β sheet formation. In addition changes in proteins and carbohydrates due to Maillard reaction were present but were less intense likely due to the duration of storage study. In addition, to fully establish the reasons related in changes in SM, but not in WM at 20 and 30 °C, which resulted in enhanced sedimentation, requires a long term study. The extension of storage time would also enable detection of specific markers, which can then be employed for prediction of shelf life of UHT milk via spectral analysis.

Acknowledgements

This work was supported by the Department of Business and Innovation of the Victorian Government, through its Victoria India

Doctoral Scholarship Program (managed by the Australia India Institute). The first author also acknowledges her employer Indian Council of Agricultural Research for granting study leave to pursue Ph.D.

References

Anderle, G., & Mendelsohn, R. (1987). Thermal denaturation of globular proteins. Fourier transform-infrared studies of the amide III spectral region. *Biophysical Journal, 52*, 69–74.

Andrews, A. (1975). Properties of aseptically packed ultra-high-temperature milk: III. Formation of polymerized protein during storage at various temperatures. *Journal of Dairy Research, 42*, 89–99.

Boubellouta, T., & Dufour, É. (2012). Cheese-matrix characteristics during heating and cheese melting temperature prediction by synchronous fluorescence and mid-infrared spectroscopies. *Food and Bioprocess Technology, 5*, 273–284.

Boumpa, T., Tsioulpas, A., Grandison, A. S., & Lewis, M. J. (2008). Effects of phosphates and citrates on sediment formation in UHT goats' milk. *Journal of Dairy Research, 75*, 160–166.

Choperena, A., & Painter, P. (2009). Hydrogen bonding in polymers: Effect of temperature on the OH stretching bands of poly(vinylphenol). *Macromolecules, 42*, 6159–6165.

Curley, D. M., Kumosinski, T. F., Unruh, J. J., & Farrell, H. M. (1998). Changes in the secondary structure of bovine casein by Fourier transform infrared spectroscopy: Effects of calcium and temperature. *Journal of Dairy Science, 81*, 3154–3162.

Dalgleish, D. G. (1992). Sedimentation of casein micelles during the storage of ultra-high temperature milk products—a calculation. *Journal of Dairy Science, 75*, 371–379.

Datta, N., Elliott, A. J., Perkins, M. L., & Deeth, H. C. (2002). Ultra-high-temperature (UHT) treatment of milk: Comparison of direct and indirect modes of heating. *Australian Journal of Dairy Technology, 57*, 211–227.

De Koning, P. J., Badings, H. T., Van der Pol, J. J. G., Kaper, J., & Vos-Klompmaker, E. A. J. (1990). Effect of heat treatment and fat content on the properties of UHT-milk. *Voedingsmiddelentechnologie, 23*, 11–14.

Deeth, H., & Lewis, M. (2016). Protein stability in sterilised milk and milk products. In P. L. H. McSweeney, & J. A. O'Mahony (Eds.), *Advanced dairy chemistry. Vol. 1B. Applied aspects* (4th ed., pp. 247–286). New York, NY, USA: Springer.

Donato, L., & Guyomarc'h, F. (2009). Formation and properties of the whey protein/$\ kappa $-casein complexes in heated skim milk—A review. *Dairy Science and Technology, 89*, 3–29.

Dufour, E., Mazerolles, G., Devaux, M. F., Duboz, G., Duployer, M. H., & Mouhous Riou, N. (2000). Phase transition of triglycerides during semi-hard cheese ripening. *International Dairy Journal, 10*, 81–93.

Dufour, E., & Riaublanc, A. (1997). Potentiality of spectroscopic methods for the characterisation of dairy products. II. Mid infrared study of the melting temperature of cream triacylglycerols and of the solid fat content in cream. *Lait, 77*, 671–681.

Fu, F.-N., Deoliveira, D. B., Trumble, W. R., Sarkar, H. K., & Singh, B. R. (1994). Secondary structure estimation of proteins using the amide III region of fourier transform infrared spectroscopy: Application to analyze calcium-binding-induced structural changes in calsequestrin. *Applied Spectroscopy, 48*, 1432–1441.

Garcia-Risco, M. R., Ramos, M., & Lopez-Fandino, R. (1999). Proteolysis, protein distribution and stability of UHT milk during storage at room temperature. *Journal of the Science of Food and Agriculture, 79*, 1171–1178.

Gebhardt, R., Takeda, N., Kulozik, U., & Doster, W. (2011). Structure and stabilizing interactions of casein micelles probed by high-pressure light scattering and FTIR. *The Journal of Physical Chemistry B, 115*, 2349–2359.

Grewal, M. K., Chandrapala, J., Donkor, O., Apostolopoulos, V., & Vasiljevic, T. (2016). Electrophoretic characterization of protein interactions suggesting limited feasibility of accelerated shelf life testing of UHT milk. *Journal of Dairy Science*. http://dx.doi.org/10.3168/jds.2016-11278 [In press].

Harty-Major, S. (1997). *Investigation of the chemistry of 1-hydroxyacetone by Fourier transform infrared spectroscopy* (MSc thesis). Motreal, QC, Canada: McGill University.

Henle, T., Schwarzenbolz, U., & Klostermeyer, H. (1996). Irreversible crosslinking of casein during storage of UHT-treated skim milk. In *Heat treatments and alternative methods. IDF symposium (6–8 Sep 1995), Vienna, Austria*.

Holland, J. W., Gupta, R., Deeth, H. C., & Alewood, P. F. (2011). Proteomic analysis of temperature-dependent changes in stored UHT milk. *Journal of Agricultural and Food Chemistry, 59*, 1837–1846.

Iñón, F. A., Garrigues, S., & de la Guardia, M. (2004). Nutritional parameters of commercially available milk samples by FTIR and chemometric techniques. *Analytica Chimica Acta, 513*, 401–412.

Jaiswal, P., Jha, S. N., Borah, A., Gautam, A., Grewal, M. K., & Jindal, G. (2015). Detection and quantification of soymilk in cow–buffalo milk using Attenuated Total Reflectance Fourier Transform Infrared spectroscopy (ATR–FTIR). *Food Chemistry, 168*, 41–47.

Karoui, R., Mazerolles, G., & Dufour, É. (2003). Spectroscopic techniques coupled with chemometric tools for structure and texture determinations in dairy products. *International Dairy Journal, 13*, 607–620.

Kher, A., Udabage, P., McKinnon, I., McNaughton, D., & Augustin, M. A. (2007). FTIR investigation of spray-dried milk protein concentrate powders. *Vibrational Spectroscopy, 44*, 375–381.

Kocak, H. R., & Zadow, J. G. (1985). Age gelation of UHT whole milk as influenced by storage temperature. *Australian Journal of Dairy Technology, 40*, 14–21.

Lee, S. J., & Sherbon, J. W. (2002). Chemical changes in bovine milk fat globule membrane caused by heat treatment and homogenization of whole milk. *Journal of Dairy Research, 69*, 555–567.

López-Fandiño, R., Olano, A., Corzo, N., & Ramos, M. (1993). Proteolysis during storage of UHT milk: Differences between whole and skim milk. *Journal of Dairy Research, 60*, 339–347.

Masmoudi, H., Dréau, Y. L., Piccerelle, P., & Kister, J. (2005). The evaluation of cosmetic and pharmaceutical emulsions aging process using classical techniques and a new method: FTIR. *International Journal of Pharmaceutics, 289*, 117–131.

Mazerolles, G., Devaux, M.-F., Duboz, G., Duployer, M.-H., Riou, N. M., & Dufour, É. (2001). Infrared and fluorescence spectroscopy for monitoring protein structure and interaction changes during cheese ripening. *Lait, 81*, 509–527.

McMahon, D. J. (1996). Age-gelation of UHT milk: Changes that occur during storage, their effect on shelf life and the mechanism by which age-gelation occurs. In *Heat treatments and alternative methods. IDF symposium (6–8 Sep 1995), Vienna, Austria*.

Mendelsohn, R., & Flach, C. R. (2002). Infrared reflection-absorption spectroscopy of lipids, peptides, and proteins in aqueous monolayers. *Current Topics in Membranes, 52*, 57–88.

Mendelsohn, R., Mao, G., & Flach, C. R. (2010). Infrared reflection–absorption spectroscopy: Principles and applications to lipid–protein interaction in Langmuir films. *Biochimica et Biophysica Acta (BBA) – Biomembranes, 1798*, 788–800.

Murphy, E. G., Fenelon, M. A., Roos, Y. H., & Hogan, S. A. (2014). Decoupling macronutrient interactions during heating of model infant milk formulas. *Journal of Agricultural and Food Chemistry, 62*, 10585–10593.

Ngarize, S., Herman, H., Adams, A., & Howell, N. (2004). Comparison of changes in the secondary structure of unheated, heated, and high-pressure-treated β-lactoglobulin and ovalbumin proteins using Fourier transform Raman spectroscopy and self-deconvolution. *Journal of Agricultural and Food Chemistry, 52*, 6470–6477.

Nieuwenhuijse, J. A., & van Boekel, M. A. (2003). Protein stability in sterilised milk and milk products. In P. L. H. McSweeney, & J. A. O'Mahony (Eds.), *Advanced dairy chemistry. Vol. 1B. Applied aspects* (pp. 947–974). New York, NY, USA: Springer.

Pellegrino, L. (1994). Influence of fat content on some heat-induced changes in milk and cream. *Nederlands melk en Zuiveltijdschrift, 48*, 71–80.

Qi, X., Holt, C., Mcnulty, D., Clarke, D., Brownlow, S., & Jones, G. (1997). Effect of temperature on the secondary structure of β-lactoglobulin at pH 6.7, as determined by CD and IR spectroscopy: A test of the molten globule hypothesis. *Biochemical Journal, 324*, 341–346.

Ramsey, J. A., & Swartzel, K. R. (1984). Effect of ultra high temperature processing and storage conditions on rates of sedimentation and fat separation of aseptically packaged milk. *Journal of Food Science, 49*, 257–262.

Sankaram, M. B., & Marsh, D. (1993). Protein–lipid interactions with peripheral membrane proteins. *New Comprehensive Biochemistry, 25*, 127–162.

Sharma, S. K., & Dalgleish, D. G. (1993). Interactions between milk serum proteins and synthetic fat globule membrane during heating of homogenized whole milk. *Journal of Agricultural and Food Chemistry, 41*, 1407–1412.

Sharma, S. K., & Dalgleish, D. G. (1994). Effect of heat treatments on the incorporation of milk serum proteins into the fat globule membrane of homogenized milk. *Journal of Dairy Research, 61*, 375–384.

Singh, H. (1991). Modification of food proteins by covalent crosslinking. *Trends Food Science and Technology, 2*, 196–200.

Surewicz, W. K., Moscarello, M. A., & Mantsch, H. H. (1987). Fourier transform infrared spectroscopic investigation of the interaction between myelin basic protein and dimyristoylphosphatidylglycerol bilayers. *Biochemistry, 26*, 3881–3886.

Turner, J. A., Sivasundaram, L. R., Ottenhof, M.-A., Farhat, I. A., Linforth, R. S. T., & Taylor, A. J. (2002). Monitoring chemical and physical changes during thermal flavor generation. *Journal of Agricultural and Food Chemistry, 50*, 5406–5411.

Walstra, P., Jenness, R., & Badings, H. T. (1984). *Dairy chemistry and physics*. New York, NY, USA: Wiley.

Whittinghill, J. M., Norton, J., & Proctor, A. (1999). A fourier transform infrared spectroscopy study of the effect of temperature on soy lecithin-stabilized emulsions. *Journal of the American Oil Chemists' Society, 76*, 1393–1398.

Zhou, Q., Sun, S.-Q., Yu, L., Xu, C.-H., Noda, I., & Zhang, X.-R. (2006). Sequential changes of main components in different kinds of milk powders using two-dimensional infrared correlation analysis. *Journal of Molecular Structure, 799*, 77–84.

CHAPTER 5

Predicting sediment formation in ultra high temperature-treated whole and skim milk using attenuated total reflectance-Fourier transform infrared spectroscopy

This chapter has been published as a research paper entitled "Predicting sediment formation in ultra high temperature-treated whole and skim milk using attenuated total reflectance-Fourier transform infrared spectroscopy" by Manpreet Kaur Grewal, Jayani Chandrapala, Osaana Donkor, Vasso Apostolopoulos, and Todor Vasiljevic in the peer reviewed International Dairy Journal,74, 39-48 (2017).

VICTORIA UNIVERSITY
MELBOURNE AUSTRALIA

GRADUATE RESEARCH CENTRE

DECLARATION OF CO-AUTHORSHIP AND CO-CONTRIBUTION: PAPERS INCORPORATED IN THESIS BY PUBLICATION

This declaration is to be completed for each conjointly authored publication and placed at the beginning of the thesis chapter in which the publication appears.

1. PUBLICATION DETAILS (to be completed by the candidate)

Title of Paper/Journal/Book:	Predicting sediment formation in ultra high temperature-treated whole and skim milk using attenuated total reflectance-Fourier transform infrared spectroscopy
Surname:	Grewal
First name:	Manpreet Kaur
College:	College of Health & Biomedicine
Candidate's Contribution (%):	80

Status:

Accepted and in press:	☐	Date:	
Published:	☑	Date:	19 1 2017

2. CANDIDATE DECLARATION

I declare that the publication above meets the requirements to be included in the thesis as outlined in the HDR Policy and related Procedures – policy.vu.edu.au.

Manpreet Kaur Grewal Digitally signed by Manpreet Kaur Grewal Date: 2018.02.18 10:50:38 +11'00'	18.02.2018
Signature	**Date**

3. CO-AUTHOR(S) DECLARATION

In the case of the above publication, the following authors contributed to the work as follows:

The undersigned certify that:

1. They meet criteria for authorship in that they have participated in the conception, execution or interpretation of at least that part of the publication in their field of expertise;
2. They take public responsibility for their part of the publication, except for the responsible author who accepts overall responsibility for the publication;
3. There are no other authors of the publication according to these criteria;
4. Potential conflicts of interest have been disclosed to a) granting bodies, b) the editor or publisher of journals or other publications, and c) the head of the responsible academic unit; and

VICTORIA UNIVERSITY
MELBOURNE AUSTRALIA

5. The original data will be held for at least five years from the date indicated below and is stored at the following **location(s)**:

College of Health & Biomedicine
Institute of Sustainable Industries and Liveable cities
Victoria University
Australia

Name(s) of Co-Author(s)	Contribution (%)	Nature of Contribution	Signature	Date
Manpreet Kaur Grewal	80	Concept development, research design, experiment execution, statistical analysis, interpretation, drafting manuscript and its revision	Manpreet Kaur Grewal Digitally signed by Manpreet Kaur Grewal Date: 2018.02.22 16:01:54 +11'00'	22 02 18
Jayani Chandrapala	6	Concept development, support and technical expertise, manuscript revision	Jayani Chandrapala Digitally signed by Jayani Chandrapala DN: cn=Jayani Chandrapala, o=RMIT University, ou=School of Science, email=jayani.chandrapala@rmit.edu.au, c=AU Date: 2018.02.26 08:25:59 +11'00'	26022018
Osaana Donkor	2	Concept development, manuscript revision	Osaana Donkor Digitally signed by Osaana Donkor DN: cn=Osaana Donkor, o=Victoria University, ou, email=osaana.donkor@vu.edu.au, c=AU Date: 2018.02.26 10:37:05 +11'00'	20.02.2018
Vasso Apostolopoulos	2	Concept development, manuscript revision	[redacted] gitally signed by Vasso N: cn=Vasso, o, ou, mail=vasso.apostolopo os@vu.edu.au, c=AU te: 2018.02.26 0:51:40 +10'00'	26/02/2018
Todor Vasiljevic	10	Concept development, experimental design, illustrations, manuscript draft and revision	Todor Vasiljevic Digitally signed by Todor Vasiljevic DN: cn=Todor Vasiljevic, o, ou, email=todor.vasiljevic@vu.edu.au, c=AU Date: 2018.02.23 14:00:01 +11'00'	23.02.2018

International Dairy Journal xxx (2017) 1–10

Contents lists available at ScienceDirect

International Dairy Journal

journal homepage: www.elsevier.com/locate/idairyj

Predicting sediment formation in ultra high temperature-treated whole and skim milk using attenuated total reflectance-Fourier transform infrared spectroscopy

Manpreet Kaur Grewal [a], Jayani Chandrapala [a], Osaana Donkor [a], Vasso Apostolopoulos [b], Todor Vasiljevic [a, *]

[a] Advanced Food Systems Research Unit, College of Health and Biomedicine, Victoria University, Melbourne, VIC 8001, Australia
[b] Immunology in Chronic Diseases Program, Centre for Chronic Disease, College of Health and Biomedicine, Victoria University, Melbourne, VIC 8001, Australia

ARTICLE INFO

Article history:
Received 9 December 2016
Received in revised form
19 January 2017
Accepted 19 January 2017
Available online xxx

ABSTRACT

Establishing accelerated shelf-life testing using Fourier transform infrared spectroscopy (FTIR) as a tool for prediction of stability requires pre-assessment of correlations between spectral changes and instability development during storage at room temperature. Comparison of results with those at elevated temperatures would establish appropriateness of accelerated shelf-life testing. UHT skim milk (SM) and UHT whole milk (WM) were stored at 20 °C for 9 months to investigate the feasibility of identifying spectral markers to predict sedimentation (a measure of instability). Marker variables corresponding to changes in structure and interactions of lipids, proteins and carbohydrates successfully predicted sedimentation in SM ($R^2 = 0.92$) and WM ($R^2 = 0.60$). Low predictability in WM may be due to influence of fat. These markers were similar to those observed during accelerated shelf-life testing, hence affirming its application with further work required to develop a model able to forecast sedimentation and other instabilities in UHT milk.

1. Introduction

The prediction of shelf-life of shelf stable products may prove to be challenging and, in many instances, is cost and time intensive. One such product is ultra-high temperature (UHT) treated milk, for which long shelf-life at room temperature has made it an important product from nutritional, technological and economical point of view. However, the UHT treatment (130–140 °C for 3–5 s; Holland, Gupta, Deeth, & Alewood, 2011) required to render the product 'commercially sterile' and thus provide longer shelf-life stability in an aseptic pack induces certain chemical and physical changes that progress during storage. Some of these physiochemical changes may lead to storage instabilities involving sedimentation or age gelation (Dalgleish, 1992; McMahon, 1996; Ramsey & Swartzel, 1984). The occurrence of considerable level of sedimentation (1% dry weight basis; Deeth & Lewis, 2016) or gelation can mark the end of shelf-life and hence affects the market potential of UHT milk. For these reasons, the need of a rapid technique for predicting such storage stability of UHT milk has been emphasised in recent years.

Fourier transform infrared (FTIR) spectroscopy could potentially serve the purpose as it was able to detect changes in spectra in as little as 14 d when UHT milk was stored under elevated storage temperatures (≥40 °C) (Grewal et al., 2017a). Changes in spectra appeared to correlate with trends in sedimentation. FTIR was also able to detect changes concurrent with increased sedimentation in UHT skim milk (SM) at temperatures lower than 40 °C, but only after 28 d. Spectral regions representing structure and interactions of milk lipids and proteins change the most, and are impacted by storage temperature and time in both SM and UHT whole milk (WM). Therefore, storage at high temperature could act as a rapid alternative to long, real time, analysis. However, intense browning, visually observed at higher temperatures, suggests that probably the rate and type of these reactions are different at lower temperatures. Thus, to establish FTIR as a tool to predict the storage stability of UHT milk, a confirmatory long term storage study at room temperature (20 °C) was required. Gelation was not observed in samples during storage, thus the build-up of sediment was taken as a measure of storage instability. This long term study would also

* Corresponding author. Tel.: +61 3 9919 8062.
E-mail address: todor.vasiljevic@vu.edu.au (T. Vasiljevic).

http://dx.doi.org/10.1016/j.idairyj.2017.01.004
0958-6946/

establish the appropriateness of the use of accelerated shelf-life testing in predicting the shelf-life of UHT milk by comparing the findings to those reported previously obtained during accelerated testing (Grewal et al., 2017a).

In the current study, the spectral markers were identified and their feasibility in predicting changes in the amount of sediment formed in SM and WM stored at 20 °C for a period of 9 months was investigated. The study was thought to be able to also bring a greater understanding of physiochemical changes that occur during long term storage of SM and WM at room temperature and their correlation with changes in the spectral profiles.

2. Materials and methods

2.1. Materials

Commercial SM and WM samples were kindly provided by Murray Goulburn Co-operative Co., Ltd. (Melbourne, VIC, Australia) and prepared as described previously (Grewal, Chandrapala, Donkor, Apostolopoulos, & Vasiljevic, 2017b). Both SM and WM packs were produced on the same day. The composition of WM as reported by the manufacturer per litre of milk was 33 g protein, 34 g fat, 53 g carbohydrate, 0.55 g Na and 1.2 g Ca. SM was reported to contain 34 g protein, 1 g fat, 53 g carbohydrate, 0.55 g Na and 1.2 g Ca per litre of milk. The UHT milk packs were stored at 20 °C for 9 months. Milk packs were analysed on the day of manufacture (day 0), after 1 month and then at bimonthly intervals during storage.

2.2. Changes in protein interactions

The change in interactions of milk proteins during storage of UHT milk packs were investigated using polyacrylamide gel electrophoresis (PAGE), i.e., native-PAGE and sodium dodecylsulphate-(SDS-) PAGE under reducing and non-reducing conditions as previously described (Grewal et al., 2017b). All gels were scanned using a ChemiDoc imager (ChemiDoc MP, Bio-Rad Laboratories, Richmond, CA, USA).

2.3. Physicochemical changes

The pH was measured at room temperature using a pH meter (Hanna Instruments, Singapore). The average particle size was determined using a Zetasizer Nano ZS (Malvern Instruments Ltd., Malvern, UK) after appropriate dilutions (1:100) with Milli-Q water. All the measurements were performed at 25 °C using 1.349, 1.354 and 1.33 as the refractive indices of WM, SM and water, respectively. Zeta potential (ζ) was also determined using the same instrument at 25 °C after appropriate dilutions with the corresponding milk ultrafiltrate in a ratio of 1:50. Prior to measurement, the samples were filtered through a membrane with a pore size of 0.8 μm to exclude possible large aggregates. The refractive index and viscosity of milk ultrafiltrate were set at 1.342 and 0.99 mPa s, respectively. Milk ultrafiltrate was used for dilutions in zeta potential measurements since use of Milli-Q water resulted in high standard deviation and low reproducibility.

The calcium content in bulk and serum phase in UHT milk during storage was determined using an inductively coupled plasma atomic emission spectrometer (ICP-AES) sequential plasma spectrometer (ICPE-9000 system, Shimadzu Corporation, Kyoto, Japan). For total calcium in bulk, aliquots (5 mL) from each milk pack were first dried and then ashed in a muffle furnace. For soluble calcium content, milk samples were ultracentrifuged at 100,000× *g* for 90 min using a Beckman Optima L-70 ultracentrifuge with a type 70.ITI rotor (Beckman Instruments Inc., Palo Alto, CA, USA). The casein micelle-free milk serum or supernatant was carefully removed from the ultracentrifugal pellet after removing the top fat layer. Supernatant (5 mL) was dried as described above. The ash obtained was dissolved in 10 mL of 1 M nitric acid and diluted with 90 mL Milli-Q water, giving a total concentration of solids of less than 0.1%. Calibration ($R^2 = 0.99$) was performed using a blank and five standard concentrations (2, 4, 6, 8 and 10 mg L^{-1} Ca).

Ionic calcium content was measured using a calcium ion selective electrode (Ca^{2+}) connected to a pH meter (inoLab, WTW GmbH, Ingolstadt, Germany). The electrode was calibrated before all storage analysis openings of milk packs using calcium chloride solutions with concentrations ranging from 0.5 mM to 20 mM. The R^2 value for the standard curve ranged from 0.90 to 0.96. Ionic strength was adjusted by the addition of 80 mM KCl to the standards (Chandrapala, McKinnon, Augustin, & Udabage, 2010).

2.4. Sediment measurement

Sedimentation was measured using a method as previously described (Grewal et al., 2017a). Briefly, milk packs were manually shaken and an aliquot was centrifuged at 2760× *g* for 15 min (Beckman Coulter Avanti J-26S XP Centrifuge; Beckman Instruments Inc.). The sediment was oven-dried to a constant weight and expressed as the amount of sediment (mg 100 g^{-1} milk).

2.5. FTIR spectra acquisition and multivariate data analysis

Sample spectra were acquired in the range of 4000–600 cm^{-1} using a PerkinElmer Frontier FTIR spectrometer (PerkinElmer, Torrence, MA, USA) with a resolution of 4 cm^{-1} and averaging 16 scans for each spectrum. Three milk packs corresponding to each storage time were analysed. Contents of the packs were mixed and approximately 0.5 mL of sample was added onto an attenuated total reflectance (ATR) cell. The spectra of three sub samples of each sample were taken by refilling the ATR cell. Background spectrum was scanned at the beginning of the measurements with a blank Diamond ATR cell using same instrumental conditions as for the sample spectra acquisition.

The FTIR spectra of all samples corresponding to different storage times were exported to Unscrambler software (Version 10.2, CAMO AS, Trondheim, Norway). Spectra were baseline corrected and then the water spectrum was subtracted, as described previously (Grewal et al., 2017a). The spectra of the milk showed five major characteristic regions after subtraction of water bands, namely: 3700–3000 cm^{-1} [hydrogen bonding (water-related)], 3000–2800 cm^{-1} [lipids (fat B)], 1800–1700 cm^{-1} [lipids (fat A)], 1700–1500 cm^{-1} (amide I and II) and 1500–900 cm^{-1} (amide III and carbohydrates). Principal component analysis (PCA) was employed on both the full range and separately on regions identified above to determine the storage based classifications in UHT milk samples. PCA score plots obtained demonstrate groupings, whereas loading plots aided identification of wavenumbers (spectral markers) that have high loadings or contributed the most in the classification of samples into different groups.

Once the spectral marker variables were known, the next step was to investigate the correlation between these variables and the amount of sediment using partial least-squares (PLS) regression. Absorbance values for the spectral markers were used as x-variables and the amount of sediment as the y-variable. Firstly, the samples were divided into two groups, i.e., the calibration (training) set and the test set. Every third sample was assigned membership of the test set, ensuring that samples corresponding to different storage times were well represented in both sets. Secondly, the model was developed using only the calibration set of samples employing leave-one-out cross-validation. Thirdly, the model developed was tested on test samples, i.e., samples completely

Please cite this article in press as: Grewal, M. K., et al., Predicting sediment formation in ultra high temperature-treated whole and skim milk using attenuated total reflectance-Fourier transform infrared spectroscopy, *International Dairy Journal* (2017), http://dx.doi.org/10.1016/j.idairyj.2017.01.004

unknown to the model with reference sediment values to evaluate the ability of the model to predict sedimentation.

2.6. Statistical analysis

The sediment dry weight data and other physiochemical measurements mentioned above corresponding to all determinations were analysed using a generalised linear model (GLM) procedure of SAS software (version 9.3; SAS Institute Inc., Cary, NC, USA). The effects of main factors (type of milk and storage time) and interactions were analysed in a split plot in time design at pre-set level of significance $P < 0.05$. The design was replicated 3 times.

3. Results and discussion

3.1. Effect of storage on protein interactions

UHT treatment results in changes in structure and interactions of milk proteins, which continue during storage. The foremost change induced by UHT treatment is denaturation of heat labile whey proteins, which subsequently become involved in hydrophobic and covalent, mainly disulphide, interactions with caseins (CNs) and amongst themselves. In the present study, this change was demonstrated by absence of native bands of whey proteins throughout the storage in native-PAGE patterns of both SM and WM and their reappearance in non-reducing and reducing SDS-PAGE patterns (Figs. 1a–f and 2a–f).

Furthermore, similar to storage at elevated temperatures, an increase in both disulphide and non-disulphide covalent bonding signified by rise in intensity of aggregate bands at the top of the resolving gel in non-reducing and reducing SDS-PAGE patterns, respectively, was observed in both SM (Fig. 1b–c, e–f) and WM (Fig. 2b–c, e–f). With storage, the band intensities of individual caseins, mainly κ-CN and α_{S2}-CN, continuously diminished in non-reducing SDS-PAGE patterns, but their reappearance in reducing SDS-PAGE patterns indicated their prominent involvement in disulphide bonding (Fig. 1b and e). However, unlike storage at elevated temperatures (Grewal et al., 2017b), the identity of specific milk proteins participating in non-disulphide covalent bonding was not clear from the reducing SDS-PAGE patterns in the current study (Figs. 1 and 2c,f).

Covalent crosslinking of proteins during storage in both SM and WM thus progresses even at lower storage temperatures, but at a slower rate in comparison with that at elevated storage temperatures (Grewal et al., 2017b). Also, it appeared that during storage at 20 °C, the order of different interactions in both SM and WM was disulphide >> covalent (non-disulphide) > non-covalent, which was different from that observed at higher storage temperatures (>40 °C), at which non-disulphide covalent interactions prevailed (Grewal et al., 2017b). The common observation under both conditions, storage at 20 °C and at elevated temperature, was the increase in participation of caseins in the aggregate formation.

Enhanced involvement of caseins in the aggregate formation with storage might be due to continuous dissociation of caseins from the micelle and their release into the serum phase, which is supported by appearance of native caseins (κ-CN, α_S-CN and β-CN) in native-PAGE patterns of the serum phase in both SM and WM (Figs. 1 and 2a,d). Dissociation of caseins from the micelle was also supported by concomitant increase in soluble and ionic calcium in the serum phase (Table 2), suggesting the release of colloidal calcium phosphate (CCP). However, increase in soluble calcium was not a result of acidification of milk as no significant change in pH was observed after 9 months (Table 2). It appeared that, unlike higher storage temperatures (≥30 °C) where pH decreased to as

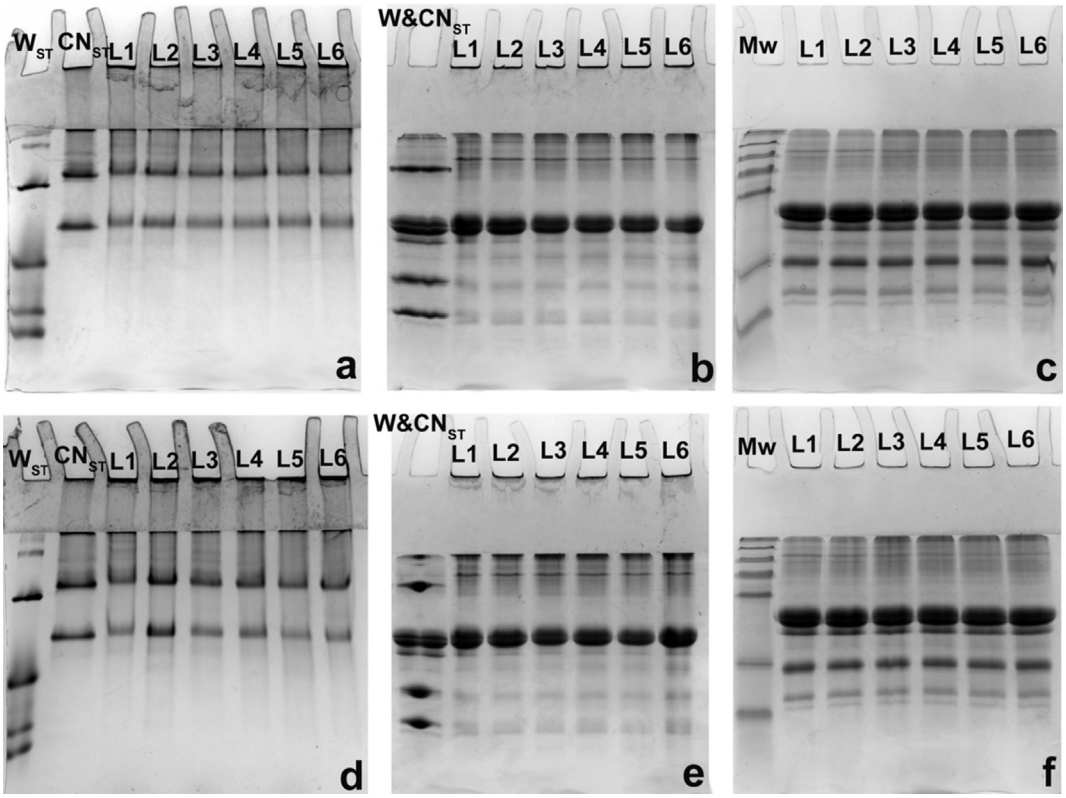

Fig. 1. Native non-reducing- and reducing-sodium dodecylsulphate gel electrophoresis patterns of UHT skim milk (SM) (a, b and c) and UHT whole milk (WM) (d, e and f) stored at 20 °C for a period of 9 months. L1, L2, L3, L4, L5 and L6 are samples on day 0 and after 1, 3, 5, 7 and 9 months of storage, respectively. W_{ST}, CN_{ST} and M_W denote whey protein standard, casein standard and molecular mass marker, respectively.

Please cite this article in press as: Grewal, M. K., et al., Predicting sediment formation in ultra high temperature-treated whole and skim milk using attenuated total reflectance-Fourier transform infrared spectroscopy, *International Dairy Journal* (2017), http://dx.doi.org/10.1016/j.idairyj.2017.01.004

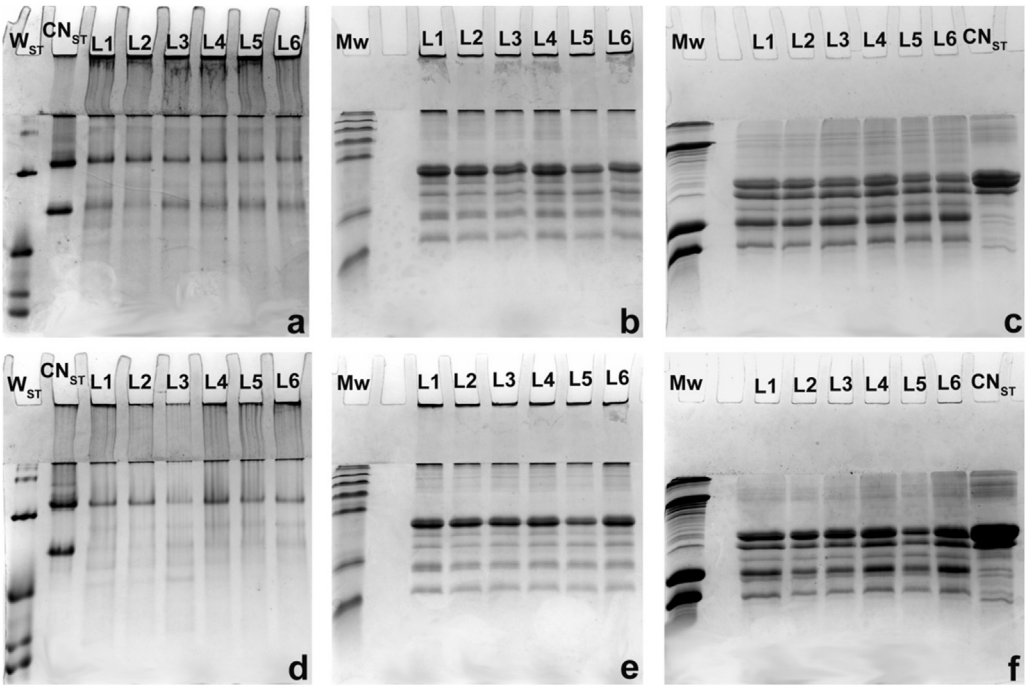

Fig. 2. Native non-reducing- and reducing-sodium dodecylsulphate gel electrophoresis patterns of supernatant (centrifuged at 2760× *g* for 15 min) of UHT skim milk (SM) (a, b and c) and UHT whole milk (WM) (d, e and f) stored at 20 °C for a period of 9 months. L1, L2, L3, L4, L5 and L6 are samples on day 0 and after 1, 3, 5, 7 and 9 months of storage, respectively. W_{ST}, CN_{ST} and M_W denote whey protein standard, casein standard and molecular mass marker, respectively.

Table 1
Effect of milk type (skim or whole milk) and storage time on amount of sediment (insoluble precipitates) formed in UHT milk.[a]

Type of milk	Sediment during storage (months)					
	0	1	3	5	7	9
Skim milk	52.5^{aA}	96.9^{bA}	112.7^{cA}	130.1^{dA}	135.9^{deA}	146.2^{eA}
Whole milk	93.6^{aB}	105.6^{abA}	110.2^{bA}	115.7^{bA}	119.8^{bB}	161.4^{cA}

[a] Values (mg 100 g^{-1} of milk) are means (standard error = 4.9); means in a row with different superscript lower case letters and in a column with different superscript upper case letters differ significantly ($P < 0.05$).

low as 5.96, the buffering capacity of milk was maintained at 20 °C. The reduction in pH at higher temperatures can be attributed to the formation of formic and acetic acid during the course of Maillard reaction (Nieuwenhuijse & van Boekel, 2003). Therefore, the considerable increase in non-disulphide protein cross-linking observed at 20 °C could be mainly due to the formation of dehydroalanine, while involvement of advanced Maillard reaction products was probably negligible.

Another explanation for dissociation of CCP could be in an increase of a negative charge of caseins in the micelle as a result of increased intra-micellar crosslinking during storage demonstrated by a significant ($P < 0.05$) increase in the zeta potential during storage (Table 2). During the early stages of Maillard reactions, lactose reacts with the positively charged amino group of lysyl and arginyl residues, and consequently the overall charge would become more negative. Indeed, an increase in b* value in SM and WM from 5.75 ± 0.02 to 8.5 ± 0.01 AU and 11.98 ± 0.04 to 13.28 ± 0.04 AU, respectively, was observed after 9 months. In addition, the deamidation of amino acid residues during storage of UHT milk (Holland et al., 2011) could also lead to an increase in negative charge and may explain the observed increase in the zeta potential. The increase in negative charge of the micellar caseins might have therefore enhanced electrostatic repulsions inside the micelle, resulting in dissociation of proteins (Nieuwenhuijse & van Boekel, 2003). Caseins, once dissociated, engage in formation of soluble aggregates with whey proteins and other caseins, indicated as an increase in intensity of aggregate bands on the top of the stacking and resolving gels in native and SDS-PAGE patterns (Figs. 1 and 2a–f). Soluble aggregates apparently reach an optimum level after which they become insoluble and precipitate as sediment.

In both SM and WM, an increase in covalent bonded aggregates was noted (Fig. 1b and e). However, the latter had higher band intensity for aggregate bands in SDS-PAGE patterns. A similar trend

Table 2
Effect of milk type (skim or whole milk) and storage time on physiochemical changes in UHT.[a]

Physicochemical parameter	Type of milk	Storage time (months)					
		0	1	3	5	7	9
pH	SM	6.52^{aA}	6.49^{bA}	6.53^{aA}	6.48^{bA}	6.51^{abA}	6.53^{aA}
	WM	6.51^{aA}	6.51^{aA}	6.52^{aA}	6.46^{bA}	6.51^{aA}	6.49^{aB}
Soluble calcium (mmol L^{-1})	SM	7.42^{aA}	8.03^{aA}	8.50^{aA}	14.20^{bA}	15.79^{bA}	10.28^{cA}
	WM	8.94^{aA}	6.88^{bA}	6.28^{bB}	14.71^{cA}	12.76^{dB}	12.85^{dB}
Ionic calcium activity	SM	0.56^{aA}	0.86^{bA}	0.84^{bA}	1.23^{cA}	1.67^{dA}	1.25^{cA}
	WM	0.58^{aA}	0.91^{bB}	0.97^{cB}	1.26^{dA}	1.65^{eA}	1.65^{eB}
Zeta potential (mV)	SM	-16.60^{aA}	-18.72^{bA}	-16.20^{aA}	-15.99^{aA}	-17.31^{cA}	-21.72^{dA}
	WM	-17.53^{aB}	-19.89^{bB}	-16.81^{cA}	-16.96^{caB}	-20.92^{dB}	-24.20^{eB}

[a] Means in a row with different superscript lower case letters and in a column with different superscript upper case letters differ significantly ($P < 0.05$).

Please cite this article in press as: Grewal, M. K., et al., Predicting sediment formation in ultra high temperature-treated whole and skim milk using attenuated total reflectance-Fourier transform infrared spectroscopy, *International Dairy Journal* (2017), http://dx.doi.org/10.1016/j.idairyj.2017.01.004

was apparent in WM stored at temperature ≥40 °C and was attributed to a phase change of milk fat at these temperatures, leading to changes in conformation of milk lipids. Caseins are absorbed on the modified fat globule membrane apparently via complex formation with surface active phospholipids or hydrophobic triglycerides through non-polar van der Waals, polar hydrogen bonds and electrostatic interactions of charged groups (Brunner, 1962). Structural changes in the lipids can hence affect lipid–protein interactions (Grewal et al., 2017a). Furthermore, at higher temperatures oxidative deterioration of lipids enhances the formation of lipid protein complexes (Brunner, 1962). However, high intensity of aggregate bands during storage at 20 °C implied changes in structure of lipids and their interactions even at comparatively lower temperatures.

Dispersion of fat globules due to upstream homogenisation results in their coverage with caseins (predominantly) and whey proteins, thus increasing their density. Casein micelles absorbed on the surface of homogenised fat globules tend to show some spreading. Hence, these casein micelles are not entirely covered by κ-casein molecules (Huppertz, 2016), which may expose Ca-sensitive micellar caseins to destabilisation due to the steady rise in ionic calcium observed during storage (Table 2; Huppertz, 2016). Ionic calcium in the serum phase may thus act as a medium for interactions between fat globules and surrounding caseins, casein micelles or denatured whey proteins.

After UHT treatment, some whey proteins may also complex via disulphide interactions with caseins and native membrane proteins, increasing the density of fat globules (Sharma & Dalgleish, 1993; Ye, Singh, Taylor, & Anema, 2002). Involvement of modified fat globules with greater density into aggregate formation leads to enlargement of the particles, which, according to Stokes' law, would enhance sedimentation (Walstra, Jenness, & Badings, 1984). The inclusion of fat in aggregates was also corroborated by an increase in a size of the casein micelles and reduction in a size of homogenised fat globules (data not shown). Fat–protein association in WM was also supported by a lower band intensity of reduced, as well as non-reduced, proteins and suspended aggregates in the serum phase compared with SM (Fig. 2a–e). It is probable that inclusion of fat globules into aggregates resulted in greater precipitation of these aggregates upon centrifugation.

3.2. Sedimentation during storage

A steady rise ($P < 0.5$) in sedimentation in SM was observed during the 9 month storage period. In contrast, in WM, the amount of sediment remained constant until 7 months of storage followed by a significant surge after 9 months of storage (Table 1). The trend in both SM and WM was similar to that noted in our previous study (Grewal et al., 2017a), in which SM and WM were stored at elevated storage temperatures, implying that accelerated shelf-life stability testing produces similar results in comparatively shorter time. Another implication is that fat content has an influence on the formation of sediment during storage.

In addition, WM contained a higher ($P < 0.5$) amount of sediment than did SM at the start of storage, as observed previously (Grewal et al., 2017a). It appears that homogenisation followed by UHT treatment may have a great impact on WM on day 0. Dispersion of fat globules and modification of fat globule membrane by homogenisation and then association of denatured whey proteins as a consequence of UHT treatment increases density of fat globules producing comparatively higher amount of sediment. However, during storage, the amount of sediment remains more or less stable (Table 1). Apparently in WM, dissociated micellar caseins interact with whey proteins to form soluble aggregates. These soluble aggregates further associate with milk fat to form suspended aggregates, which on reaching a maximum size sediment as insoluble precipitates. While fat precipitates in these associations, at the same time it may also act as a hindrance to precipitation due to its low density, which could explain slight but not significant increase of the sediment in WM up to 7 months of storage.

The steady increase in sediment in SM during storage could be attributed to pronounced protein–protein interactions in SM compared with WM (Grewal et al., 2017a). Reactive denatured whey proteins are comparably less associated with the casein micelle surface in SM than WM (Garcia-Risco, Ramos, & Lopez-Fandino, 1999; Grewal et al., 2017a). This increases their availability for crosslinking reactions that take place in the solution (Grewal et al., 2017a). The increase in ionic calcium (Table 2) might also have contributed to the greater amount of sediment in SM. Furthermore, in SM due to a comparatively lower content of fat, the formation of sediment involves primarily association of dissociated micellar caseins and whey proteins forming soluble aggregates that grow in size and finally sediment as insoluble precipitates.

3.3. Effects of storage time on FTIR spectra

The increase in covalent protein–protein and protein–lipid interactions observed above during storage indicate underlying conformational changes in the proteins and lipids. The PCA of the full range classified the samples into different groups in both SM (Fig. 3a) and WM according to the storage time, implying that definite changes progressed in FTIR spectra during storage at 20 °C. Different clusters had been named as D0, M1, M3, M5, M7 and M9 representing samples analysed on day 0, 1, 3, 5, 7 and 9 months of storage, respectively.

Spectral regions contributing the most to the classification were (Figs. 3b and 4b): region I, 3700–3000 cm^{-1} [hydrogen bonding (water related)]; region II, 3000–2800 cm^{-1} [lipids (fat B)]; region III, 1800–1700 cm^{-1} [lipids (fat A)]; region IV, 1700–1500 cm^{-1} (amide I and II) and region V, 1500–900 cm^{-1} (amide III and carbohydrates). To select marker variables out of these regions, PCA was applied separately to all five regions. Variables with highest loading were selected and PCA was applied only using these. If a sample classification produced was similar as the whole region, these selected variables were considered as marker variables for further use in the prediction analysis discussed later in the study.

3.3.1. Region I, 3700–3000 cm^{-1}

The region registered substantial changes and was able to classify samples into different groups in both SM (Fig. 3c) and WM. In SM, PC1 and PC2 explained 97% and 2% of the variance, respectively. In WM, PC1 explained 99% and 1% of the variance, respectively (Fig. 4c). Variables with highest loadings in WM, able to produce similar classification as produced by whole region, were 3587, 3419, 3197–3195 and 3158 cm^{-1}. Similarly, variables with highest loading in SM were 3587, 3450, 3202–3192, 3142–3141 cm^{-1}. While these markers were slightly different from WM, they were also able to classify in the same way as the whole region (Fig. 3d). After 1 month in SM samples and after 2 months in WM, a shift was observed in a band corresponding to O–H stretch to higher wavenumbers resulting in depression around 3194 cm^{-1}. A similar pattern during storage at a high temperature was attributed to decrease in extent of hydrogen bonding (water related) (Grewal et al., 2017a), which shifts the O–H stretching frequency to higher wavenumbers (Choperena & Painter, 2009). Thus, similar changes in spectra were produced with storage time as by applying an accelerated storage temperature but during a shorter period.

3.3.2. Fat B, 3000–2800 cm^{-1}

Irrespective of fat content, the region was able to classify samples in both SM and WM. In SM, PC1 explained 98% of the variance

Please cite this article in press as: Grewal, M. K., et al., Predicting sediment formation in ultra high temperature-treated whole and skim milk using attenuated total reflectance-Fourier transform infrared spectroscopy, *International Dairy Journal* (2017), http://dx.doi.org/10.1016/j.idairyj.2017.01.004

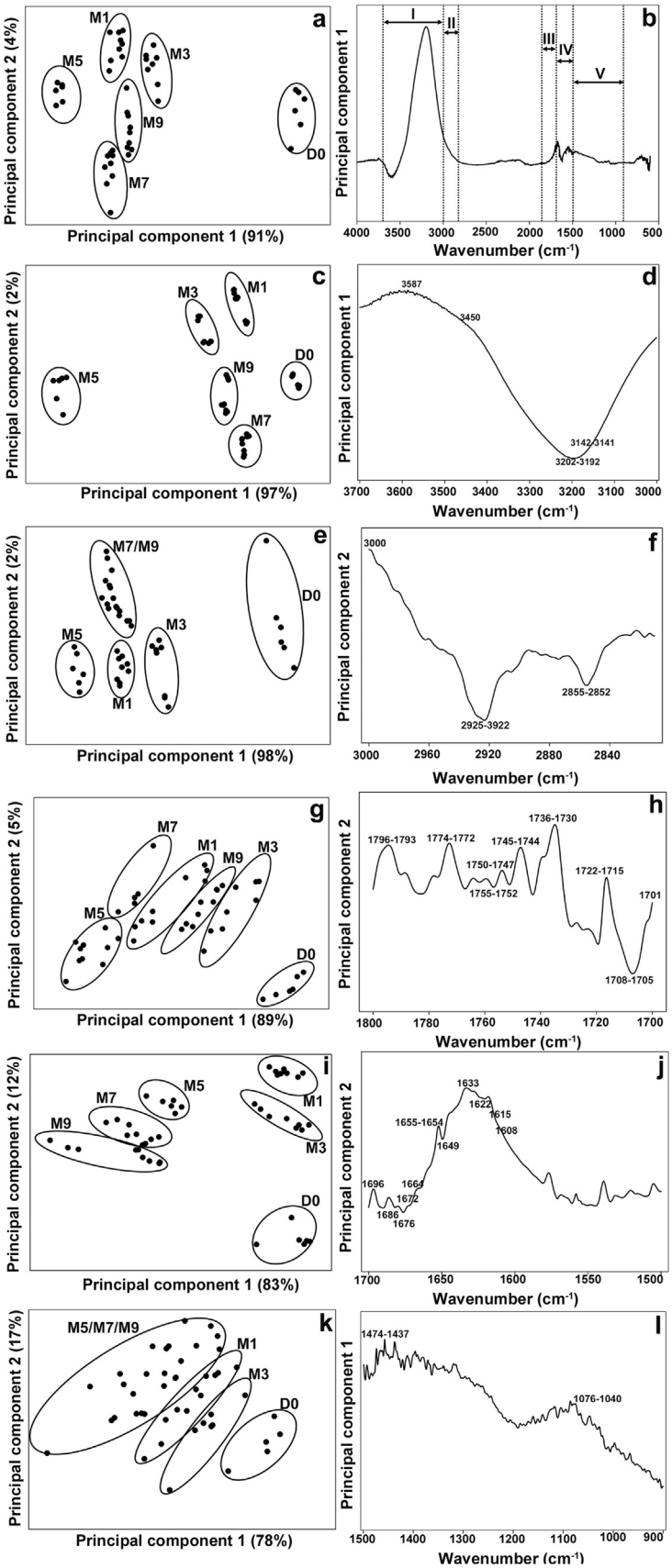

Fig. 3. Principal component scores and loading plots of spectra of UHT skim milk samples acquired at day 0 (D0) and after 1, 3, 5, 7 and 9 months (M1, M3, M5, M7 and M9, respectively) storage for spectral ranges: (a, b) 4000–600 cm^{-1}; (c, d) region I, 3700–3000 cm^{-1}; (e, f) region II, 3000–2800 cm^{-1}; (g, h) region III, 1800–1700 cm^{-1}; (i, j) region IV, 1700–1500 cm^{-1}; (k, l) region V, 1500–900 cm^{-1}.

Please cite this article in press as: Grewal, M. K., et al., Predicting sediment formation in ultra high temperature-treated whole and skim milk using attenuated total reflectance-Fourier transform infrared spectroscopy, *International Dairy Journal* (2017), http://dx.doi.org/10.1016/j.idairyj.2017.01.004

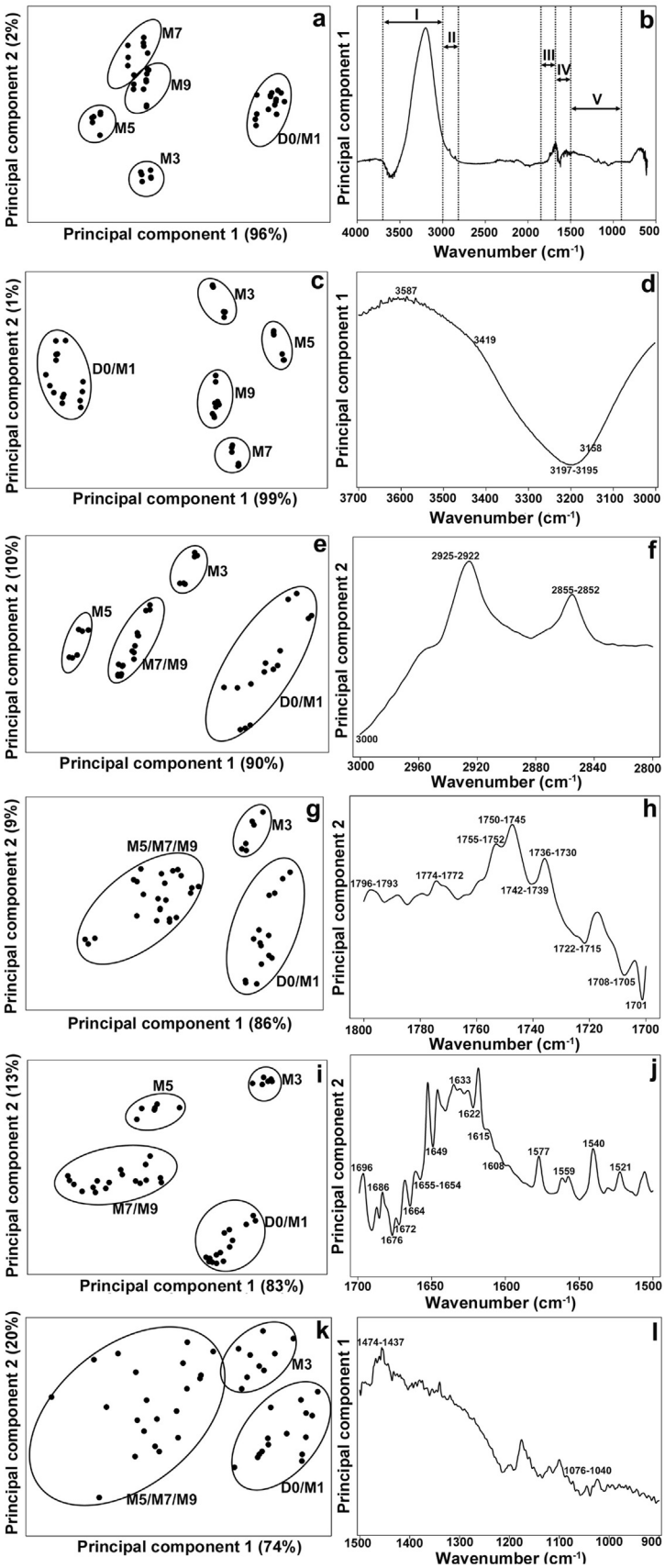

Fig. 4. Principal component scores and loading plots of spectra of UHT whole milk samples acquired at day 0 (D0) and after 1, 3, 5, 7 and 9 months (M1, M3, M5, M7 and M9, respectively) of storage for spectral ranges: (a, b) 4000–600 cm^{-1}; (c, d) region I, 3700–3000 cm^{-1}; (e, f) region II, 3000–2800 cm^{-1}; (g, h) region III, 1800–1700 cm^{-1}; (i, j) region IV, 1700–1500 cm^{-1}; (k, l) region V, 1500–900 cm^{-1}.

Please cite this article in press as: Grewal, M. K., et al., Predicting sediment formation in ultra high temperature-treated whole and skim milk using attenuated total reflectance-Fourier transform infrared spectroscopy, *International Dairy Journal* (2017), http://dx.doi.org/10.1016/j.idairyj.2017.01.004

separating D0 samples from the others. PC2 explained 2% of the variance and classified storage samples except D0 into different groups (Fig. 3e). Similar trend was observed in WM with PC1 and PC2 explaining 90% and 10% of the variance, respectively. Variables with highest loadings in both SM (Fig. 3f) and WM, and able to produce similar classification patterns as the whole region were 3000, 2925–2922, 2855–2852 cm^{-1}. Changes in fat B region clearly separated M1 samples from D0 samples, implying a marked change in SM only after a month-long storage at 20 °C. In contrast, in WM, M1 samples were not placed far from D0 samples in the score plot (Fig. 4f). The changes were in accordance with the trend of sedimentation (Table 1). In contrast to a significant increase in SM, sedimentation in WM did not increase substantially ($P > 0.05$) during the first month of storage.

Similar patterns were observed during 28 days storage under accelerated storage conditions (Grewal et al., 2017a). Decrease in loadings for 2926 cm^{-1} (asymmetric stretching modes of CH_2 groups of acyl chains of milk lipids) and 2857 cm^{-1} (symmetric stretching modes of CH_2 groups of acyl chains of triglycerides and phospholipids) with storage time could be due to building up of protein-lipid associations resulting in decrease in their intensity. These associations may be due to structural changes in lipids itself or in milk proteins, which are constituents of homogenised fat globule membrane.

3.3.3. Fat A, 1800–1700 cm^{-1}

Similar to fat B region, fat A also classified storage samples into different groups in both SM and WM irrespective of fat content implying significant changes in this region. In SM, first two principal components explained 89% and 5% of variance, respectively (Fig. 3g). In WM first two principal components explained 86% and 9% of variance, respectively (Fig. 4g). The variables with highest loading in SM and WM, able to produce similar classification patterns as the whole region, were 1701, 1708–1705, 1722–1715, 1736–1730, 1742–1739, 1745–1744, 1750–1747, 1755–1752, 1774–1772, 1796–1793 cm^{-1} (Figs. 3h and 4h). High loading for 1755–1752 cm^{-1} was also observed at higher storage temperatures (Grewal et al., 2017a) and could be linked to protein–lipid association via carbonyl groups (Surewicz, Moscarello, & Mantsch, 1987) thus changing C=O stretching vibrations of ester linkage pertaining to triacylglycerols (Karoui, Mazerolles, & Dufour, 2003). Higher loading around 1722–1715 cm^{-1} has been associated previously with the presence of advanced Maillard products (AMP) associated with high storage temperatures (Grewal et al., 2017a). High loadings for these samples at 20 °C also suggested the occurrence of products due to Maillard reaction even at ambient temperature, which was supported by an increase in b* value.

Similar changes were observed in SM and WM at accelerated temperatures and were attributed to a phase change of lipids above 40 °C (Grewal et al., 2017a). High loading for these wavenumbers at 20 °C in the current study also indicated structural changes in lipids and their association with proteins, progressing even at ambient temperatures which does not necessarily involve phase transition and might be due to presence of possible cross-linkers such as AMP and increase in calcium content in the serum phase (Table 2). Interestingly, changes in the fat region in SM were intense enough to be detected by FTIR despite of its lower content in these samples.

3.3.4. Amide I and II, 1700–1500 cm^{-1}

Amide I (1700–1600 cm^{-1}) and amide II (1600–1500 cm^{-1}) regions correspond to C=O stretching vibrations of the peptide bonds and C–N stretching vibrations in combination with N–H bending, respectively (Kher, Udabage, McKinnon, McNaughton, & Augustin, 2007). As expected, this region in both SM (Fig. 3i) and WM (Fig. 4i) classified storage samples into different groups. In SM, PC 1 and 2 explained 83% and 12% of the variance, respectively. In WM, PC 1 and 2 explained 83% and 13% of the variance, respectively. PC1 separated D0, M1 and M3 samples from M5, M7 and M9 samples, mainly due to increase in loadings for 1696, 1686, 1681, 1677–1676, 1672–1671, 1665–1664, 1656–1654, 1649, 1644, 1641, 1633, 1622–1621, 1615, 1608 cm^{-1} (amide I) and 1576–1575, 1557–1555 and 1542–1539 cm^{-1} (amide II) (Figs. 3j and 4j). These variables were able to produce similar classification patterns as the whole region and thus were selected as markers for prediction of sedimentation.

Interestingly, almost similar wavenumbers had the highest loadings under accelerated storage temperatures (Grewal et al., 2017a). Formation of protein aggregates with pronounced intermolecular β sheets due to protein–protein and protein–lipid associations result in increase in loading at 1697, 1686 and 1622–1621 cm^{-1} (Mendelsohn & Flach, 2002; Mendelsohn, Mao, & Flach, 2010; Ngarize, Herman, Adams, & Howell, 2004; Sankaram & Marsh, 1993). In line with our earlier observations during short term storage at elevated temperatures (Grewal et al., 2017a), an increase in intermolecular β sheets (1686 and 1622–1621 cm^{-1}) in the current study was not followed with a concomitant decline in α-helix (1656–1654 cm^{-1}) and intramolecular β-sheet structure (1633 cm^{-1}). In addition, high loadings for 1656–1654, 1676 and 1645 cm^{-1} were attributed to rise in random coil structure during storage (Grewal et al., 2017a) due to increased participation of caseins in formation of aggregates supported by trends in PAGE patterns of bulk and serum phase (Figs. 1 and 2).

The increase in participation of caseins in aggregate formation as mentioned earlier could be related to dissociation of casein micelle as a result of increase in intra-micellar crosslinking. Loadings for wavenumbers in amide II region for 1576–1575, 1557–1555 and 1542–1539 cm^{-1} had been attributed to changes in amount of β-turns, α-helices/loops and β-sheets, respectively, during storage at elevated temperatures in UHT milk (Grewal et al., 2017a). Almost similar changes in the protein secondary structure, protein–protein and protein-lipid interactions during long term storage at 20 °C as observed in short term storage at elevated temperatures favoured the use of accelerated shelf-life stability testing.

3.3.5. Region V, 1500–900 cm^{-1}

This region was not able to separate samples clearly as achieved by other regions. In SM and WM, first two principal components explained 95% and 94% of variance, respectively (Figs. 3k and 4k). Wavenumber regions with highest loadings were 1474–1437 and 1076–1040 cm^{-1} (Figs. 3l and 4l) attributed to CH_2 scissoring of acyl chains of lipids (1500–1400 cm^{-1}) and various C–O vibrations in carbohydrates, mainly lactose during storage at elevated temperatures, respectively (Grewal et al., 2017a). High loadings for wavenumbers in this region hint at protein–lipid interactions and formation of AMP even at 20 °C.

3.4. Prediction of sediment using multivariate regression

Changes in protein interactions exhibited as an increase in formation of covalent aggregates in PAGE patterns seemed to steer build-up of sediment in both SM and WM. Spectral analysis discussed above highlighted the underlying structural changes resulting in formation of aggregates and hence the formation of sediment. PLS regression technique using a calibration set of samples in both SM and WM was employed to identify correlation in changes in spectral variables with sedimentation. The identified correlation was developed as a regression model for quantitative prediction of sediment during storage of UHT milk. The PLS model for SM and WM exhibited good R^2 values for calibration and validation as 0.88 and 0.85 and 0.91 and 0.86, respectively. Low values

Please cite this article in press as: Grewal, M. K., et al., Predicting sediment formation in ultra high temperature-treated whole and skim milk using attenuated total reflectance-Fourier transform infrared spectroscopy, *International Dairy Journal* (2017), http://dx.doi.org/10.1016/j.idairyj.2017.01.004

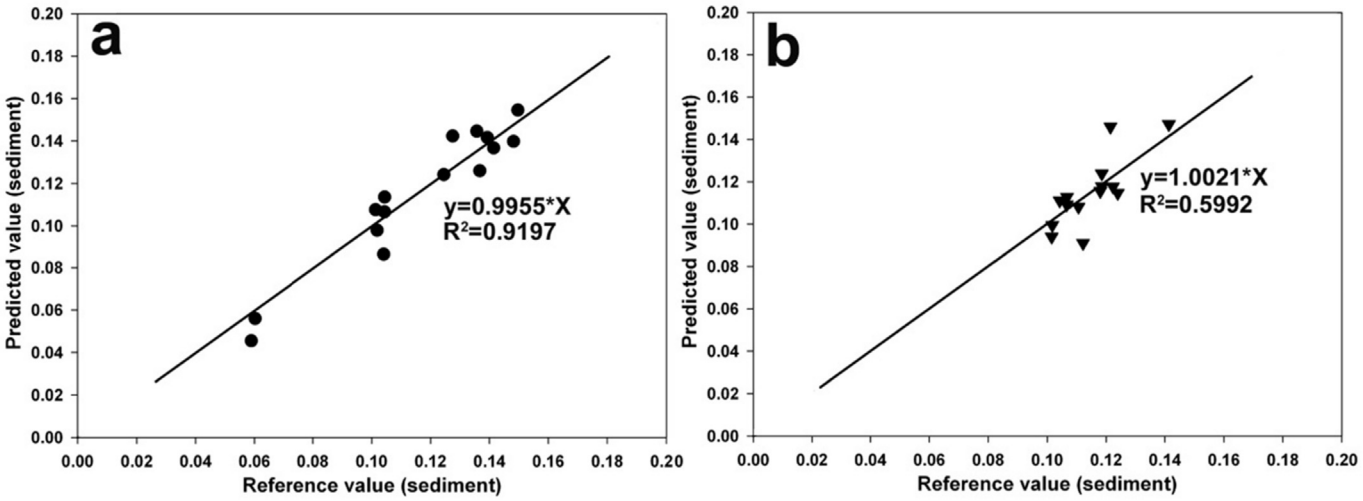

Fig. 5. Observed versus predicted amount of sediment in SM (a) and WM (b) for test set samples obtained using PLS regression.

of root mean square error of calibration and prediction in both SM (0.009 and 0.01, respectively) and WM (0.006 and 0.004, respectively) indicated better stability of prediction. However, when the developed model was tested using test SM and WM samples, prediction R^2 values were far better for SM (0.92) than for WM (0.60). The physical distribution of samples in scatter plots of observed versus predicted values (Fig. 5) obtained from the prediction model for detection for SM and WM further demonstrated that prediction in former was close to the experimental values. However, low predictability (low R^2) of the model for WM could be due to the influence of fat and can be probably improved by increasing number of samples analysed.

4. Conclusions

The increase in sediment concentration as an indicator of the shelf life stability for both SM and WM during long term storage at 20 °C was correlated with the FTIR spectral changes of the samples. PCA was able to specify marker variables, changes in which could be used to predict build-up of sediment in UHT milk, especially SM. Marker variables corresponded to structural changes in milk lipids, proteins and carbohydrates signifying that storage at 20 °C produced definite changes in these spectral regions. These changes were similar to those observed previously during accelerated shelf-life testing. Thus, our earlier concern that different types and rate of reactions at elevated storage temperatures could hinder the application of accelerated shelf-life testing appears to be unfounded. Use of accelerated temperatures could thus assist in reducing time required to predict the changes and estimate sedimentation, a measure of shelf-life of this product. In addition, though we were able to predict build-up of sediment from changes in spectral variables, further work is required to develop a model that could forecast sedimentation in advance. This would probably involve intentional inducement of instabilities in samples and identify corresponding changes in the spectra.

Acknowledgements

This work was supported by the Department of Business and Innovation of the Victorian Government, through its Victoria India Doctoral Scholarship Program (managed by the Australia India Institute). The first author also acknowledges her employer, Indian Council of Agricultural Research, for granting study leave to pursue a Ph.D.

References

Brunner, J. (1962). Protein-lipid interactions and their relation to the physical-chemical stability of concentrated milk. A review. *Journal of Dairy Science, 45*, 943–951.

Chandrapala, J., McKinnon, I., Augustin, M. A., & Udabage, P. (2010). The influence of milk composition on pH and calcium activity measured in situ during heat treatment of reconstituted skim milk. *Journal of Dairy Research, 77*, 257–264.

Choperena, A., & Painter, P. (2009). Hydrogen bonding in polymers: Effect of temperature on the OH stretching bands of poly(vinylphenol). *Macromolecules, 42*, 6159–6165.

Dalgleish, D. G. (1992). Sedimentation of casein micelles during the storage of ultra-high temperature milk products—A calculation. *Journal of Dairy Science, 75*, 371–379.

Deeth, H., & Lewis, M. (2016). Protein stability in sterilised milk and milk products. In P. L. H. McSweeney, & J. A. O'Mahony (Eds.), *Proteins: Applied aspects: Vol. 1B. Advanced dairy chemistry* (pp. 247–286). New York, NY, USA: Springer US.

Garcia-Risco, M. R., Ramos, M., & Lopez-Fandino, R. (1999). Proteolysis, protein distribution and stability of UHT milk during storage at room temperature. *Journal of the Science of Food and Agriculture, 79*, 1171–1178.

Grewal, M. K., Chandrapala, J., Donkor, O., Apostolopoulos, V., Stojanovska, L., & Vasiljevic, T. (2017a). Fourier transform infrared spectroscopy analysis of physicochemical changes in UHT milk during accelerated storage. *International Dairy Journal, 66*, 99–107.

Grewal, M. K., Chandrapala, J., Donkor, O., Apostolopoulos, V., & Vasiljevic, T. (2017b). Electrophoretic characterization of protein interactions suggesting limited feasibility of accelerated shelf-life testing of ultra-high temperature milk. *Journal of Dairy Science, 100*, 76–88.

Holland, J. W., Gupta, R., Deeth, H. C., & Alewood, P. F. (2011). Proteomic analysis of temperature-dependent changes in stored UHT milk. *Journal of Agricultural and Food Chemistry, 59*, 1837–1846.

Huppertz, T. (2016). Heat stability of milk. In P. L. H. McSweeney, & J. A. O'Mahony (Eds.), *Proteins: Applied aspects: Vol. 1B. Advanced dairy chemistry* (pp. 179–196). New York, NY, USA: Springer US.

Karoui, R., Mazerolles, G., & Dufour, É. (2003). Spectroscopic techniques coupled with chemometric tools for structure and texture determinations in dairy products. *International Dairy Journal, 13*, 607–620.

Kher, A., Udabage, P., McKinnon, I., McNaughton, D., & Augustin, M. A. (2007). FTIR investigation of spray-dried milk protein concentrate powders. *Vibrational Spectroscopy, 44*, 375–381.

McMahon, D. J. (1996). Age-gelation of UHT milk: Changes that occur during storage, their effect on shelf life and the mechanism by which age-gelation occurs. In *Heat treatments and alternative methods. IDF Symposium, Vienna (Austria), 6–8 Sep 1995*. International Dairy Federation.

Mendelsohn, R., & Flach, C. R. (2002). Infrared reflection-absorption spectroscopy of lipids, peptides, and proteins in aqueous monolayers. *Current Topics in Membranes, 52*, 57–88.

Mendelsohn, R., Mao, G., & Flach, C. R. (2010). Infrared reflection–absorption spectroscopy: Principles and applications to lipid–protein interaction in Langmuir films. *Biochimica et Biophysica Acta (BBA) – Biomembranes, 1798*, 788–800.

Ngarize, S., Herman, H., Adams, A., & Howell, N. (2004). Comparison of changes in the secondary structure of unheated, heated, and high-pressure-treated β-lactoglobulin and ovalbumin proteins using Fourier transform Raman spectroscopy and self-deconvolution. *Journal of Agricultural and Food Chemistry, 52*, 6470–6477.

Nieuwenhuijse, J. A., & van Boekel, M. A. (2003). Protein stability in sterilised milk and milk products. In P. L. H. McSweeney, & J. A. O'Mahony (Eds.), *Proteins:*

Please cite this article in press as: Grewal, M. K., et al., Predicting sediment formation in ultra high temperature-treated whole and skim milk using attenuated total reflectance-Fourier transform infrared spectroscopy, *International Dairy Journal* (2017), http://dx.doi.org/10.1016/j.idairyj.2017.01.004

Applied aspects: Vol. 1B. Advanced dairy chemistry (pp. 947–974). New York, NY, USA: Springer US.

Ramsey, J. A., & Swartzel, K. R. (1984). Effect of ultra high temperature processing and storage conditions on rates of sedimentation and fat separation of aseptically packaged milk. *Journal of Food Science, 49*, 257–262.

Sankaram, M. B., & Marsh, D. (1993). Protein-lipid interactions with peripheral membrane proteins. *New Comprehensive Biochemistry, 25*, 127–162.

Sharma, S. K., & Dalgleish, D. G. (1993). Interactions between milk serum proteins and synthetic fat globule membrane during heating of homogenized whole milk. *Journal of Agricultural and Food Chemistry, 41*, 1407–1412.

Surewicz, W. K., Moscarello, M. A., & Mantsch, H. H. (1987). Fourier transform infrared spectroscopic investigation of the interaction between myelin basic protein and dimyristoylphosphatidylglycerol bilayers. *Biochemistry, 26*, 3881–3886.

Walstra, P., Jenness, R., & Badings, H. T. (1984). *Dairy chemistry and physics*. New York, NY, USA: Wiley.

Ye, A., Singh, H., Taylor, M. W., & Anema, S. (2002). Characterization of protein components of natural and heat-treated milk fat globule membranes. *International Dairy Journal, 12*, 393–402.

Please cite this article in press as: Grewal, M. K., et al., Predicting sediment formation in ultra high temperature-treated whole and skim milk using attenuated total reflectance-Fourier transform infrared spectroscopy, *International Dairy Journal* (2017), http://dx.doi.org/10.1016/j.idairyj.2017.01.004

CHAPTER 6

FTIR fingerprinting of structural changes of milk proteins induced by heat treatment, deamidation and dephosphorylation

This chapter has been published as a research paper entitled "FTIR fingerprinting of structural changes of milk proteins induced by heat treatment, deamidation and dephosphorylation" by Manpreet Kaur Grewal, Thom Huppertz. and Todor Vasiljevic in the peer reviewed journal, Food Hydrocolloids 80, 160-167 (2018).

VICTORIA UNIVERSITY
MELBOURNE AUSTRALIA

GRADUATE RESEARCH CENTRE

DECLARATION OF CO-AUTHORSHIP AND CO-CONTRIBUTION: PAPERS INCORPORATED IN THESIS BY PUBLICATION

This declaration is to be completed for each conjointly authored publication and placed at the beginning of the thesis chapter in which the publication appears.

1. PUBLICATION DETAILS (to be completed by the candidate)

Title of Paper/Journal/Book:	FTIR fingerprinting of structural changes of milk proteins induced by heat treatment, deamidation and dephosphorylation
Surname:	Grewal
First name:	Manpreet Kaur
College:	College of Health & Biomedicine
Candidate's Contribution (%):	80

Status:

Accepted and in press:	☑	Date:	08 02 2018
Published:	☐	Date:	

2. CANDIDATE DECLARATION

I declare that the publication above meets the requirements to be included in the thesis as outlined in the HDR Policy and related Procedures – policy.vu.edu.au.

Manpreet Kaur Grewal Digitally signed by Manpreet Kaur Grewal Date: 2018.02.18 10:50:38 +11'00'	18.02.2018
Signature	**Date**

3. CO-AUTHOR(S) DECLARATION

In the case of the above publication, the following authors contributed to the work as follows:

The undersigned certify that:

1. They meet criteria for authorship in that they have participated in the conception, execution or interpretation of at least that part of the publication in their field of expertise;
2. They take public responsibility for their part of the publication, except for the responsible author who accepts overall responsibility for the publication;
3. There are no other authors of the publication according to these criteria;
4. Potential conflicts of interest have been disclosed to a) granting bodies, b) the editor or publisher of journals or other publications, and c) the head of the responsible academic unit; and

VICTORIA UNIVERSITY
MELBOURNE AUSTRALIA

5. The original data will be held for at least five years from the date indicated below and is stored at the following **location(s)**:

College of Health & Biomedicine
Institute of Sustainable Industries and Liveable cities
Victoria University
Australia

Name(s) of Co-Author(s)	Contribution (%)	Nature of Contribution	Signature	Date
Manpreet Kaur Grewal	80	Concept development, research design, experiment execution, statistical analysis, interpretation, drafting manuscript and its revision	Manpreet Kaur Grewal Digitally signed by Manpreet Kaur Grewal Date: 2018.02.22 16:03:35 +11'00'	22 02 2018
Todor Vasiljevic	10	Concept development, experimental design, illustrations and manuscript revision	Todor Vasiljevic Digitally signed by Todor Vasiljevic DN: cn=Todor Vasiljevic, o, ou, email=todor.vasiljevic@vu.edu.au, c=AU Date: 2018.02.23 14:01:07 +11'00'	23.02.18
Thom Huppertz	10	Concept and concept development, manuscript revision	Thom Huppertz Digitally signed by Thom Huppertz Date: 2018.02.23 10:19:18 +01'00'	23.02.18

Food Hydrocolloids 80 (2018) 160–167

Contents lists available at ScienceDirect

Food Hydrocolloids

journal homepage: www.elsevier.com/locate/foodhyd

FTIR fingerprinting of structural changes of milk proteins induced by heat treatment, deamidation and dephosphorylation

Manpreet Kaur Grewal [a], Thom Huppertz [a, b], Todor Vasiljevic [a, *]

[a] Advanced Food Systems Research Unit, College of Health and Biomedicine, Victoria University, Melbourne, VIC 8001, Australia
[b] Friesland Campina, Amersfoort, The Netherlands

ARTICLE INFO

Article history:
Available online 8 February 2018

ABSTRACT

Changes in protein structure and interactions during processing and storage of UHT milk affect its shelf-life. In our previous study, we demonstrated that changes in FTIR spectra correlate well with the development of a sediment (a storage instability) during storage. However, due to a number of possible changes during heating and storage, conformational changes specific to a particular interaction among milk proteins remain largely unknown. The aim of the current study was to evaluate the possibility of fingerprinting two selected changes, i.e., deamidation and dephosphorylation, using FTIR. Enzymatic deamidation and dephosphorylation were carried out prior to heat treatment. Principal component analysis revealed that heat treatment induced different changes in their secondary structure of control, deamidated and dephosphorylated milk samples. In contrast to a significant ($P < 0.05$) decrease in β-sheet (1624 cm^{-1}) with rise in β-turns (1674 cm^{-1}) in heated control samples, both deamidation and dephosphorylation of skim milk before heat treatment created more ordered secondary structure, significant ($P < 0.05$) increase in α-helix (1650-52 cm^{-1}) and β-sheet in milk proteins at expense of 3_{10}-helix (1661 cm^{-1}), random (1645-46 cm^{-1}) and β-turn (1674 cm^{-1}). The only difference between heated deamidated and dephosphorylated samples, when compared to unheated samples, was decrease in large loops (1656 cm^{-1}) in the latter opposed to the increase in the former. The outcomes from this study can be applied for different interactions and help to arrive to a complete understanding of the conformational changes affecting the storage stability of UHT milk.

1. Introduction

Milk is kinetically stable mixture of mainly three colloidal particles, namely fat droplets stabilized by mixture of lipoproteins and bilayer structures, casein micelles sterically stabilized by hairy layer of κ-casein, and whey proteins and their oligomers. Raw milk is largely stable against aggregation, flocculation or coalescence with the exception of creaming of fat globules due to gravitational effects. However, heat treatment, necessary to provide required safety levels and stabilize the system against spoilage, affects the original colloidal structure and these otherwise non-interacting colloids start to interact resulting in both desired and undesired changes in the milk depending on the end use. One such heat treatment of milk, which is the focus of the current work, ultra-high temperature (UHT) processing involves heating of milk at a high temperature (135–145 °C) for a short duration (1–10 s) followed by aseptic packaging, enabling its storage at room temperature for up to 9 months (Deeth & Lewis, 2016; Malmgren et al., 2017). In addition to long shelf-life, high temperature treatment induces certain physio-chemical changes, which progress during storage and may sometimes detrimentally affect the stability and hence the shelf life of UHT milk.

Some of the storage instabilities namely, sedimentation and gelation, involve aggregation of milk proteins, which is preceded by changes in their structure and interactions. In our previous study, we have observed that changes in FTIR spectra during storage could successfully predict development of a sediment (Grewal et al., 2017a; Grewal, Chandrapala, Donkor, Apostolopoulos, & Vasiljevic, 2017c). Increases in the sediment weight during long term storage of UHT milk were preceded by a rise in intermolecular β-sheet (1618, 1687 and 1696 cm^{-1}), without an expected decrease in the intramolecular β-sheet (1630 cm^{-1}) and α-helix structures (1653 cm^{-1}) of milk proteins. These overall changes in the structure of proteins were attributed to different heat- and storage-induced

* Corresponding author.
E-mail address: todor.vasiljevic@vu.edu.au (T. Vasiljevic).

https://doi.org/10.1016/j.foodhyd.2018.02.010
0268-005X/

structural modifications and interactions of proteins. These changes involve denaturation of β-lactoglobulin (β-Lg) and α-lactalbumin (α-La) on heating leading to intramolecular and intermolecular thiol-disulfide exchange reactions with mainly κ-casein (κ-CN) present on the surface of the casein micelles (Sharma & Dalgleish, 1993), reactions between lactose and lysine residues initiating covalent crosslinking via Maillard reaction products, dephosphorylation of phosphoserine residues and deamidation of asparagine and glutamine residues (Deeth & Lewis, 2016). Heat-induced dephosphorylation of phosphoserine residues proceeds mainly by hydrolysis, resulting in the formation of serine residue, and to a comparatively lesser extent formation of dehydroalanine via β-elimination (van Boekel, 1999). The dehydroalanine formed may further react with the ε-amino group of lysine residues, imidazole group of histidine or thiol group of cysteine resulting in intra or intermolecular crosslinks, respectively (Al-Saadi & Deeth, 2008; Holland, Gupta, Deeth, & Alewood, 2011; Horne, 2016; O'connell & Fox, 2003; Singh, 1991). Deamidation has been reported to increase significantly with storage of UHT milk especially at elevated storage temperatures (Deeth & Lewis, 2016; Holland et al., 2011). Deamidation of the casein residues increased the negative charge on the protein, which may destabilise the micelle or even lead to micellar disintegration (Miwa, Yokoyama, Wakabayashi, & Nio, 2010). Furthermore, high rates of sedimentation were also observed at elevated storage temperatures (Grewal et al., 2017a; Malmgren et al., 2017; Nieuwenhuijse & van Boekel, 2003).

Nevertheless, we now have an idea of overall changes in the secondary structure and related protein interactions leading to storage instability in UHT milk, however conformational adjustments corresponding to individual protein interactions remain largely unknown. This information could assist in improving predictive ability of our model to predict sedimentation in UHT milk and identify the main interactions responsible for this storage instability. Thus, the aim of the current research paper was to evaluate possibility of fingerprinting several selected mechanisms involved in structural changes of proteins using FTIR. Raw skim milk was thus enzymatically deamidated or dephosphorylated before heat treatment under simulated UHT conditions (143 °C for 3 s). The extent of deamidation and dephosphorylation was chosen based on a preliminary study, in which several levels of enzyme additions were tested to provide impacts comparable to those observed in UHT skim milk samples stored at 20 °C for twelve months. The samples were then investigated for changes in their FTIR spectra with the aim to identify and quantify underlying changes in the secondary structure of proteins associated specifically with deamidation and dephosphorylation.

2. Material and methods

2.1. Materials

Protein-glutaminase (PG) (glutaminase SD-C100S with activity of 100 GTU/g) was obtained from Amano Enzyme, Inc. (Nagoya, Japan). One glutaminase unit (GTU) of activity was defined as the amount of enzyme that formed 1 μmol of L-glutamic acid from L-glutamine (final concentration 1%) at 37 °C, pH 6.0. Calf intestinal alkaline phosphatase (AP) (20 units/μl) was purchased from Promega Corporation (Madison, WI, USA). One unit of activity was defined as the amount of enzyme required to catalyze the hydrolysis of 1 μmol of 4-nitrophenyl phosphate per minute at 37 °C in 1 M diethanolamine, 10.9 mM 4-nitrophenyl phosphate and 0.5 mM $MgCl_2$ (pH 9.8).

2.2. Deamidation and dephosphorylation of milk and heat treatment

Raw milk was obtained from Murray Goulburn Cooperative Co. Ltd (Laverton, Victoria, Australia). Experimental skim milk samples were prepared by adding sodium azide (0.02%) followed by equilibration to 40 °C for 30 min and then centrifuging at 40 °C at 3220 g for 30 min (Eppendorf AG, Hamburg, Germany) to remove the fat. Skimmed milk samples were again equilibrated to 40 °C for 1 h before incubating with 0.065 units of PG or 720 units AP per g milk protein for 3 h at 40 °C. After incubation, all samples were heated using an oil bath to 143 °C (heating rate of 93 °C/min), held for 3 s at this temperature and then cooled immediately by immersion in an ice bath. The control sample was not treated with an enzyme but was subjected to the same incubation and heat treatment. Raw, control, PG- and AP-treated samples were referred in the following text as unheated, heated, heated PG-treated and heated AP-treated samples respectively. The samples were prepared in duplicate.

UHT skim milk samples from the previous storage study (Grewal et al., 2017c) were stored for 12 months at 20 °C and assessed for the extent of deamidation and dephosphorylation at the start and end of the storage study. The skim milk was processed using an indirect UHT treatment (138 °C, 6s) as described in detail in Grewal et al. (2017a).

2.3. Determination of extent of deamidation and dephosphorylation

The amount of ammonia released in heated PG-treated and commercial UHT milk samples was used as an indicator of the extent of deamidation and was determined using an ammonia kit (R-Biopharm – Laboratory Diagnostics Pty Ltd, Sydney, New South Wales, Australia) as described previously (Miwa et al., 2010). The deamidation degree was expressed as the percentage of the total released ammonia when milk was treated with 2 N HCl at 100 °C for 4 h, i.e., after complete deamidation. The extent of dephosphorylation was estimated in heated AP-treated and commercial UHT milk samples by quantifying soluble inorganic phosphate content, which increases on dephosphorylation of SerP residues, following a method developed by Lorient and Linden (1976) and improved by McKie and McCleary (2016) with minor modifications. The quantification was carried out with a standard curve of potassium dihydrogen phosphate with a concentration range of 0–200 mg L^{-1}. The supernatant (1mL) from the ultracentrifuged milk (100,000 g for 90 min using a Beckman Optima L-70 ultracentrifuge with a type 70. ITI rotor; Beckman Instruments Inc., Palo Alto, CA, USA) was treated with 24% TCA (4 mL), vortexed and held for 10 min to allow for a complete protein precipitation. The treated sample was then centrifuged (Eppendorf AG, Hamburg, Germany) at 20 °C and 3000 g for 15 min. The supernatant was decanted and exactly was made up to 10 mL with Milli-Q water and the absorbance was recorded at 655 nm using a spectrophotometer (Biochrom LibraS11, Cambridge, UK). The blank included Milli-Q water instead of the sample. Extent of dephosphorylation was calculated from the increase in the amount of soluble inorganic phosphate in the heated AP-treated sample relative to the heated control and based on the theoretical amount of phosphoserine (SerP) residues in the samples. The measured protein content in the UHT and treated raw samples was 34.0 and 37.1 g/L, respectively. The theoretical calculation was based on the casein/whey protein ratio of 4:1, and a ratio of individual caseins for α_{s1}, α_{s2}, β and κ-caseins of 4:1:3.5:1.5, respectively (Huppertz, 2013). The levels of phosphorylation were assumed to be 8, 11, 5 and 1 for α_{s1}, α_{s2}, β and κ-casein, respectively (Huppertz, 2013).

2.4. FTIR measurements

FTIR spectra were acquired in duplicate in the range of 4000–600 cm^{-1} using a PerkinElmer Frontier FTIR spectrometer (PerkinElmer, Boston, MA, USA) with a resolution of 2 cm^{-1} and averaging 16 scans for each spectrum. Approximately 0.5 mL of sample was added onto an attenuated total reflectance (ATR) cell. The spectra of three sub samples of each sample were taken by refilling the ATR cell. A background spectrum was scanned at the beginning of the measurements with a blank Diamond ATR cell using same instrumental conditions as for the sample spectra acquisition.

2.5. Spectral data analysis

The FTIR spectra of all samples were exported to an Unscrambler software (Version 10.2, CAMO AS, Trondheim, Norway). Spectra were baseline corrected, normalized and then the water spectrum was subtracted as described previously (Grewal et al., 2017a). The spectra of the milk showed five major characteristic regions after subtraction of water bands namely 3700-3000 cm^{-1} (hydrogen bonding; water-related), 3000-2800 cm^{-1} (lipids; fat B); 1800-1700 cm^{-1} (lipids; fat A), 1700-1500 cm^{-1} (amide I and II) and 1500-900 cm^{-1} (amide III and carbohydrates). As this study aimed at establishing changes in the secondary structure of proteins produced by deamidation and dephosphorylation, principal component analysis (PCA) was employed only on the protein amide I and II region spanning from 1700 to 1500 cm^{-1}. PCA assisted in investigating whether the changes recorded by this protein region were significant enough to classify milk samples into different groups. PCA score plots obtained demonstrate groupings whereas loading plots aided to identify wavenumbers which have high loadings or contributed the most in classification of samples into different groups.

Based on PCA results, only the amide I spectra were further subjected to quantitative analysis of the secondary structure using a nonlinear curve fitting procedure. Amide I was preferred because of its high sensitivity to small variations in molecular geometry and hydrogen bonding patterns originating mainly from C=O stretching frequency unlike combination of C-N and N-H bending in amide II. Furthermore, the amide II region has also been reported to have indistinct peaks and large errors associated with their integrated areas (Curley, Kumosinski, Unruh, & Farrell, 1998).

2.5.1. Quantitative analysis of changes in secondary structure

Changes in the secondary structure of proteins were obtained by curve fitting of the second derivative of amide I envelope by a procedure described elsewhere (Yang, Yang, Kong, Dong, & Yu, 2015). Curve fitting process was applied to the second derivative spectra and not to the deconvoluted one to ensure the fitted curves reflect closely the secondary structure of the samples (Yang et al., 2015). Briefly, the water-subtracted spectra of the amide I region were derivatized (polynomial order 2, Savitzky-Golay algorithm with 11-point smoothing). The derivatized spectra were further smoothed (moving average 7 points) and normalized for amide I band to remove the white noise resulting from the calculation of the second derivative function. The peaks were identified and fitted with a Gaussian function using the Peak fit procedure in an Origin software (Origin Pro 2017, Origin Lab Corp, Northampton, MA, USA). The program iterated the curve-fitting process, and in each iteration, the characteristic parameters (height, bandwidth, position and baseline) were varied to calculate the parameters that would result in the best fit of the original protein spectrum using Gaussian shaped curves. Optimal fits to spectra were indicated by reduced chi-square values and it was ensured visually that fit does not include assigned peaks below the baseline or with too broad or too narrow bandwidths. The peak fit observed in this study had chi-square values in the range of 1.5×10^{-6}. Fig. 3a-c shows a typical curve fit with the residual plots indicating quality of the fit. The residuals for the Gaussian fits were random and also had low values (±0.006) implying a good fit (Curley et al., 1998). Once the fit was found satisfactory, the band area for each component peak assigned to specific secondary structure described below was used to calculate the relative contribution of component to a particular secondary structure. Significance of changes in the secondary structure was further evaluated at 95% confidence level using one way ANOVA followed by Tukey's HSD multi-comparison test (IBM SPSS Statistics 25).

2.5.2. Assignment of the fitted peaks

The assignment of the fitted peaks to specific secondary structures was based on the information in the literature, generally obtained from known globular proteins. In this study, we mainly followed band assignments compiled by Yang et al. (2015) for proteins in the aqueous solution. Six protein secondary structural types namely α-helix (1654-1658 cm^{-1}), β-sheet (1623-43 and 1689-1698 cm^{-1}), β-turns (1666-1687 cm^{-1}), random coils (1646-1650 cm^{-1}) and 3_{10}-helix (1660-1666) were assigned to different peaks in the second derivative spectra. However, as reported by Curley et al. (1998), we also observed that milk spectra after derivatization contained a band around 1656 cm^{-1}. Therefore, in order to avoid overestimating the content of α-helix structural element in the milk sample which contains 80% caseins, we used the rationale developed by Curley et al. (1998) and placed the elements centering on 1656 cm^{-1} into a separate category termed large loops. Curley et al. (1998) arrived on this band assignment for large loops on the basis of NMR structural studies of the α_{s1}-CN peptide (f 59-79) (Huq, Cross, & Reynolds, 1995) and β-CN peptide (Wahlgren, Léonil, Dejmek, & Drakenberg, 1993) demonstrating large loop structures for the phosphoserine-containing segment. The summary of assignments of the secondary structure for unheated, heated, heated PG-treated and heated AP-treated skim milk samples are shown in Tables 1 and 2.

3. Results

3.1. Extent of deamidation and dephosphorylation

The degree of deamidation in heated PG-treated milk was assessed as 2.26% which corresponded to 0.86 mM of ammonia released. Similarly, the percent dephosphorylation in heated AP-treated milk was 1.29% derived from 0.10 mM rise in inorganic phosphate concentration in the serum in heated AP-treated compared to the control and the theoretically calculated content of SerP in the sample of 7.7 mM. The values were comparable to the degree of deamidation and the recorded in UHT milk after one year of storage at 20 °C, which were 1.79% (corresponding to 0.76 mM of ammonia released) and 1.26% dephosphorylation, which corresponded to 0.09 mM of released inorganic phosphate and based on the theoretically calculated content of SerP in the sample of 7.1 mM, respectively.

3.2. FTIR spectra

Water subtracted and smoothed spectra of unheated, heated, heated PG-treated and heated AP-treated skim milk were shown for the amide I and II regions in Fig. 1. Amide I (1700-1600 cm^{-1}) corresponds mainly to C=O stretching vibrations of the peptide bonds and amide II (1600-1500 cm^{-1}) attributed to C-N stretching vibrations in combination with N-H bending (Curley et al., 1998;

Table 1
Total percentage areas of different secondary structures in amide I.

Conformational element	Wavenumber	Area, %				SE[a]
		Unheated	Heated	Heated PG-treated	Heated AP-treated	
Total β-sheet	1619-1642 1688-1697	49.2^{ab}	44.8^{a}	52.0^{b}	52.3^{b}	1.3
Random	1644–48	14.6^{a}	13.8^{ba}	12.8^{b}	12.5^{b}	0.4
α-helix	1651–53	3.6^{a}	3.5^{a}	7.8^{b}	13.0^{c}	0.4
Large loops	1656–58	3.6^{ac}	5.4^{ba}	6.1^{b}	2.6^{c}	0.4
3_{10}-helices	1661–64	6.1^{a}	8.4^{a}	2.5^{b}	3.5^{b}	0.7
Total β-turn	1667–1684	16.4^{a}	20.2^{b}	14.3^{c}	14.0^{c}	0.4

[a,b,c] Means in the same row that do not share the same small letters differ significantly ($P < 0.05$).
[a] Standard error for all summed up data for a particular secondary structure; n = 2.

Table 2
Percentage area of different peaks in amide I.

Band assignment	Unheated		Heated		Heated PG-treated		Heated AP-treated		SE[a]
	Band frequency	Area %	Band frequency	Area %	Band frequency	Area %	Band frequency	Area %	
β-sheet	1619	2.0	1619–20	2.3	1619	1.7	1619–21	2.6	1.5
β-sheet	1624	10.0^{a}	1623–24	4.6^{b}	1623	8.9^{a}	1623–25	4.9^{b}	0.8
β-sheet	1629–30	11.2^{a}	1628–1630	5.6^{a}	1629	13.8^{ab}	1630	21.9^{b}	3.0
β-sheet	1633–34	10.9	1633–34	13.8	1634–35	10.3	1635	9.0	5.0
β-sheet	1640	9.6	1640–41	9.6	1639–40	9.2	1639	6.2	2.7
β-sheet	1689	6.1	1688–89	4.4	1688	3.4	1690	5.0	2.8
β-sheet	1694	2.1^{a}	1693–94	4.5^{bc}	1692–93	4.7^{c}	1695	2.7^{ab}	0.7
β turn	1669	6.7^{a}	1668	5.8^{ba}	1668	4.78^{cb}	1666–67	2.8^{d}	0.4
β turn	1674	2.4^{a}	1674	6.4^{b}	1672–73	1.3^{a}	1674	2.4^{a}	0.3
β turn	1679	4.8^{a}	1678–79	6.8^{a}	1678–79	4.3^{ba}	1678	7.2^{ca}	0.7
β turn	1683	2.4^{a}	1682–83	1.2^{ba}	1682	4.0^{ca}	1683	1.6^{ba}	0.4

[a,b,c,d] Means in the same row that do not share the same small letters differ significantly ($P < 0.05$).
[a] Standard error for all summed up data for a particular secondary structure; n = 2.

Kher, Udabage, McKinnon, McNaughton, & Augustin, 2007).

Original spectra (Fig. 1A) revealed that heating without enzymes (heated) reduced the intensity for amide I and II bands as expected due to denaturation of whey proteins. Deamidating or dephosphorylating unheated milk enzymatically before heat treatment further reduced the intensity of these bands. The original spectra did not reveal sufficient information. However, when the above spectra were derivatized (polynomial order 2, Savitzky-Golay algorithm with 11-point smoothing), overlapping bands were clearly separated into distinct peaks and hence changes due to different treatments could be visualized (Fig. 1B). For example, a marked increase in a band around 1653 cm^{-1} was observed indicating increase in α-helical structure upon deamidation and dephosphorylation of milk prior to heat treatment. Other bands e.g. 1620, 1631, 1645, 1678, 1684, 1693 cm^{-1} also shifted, rearranged, increased or decreased (Fig. 1B). Before quantifying the changes in different bands and hence the corresponding secondary structure, PCA was employed to investigate whether the changes observed in the bands were significant enough to classify samples into different groups.

3.3. Principal component analysis

PCA was performed in the region 1700-1500 cm^{-1}. PC1, PC2 and PC3 explained 93, 4 and 2% of the variance, respectively (Fig. 2A). The PCA clearly separated unheated milk from heated, heated PG-treated and heated AP-treated samples implying significant changes in the protein secondary structure in each group (Karoui, Mazerolles, & Dufour, 2003; Mendelsohn, Mao, & Flach, 2010; Sankaram & Marsh, 1993). Wavenumbers with the greatest loading in amide I region were 1696, 1665-1667, 1646, 1653-56, 1631-36 and 1610-1605 cm^{-1} corresponding to intermolecular β-sheet, unordered, 3_{10}, α-helix, random, intramolecular β-sheet secondary structure and side chains of amino acids, respectively (Fig. 2B). The loading for 1697 cm^{-1} suggests varying degree of formation of aggregates consisting of intermolecular β-sheets in differently treated samples (Mendelsohn & Flach, 2002; Mendelsohn et al., 2010; Ngarize, Herman, Adams, & Howell, 2004). In addition, higher loading for random coil (1645 cm^{-1}) and turns (1676 cm^{-1}) suggest increased participation of caseins in formation of aggregates (Grewal et al., 2017a; Grewal, Chandrapala, Donkor, Apostolopoulos, & Vasiljevic, 2017b; Grewal et al., 2017c).

High loadings for wavenumbers in 1578-1555, 1555-1543 and 1542-1525 cm^{-1} region implied changes in the amount of β-turns, α-helices/loops and β sheets, respectively (Curley et al., 1998). As suggested in our previous studies (Grewal et al., 2017a; Grewal et al., 2017c), high loading for deamidated samples according to PC2 around 1575 cm^{-1} could be considered to arise from an increase in the $-COO^{-}$ asymmetric stretching vibrations of Glu residues due to deamidation of glutamine to glutamate by enzyme protein glutaminase. Similar, wavenumbers had high loadings in our previous study (Grewal et al., 2017c), in which storage of UHT milk at 20 °C induced changes in milk spectra, implying that inferences drawn in this study relate to similar interactions occurring during storage of UHT milk. However, it should be noted that loadings observed in the previous study were composite of all known and unknown interactions occurring during storage.

3.4. Quantification of changes in secondary structure

Results discussed above led us to conclude that heated, heated PG-treated and heated AP-treated samples experienced different changes in their secondary structure. The quantification of changes in the secondary structure was achieved through curve fitting of the amide I band only, as described in detail earlier in section 2.5. Table 1 summarizes the composite secondary structures from the

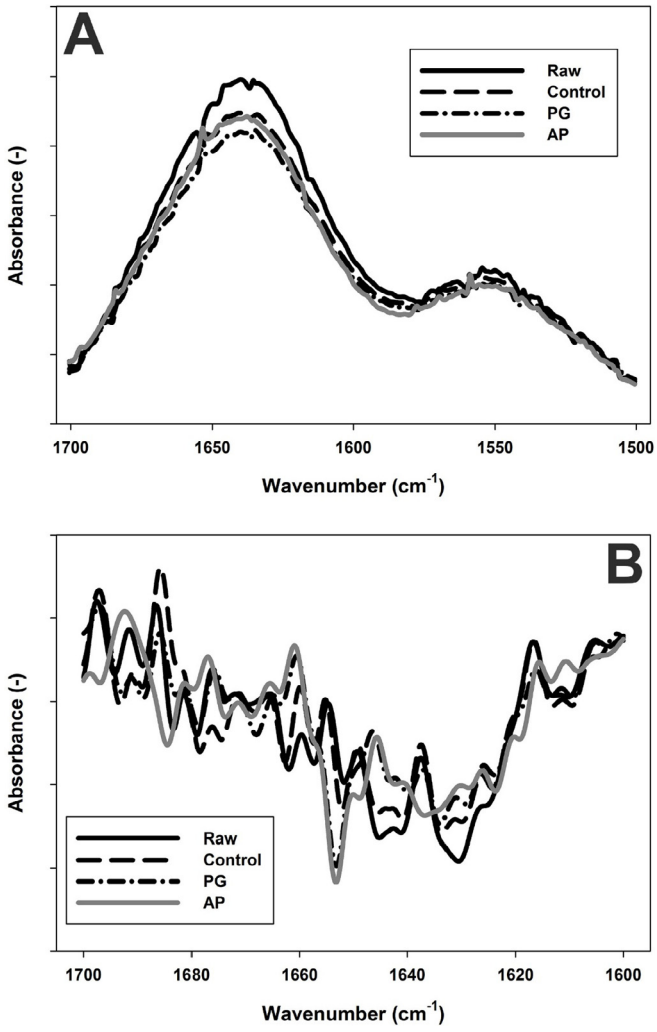

Fig. 1. Original FTIR (A) and second derivative (B) spectra of unheated, heated, heated PG-treated and heated AP-treated milk samples.

amide I region in unheated skim milk and milk subjected to different treatment combinations. Table 2 tabulates the percentage peak area of individual components of β-sheet and β turn structures.

Heating without enzymatic pre-treatment induced a significant increase only in the β-turn (1674 cm^{-1}) compared to unheated milk (Table 2). Although there was no significant change in total β-sheet (Table 1), β-sheet component at 1624 cm^{-1} corresponding to intramolecular β-sheet decreased from 10.0% to 4.6% ($P < 0.05$) and β-sheet component at 1694 cm^{-1} corresponding to intermolecular β-sheet aggregates increased from 2.1% to 4.5% (Table 2). Other secondary structures did not appear to be significantly affected by heating regime of the heated samples.

Structural changes induced by enzymatic deamidation of skim milk followed by heat treatment were quite different from those induced by heating only as also shown above by the PCA classification (Fig. 2A). On enzymatic deamidation prior to heat treatment, an overall increase ($P < 0.05$) in α-helix (1650-52 cm^{-1}), loops (1657 cm^{-1}) and β-sheet component (1694 cm^{-1}) was observed with concomitant decrease in random (1645 cm^{-1}), 3_{10}-helix (1661 cm^{-1}) and β-turn (1669 cm^{-1}) (Tables 1 and 2) indicating that the proteins had become more ordered.

Enzymatic dephosphorylation before heat treatment of skim milk samples resulted in an increase ($P < 0.05$) in α-helix (3.6–13.0%) and β-sheet component (1630 cm^{-1}) at the expense ($P < 0.05$) of β-sheet component (1624 cm^{-1}), random (14.6–12.5%), loops (3.6–2.6%), 3_{10}-helix (6.1–3.5%) and total β-turns (1668 cm^{-1}; 16.4 to 14.0%), implying an increase in an ordered structure like heated PG-treated samples (Tables 1 and 2). Although, the overall trend in the heated AP-treated samples was more or less similar to the heated PG-treated counterparts, the major difference when compared to unheated samples was variation in large loops (1656 cm^{-1}). In heated PG-treated samples, the amount of large loops increased significantly, from 3.6 to 5.4%, whereas in heated AP-treated samples, it decreased from 3.6 to 2.6%. The decrease in large loops confirmed dephosphorylation and ability of FTIR to detect it successfully as the above assignment at 1656 cm^{-1} for large loops has been assigned to the phosphoserine residues of the caseins (section 2.5.2). In addition, compared to the heated samples, both heated PG-treated and heated AP-treated samples demonstrated significant increase in total β-sheet. However, the increase in former was due to increase in the percentage area of β-sheet component at 1624 cm^{-1} whereas in the latter it was due to a component at 1630 cm^{-1}.

4. Discussion

Results above clearly demonstrate that FTIR can resolve and identify specific changes in the secondary structure of proteins in skim milk subjected to different treatments. The PCA analysis demonstrated that the treated milk samples were considerably different from each other and the principal wavenumbers corresponding to different secondary structures in amide I and II region were responsible for this difference. Further quantification of changes in secondary structure in amide I region using curve fitting helped to estimate the amount and direction of change indicated by PCA.

4.1. Effect of heating alone on the secondary structure

Heat treatment affects heat labile whey proteins the most, which have well defined secondary structure. Therefore, decrease in ordered secondary structure (mainly β-sheet, main structure in more heat labile β-Lg) on heating was expected. Thus, decrease ($P < 0.05$) in β-sheet component at 1624 cm^{-1} corresponding to intramolecular β-sheet (Table 2) could be attributed to denaturation of β-Lg (Qi, Ren, Xiao, & Tomasula, 2015). Furthermore, the observed increase ($P < 0.05$) in total β-turn could be due to interactions between κ-CN with β-Lg (predominantly) reported to lead to formation of loops, triple helices and turns (Dalgleish, 2011; Dalgleish & Corredig, 2012). Additionally, increase in β-turn could also be attributed to the dissociation of individual caseins from the casein micelles upon heating (Deeth & Lewis, 2016). Dissociation of individual caseins from the micelle was supported by an increase in the amount of caseins in the serum phase as observed in the reducing SDS-PAGE patterns in the heated compared to the unheated milk samples (data not shown).

4.2. Effect of enzymatic deamidation and dephosphorylation prior to heat treatment

Changes observed in the secondary structure in heated PG-treated and heated AP-treated samples were result of both enzymatic action and the heat treatment. Heat alone reduced significantly intramolecular β-sheet component and increased β-turn structure. However, when milk samples were deamidated or dephosphorylated before heat treatment considerable increase in α-helix was observed at expense of random, turns and triple helices

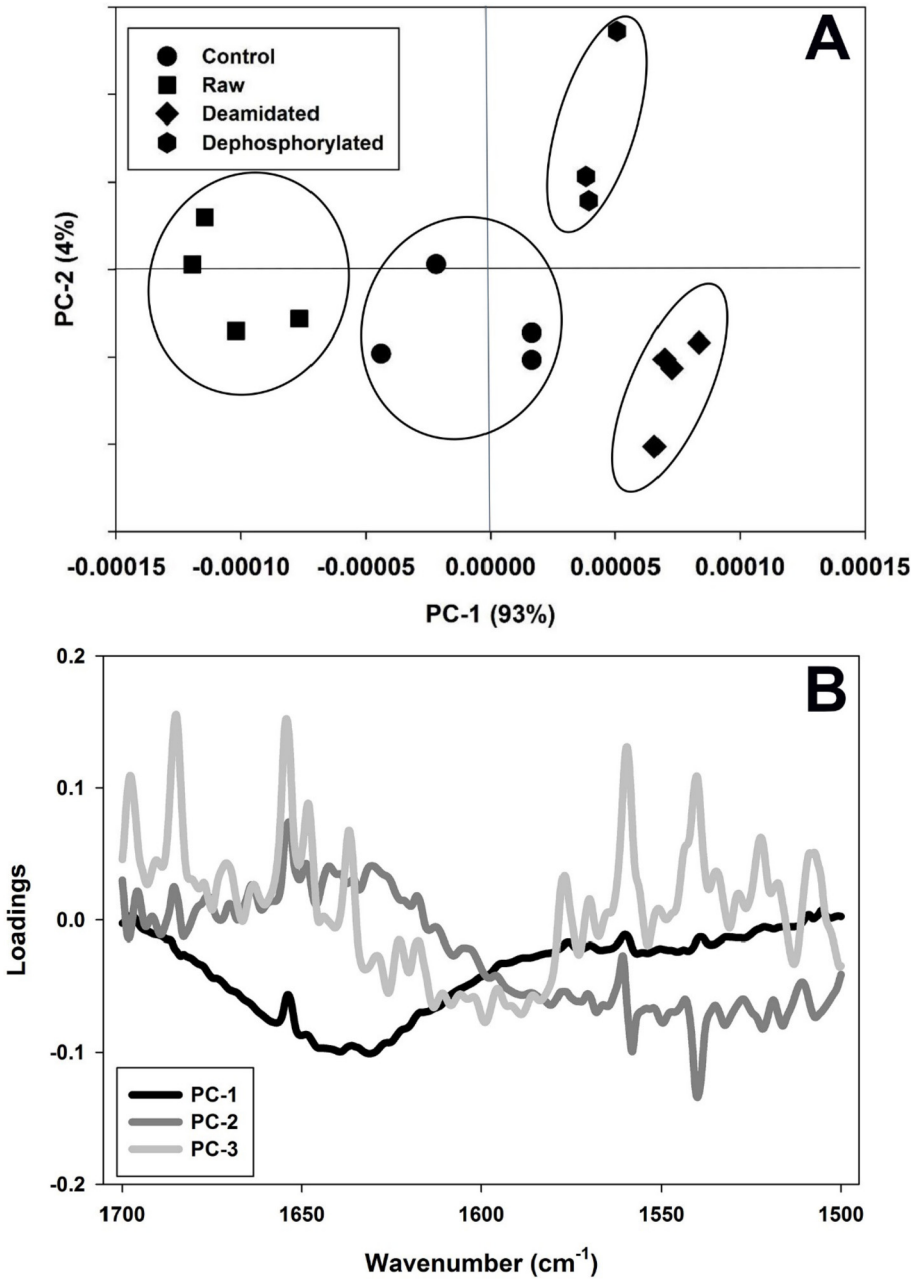

Fig. 2. Principal Component Analysis (A) score and (B) loading plot of unheated, heated, heated PG-treated and heated AP-treated skim milk samples in the 1700-1500 cm^{-1} region.

implying increase in the ordered structure. Only difference between two enzymatic treatments was significant increase in the loops on deamidation and decrease of the same upon dephosphorylation.

At low concentration of PG enzyme in milk, as used in the present study, caseins are more favorable substrate compared to whey proteins (Miwa et al., 2010). The experimental observation can also be supported by structure and amino acid composition of caseins. Glutaminase converts amide groups of specifically glutamine residues to carboxyl groups. Caseins, namely αs_1, αs_2, β, and κ CN, contain 25, 24, 19 and 12 glutamine residues, respectively, in comparatively unfolded structure to 9 and 6 glutamine residues in β-Lg and α-La, respectively, packed in a compact globular structure. Higher number of glutamine residues and randomly unfolded structure results in high accessibility of glutamine residues in caseins for enzyme PG. Hence, it could be assumed that deamidation affects structural changes of mainly caseins while heat impacts heat-labile whey proteins. Heating as observed in this study and as generally reported, reduces elements of the ordered secondary structure such as β-sheet and α-helix. However, increase in α helix and β-sheet compared to the heated samples at expense of triple helices, β-turns and random coils (Table 1) suggested that enzymatic deamidation modified casein structure into more ordered forms.

Structural changes in heated AP-treated samples were due to enzymatic dephosphorylation and subsequent heat treatment. Heat affects whey proteins and alkaline phosphatase can act only on caseins since the former lacks phosphoserine residues. The caseins in general have a high net negative charge arising from mainly phosphoserine residues and are not exceptionally hydrophobic

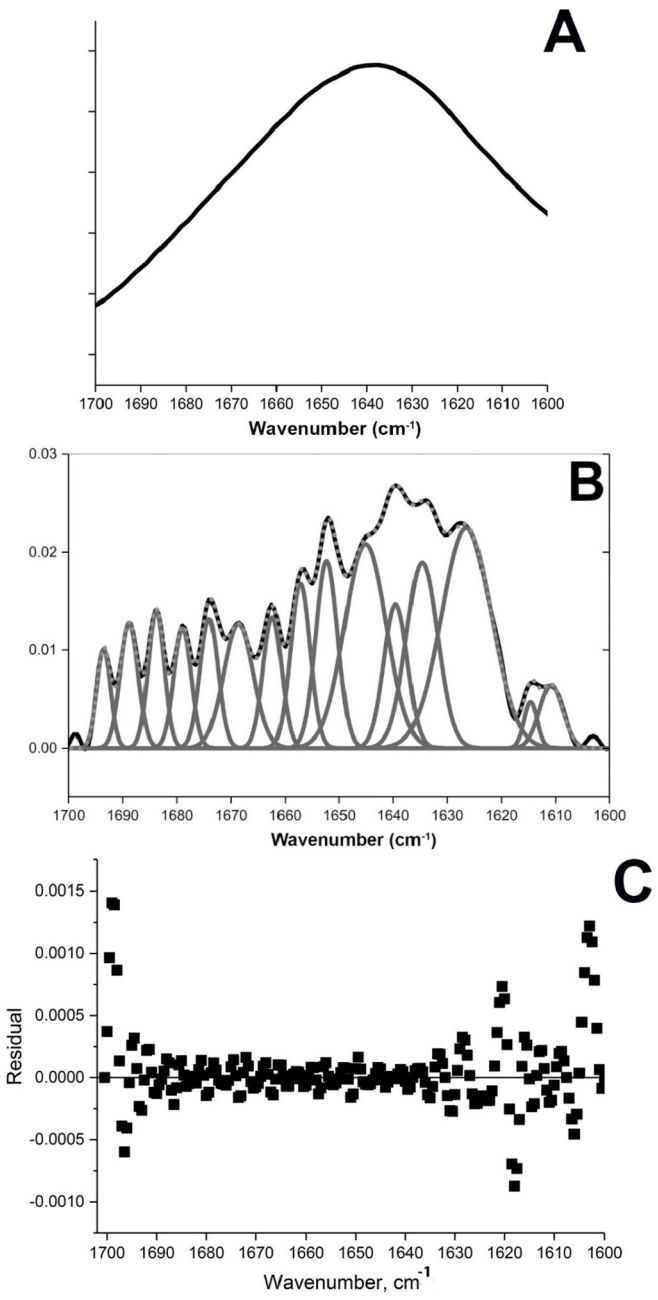

Fig. 3. Original (A) and normalized second derivative curve fitted amide I spectrum (B) of heated sample and corresponding residual plot (C).

(Swaisgood, 2003). Charge to charge repulsion of negatively charged groups and low hydrophobicity results in lower driving force for a compact structure (Koudelka, Hoffmann, & Carver, 2009; Uversky, Gillespie, & Fink, 2000). However, the removal of phosphoserine residues upon dephosphorylation significantly reduces the negative charge on the proteins and may lead to inducement of more secondary structure by increase in hydrogen bonding (Darewicz, Dziuba, Caessens, & Gruppen, 2000; Farrell, Qi, Wickham, & Unruh, 2002; Koudelka et al., 2009).

5. Conclusion

The present study for the first time has presented quantification of changes in the secondary structure of milk proteins upon deamidation and dephosphorylation followed by heat treatment. The curve fitting and assignment results, though tentative because bovine casein has never been crystallized, provide measure for changes in the secondary structure on intentional induction of structural modifications. In contrast to a decrease in ordered structure in heated samples, heated PG-treated and heated AP-treated samples demonstrated increase in ordered structure. The increase in ordered structure was in line with the observation made in our previous storage study (Grewal et al., 2017c), in which increase in sediment during storage of UHT milk at 20 °C was concomitant with the rise in inter- and intramolecular β-sheet and α-helix. However, there was no significant difference in sediment between control and treated samples (data not shown). Thus, it could not be concluded with confidence that changes in the secondary structure observed in this study were exactly similar to the ones observed in the previous storage study mainly due to three reasons. Firstly, the inferences drawn in the storage study was combined effect of all known and unknown interactions occurring during storage. Secondly, we did not quantify the changes in the secondary structure using curve fitting procedure adopted in this study. And thirdly, the enzymatic treatment prior to heating might have modified the structure of milk proteins in a way that may not really reflect the real-time mechanisms. Thus, the variations in FTIR spectra upon deamidation and dephosphorylation may or may not relate exactly to changes taking place during storage of the UHT milk. In order to do so, further work with the basic information and technique from this study should be extended to different treatment combinations like heat followed by enzymatic treatment and also to the other interactions occurring during storage of UHT milk.

Acknowledgement

This work is supported by the Department of Business and Innovation of the Victorian Government, through its Victoria India Doctoral Scholarship Program (managed by the Australia India Institute).

References

Al-Saadi, J. M., & Deeth, H. C. (2008). Cross-linking of proteins and other changes in UHT milk during storage at different temperatures. *Australian Journal of Dairy Technology, 63*(3), 93.

Curley, D. M., Kumosinski, T. F., Unruh, J. J., & Farrell, H. M. (1998). Changes in the secondary structure of bovine casein by Fourier transform infrared spectroscopy: Effects of calcium and temperature. *Journal of Dairy Science, 81*(12), 3154–3162.

Dalgleish, D. G. (2011). On the structural models of bovine casein micelles—review and possible improvements. *Soft Matter, 7*, 2265–2272.

Dalgleish, D. G., & Corredig, M. (2012). The structure of the casein micelle of milk and its changes during processing. *Annual review of food science and technology, 3*, 449–467.

Darewicz, M., Dziuba, J., Caessens, P. W., & Gruppen, H. (2000). Dephosphorylation-induced structural changes in beta-casein and its amphiphilic fragment in relation to emulsion properties. *Biochimie, 82*(3), 191–195.

Deeth, H., & Lewis, M. (2016). Protein stability in sterilised milk and milk products. In P. L. H. McSweeney, & J. A. O'Mahony (Eds.), *Proteins: Applied aspects: Vol. 1B. Advanced dairy chemistry* (pp. 247–286). New York, NY, USA: Springer US.

Farrell, H., Qi, P., Wickham, E., & Unruh, J. (2002). Secondary structural studies of bovine caseins: Structure and temperature dependence of β-casein phosphopeptide (1-25) as analyzed by circular dichroism, FTIR spectroscopy, and analytical ultracentrifugation. *Journal of Protein Chemistry, 21*(5), 307–321.

Grewal, M. K., Chandrapala, J., Donkor, O., Apostolopoulos, V., Stojanovska, L., & Vasiljevic, T. (2017). Fourier transform infrared spectroscopy analysis of physicochemical changes in UHT milk during accelerated storage. *International Dairy Journal, 66*, 99–107.

Grewal, M. K., Chandrapala, J., Donkor, O., Apostolopoulos, V., & Vasiljevic, T. (2017). Electrophoretic characterization of protein interactions suggesting limited feasibility of accelerated shelf-life testing of ultra-high temperature milk. *Journal of Dairy Science, 100*(1), 76–88.

Grewal, M. K., Chandrapala, J., Donkor, O., Apostolopoulos, V., & Vasiljevic, T. (2017). Predicting sediment formation in ultra high temperature-treated whole and skim milk using attenuated total reflectance-Fourier transform infrared spectroscopy. *International Dairy Journal, 74*, 39–48.

Holland, J. W., Gupta, R., Deeth, H. C., & Alewood, P. F. (2011). Proteomic analysis of temperature-dependent changes in stored UHT milk. *Journal of Agricultural and Food Chemistry, 59*(5), 1837–1846.

Horne, D. S. (2016). Ethanol stability and milk composition. In P. L. H. McSweeney, & J. A. O'Mahony (Eds.), *Proteins: Applied aspects: Vol. 1B. Advanced dairy chemistry* (pp. 225–246). New York, NY, USA: Springer US.

Huppertz, T. (2013). Chemistry of the caseins. In P. L. H. McSweeney, & P. F. Fox (Eds.), *Proteins: Basic aspects: Vol. 1A. Advanced dairy chemistry* (pp. 135–160). New York, NY, USA: Springer US.

Huq, N. L., Cross, K. J., & Reynolds, E. C. (1995). A 1H-NMR study of the casein phosphopeptide αs1-casein (59–79). *Biochimica et Biophysica Acta (BBA) - Protein Structure and Molecular Enzymology, 1247*(2), 201–208.

Karoui, R., Mazerolles, G., & Dufour, É. (2003). Spectroscopic techniques coupled with chemometric tools for structure and texture determinations in dairy products. *International Dairy Journal, 13*(8), 607–620.

Kher, A., Udabage, P., McKinnon, I., McNaughton, D., & Augustin, M. A. (2007). FTIR investigation of spray-dried milk protein concentrate powders. *Vibrational Spectroscopy, 44*(2), 375–381.

Koudelka, T., Hoffmann, P., & Carver, J. A. (2009). Dephosphorylation of αS-and β-caseins and its effect on chaperone activity: A structural and functional investigation. *Journal of Agricultural and Food Chemistry, 57*(13), 5956–5964.

Lorient, D., & Linden, G. (1976). Dephosphorylation of bovine casein by milk alkaline phosphatase. *Journal of Dairy Research, 43*(1), 19–26.

Malmgren, B., Ardö, Y., Langton, M., Altskär, A., Bremer, M. G., Dejmek, P., et al. (2017). Changes in proteins, physical stability and structure in directly heated UHT milk during storage at different temperatures. *International Dairy Journal, 71*, 60–75.

McKie, V. A., & McCleary, B. V. (2016). A novel and rapid colorimetric method for measuring total phosphorus and phytic acid in foods and animal feeds. *Journal of AOAC International, 99*(3), 738–743.

Mendelsohn, R., & Flach, C. R. (2002). Infrared reflection-absorption spectroscopy of lipids, peptides, and proteins in aqueous monolayers. *Current Topics in Membranes, 52*, 57–88.

Mendelsohn, R., Mao, G., & Flach, C. R. (2010). Infrared reflection–absorption spectroscopy: Principles and applications to lipid–protein interaction in Langmuir films. *Biochimica et Biophysica Acta (BBA) - Biomembranes, 1798*(4), 788–800.

Miwa, N., Yokoyama, K., Wakabayashi, H., & Nio, N. (2010). Effect of deamidation by protein-glutaminase on physicochemical and functional properties of skim milk. *International Dairy Journal, 20*(6), 393–399.

Ngarize, S., Herman, H., Adams, A., & Howell, N. (2004). Comparison of changes in the secondary structure of unheated, heated, and high-pressure-treated β-lactoglobulin and ovalbumin proteins using fourier transform Raman spectroscopy and self-deconvolution. *Journal of Agricultural and Food Chemistry, 52*(21), 6470–6477.

Nieuwenhuijse, J. A., & van Boekel, M. A. (2003). Protein stability in sterilised milk and milk products. In *Advanced dairy Chemistry—1 proteins* (pp. 947–974). Springer.

O'connell, J., & Fox, P. (2003). Heat-induced coagulation of milk. In *Advanced dairy Chemistry—1 proteins* (pp. 879–945). Springer.

Qi, P. X., Ren, D., Xiao, Y., & Tomasula, P. M. (2015). Effect of homogenization and pasteurization on the structure and stability of whey protein in milk. *Journal of Dairy Science, 98*(5), 2884–2897.

Sankaram, M. B., & Marsh, D. (1993). Protein-lipid interactions with peripheral membrane proteins. *New Comprehensive Biochemistry, 25*, 127–162.

Sharma, S. K., & Dalgleish, D. G. (1993). Interactions between milk serum proteins and synthetic fat globule membrane during heating of homogenized whole milk. *Journal of Agricultural and Food Chemistry, 41*(9), 1407–1412.

Singh, H. (1991). Modification of food proteins by covalent crosslinking. *Trends in Food Science & Technology, 2*, 196–200.

Swaisgood, H. (2003). Chemistry of the caseins. In *Advanced dairy chemistry—1 Proteins* (pp. 139–201). Springer.

Uversky, V. N., Gillespie, J. R., & Fink, A. L. (2000). Why are "natively unfolded" proteins unstructured under physiologic conditions? *Proteins: Structure, Function, and Bioinformatics, 41*(3), 415–427.

van Boekel, M. A. (1999). Heat-induced deamidation, dephosphorylation and breakdown of caseinate. *International Dairy Journal, 9*(3), 237–241.

Wahlgren, N. M., Léonil, J., Dejmek, P., & Drakenberg, T. (1993). Two-dimensional nuclear magnetic resonance study of the β-casein peptide 1–25: Resonance assignments and secondary structure. *Biochimica et Biophysica Acta (BBA) - Protein Structure and Molecular Enzymology, 1202*(1), 121–128.

Yang, H., Yang, S., Kong, J., Dong, A., & Yu, S. (2015). Obtaining information about protein secondary structures in aqueous solution using Fourier transform IR spectroscopy. *Nature Protocols, 10*(3), 382–396.

CHAPTER 7

Conclusions

7.1 Conclusions

The overall aim of this study to understand and predict the storage stability of UHT milk using FTIR spectroscopy and accelerated storage temperatures was subdivided into four objectives. Under the first objective, feasibility of using elevated temperatures during storage of UHT milk (with different fat content) to elucidate changes in interactions of milk proteins at ambient temperature was investigated. Storage of UHT whole milk (WM) and skim milk (SM) at and above 30 °C enhanced protein aggregation via covalent interactions (determined by electrophoretic analysis). Overall, the rate and type of protein crosslinking these reactions, especially at temperatures above 30 °C in WM and above 40 °C in SM, were very different from those at 20 °C, making it seem difficult to extrapolate these changes to protein interactions at lower temperatures. Hence, the electrophoretic analysis was found to be of limited use as a predictive tool. Furthermore, the fat content appeared to influence the extent and pathway of protein aggregation. Extent of aggregation was higher in WM and it appeared that covalent crosslinking in WM was attributed mainly to the products of lipid oxidation and increased access to caseins for crosslinking reactions. Whereas in SM, Maillard and dehydroalanine products appeared to be the main contributors in protein aggregation.

The knowledge generated about the involvement of individual proteins and the kinetics of changes in protein interactions under accelerated storage temperatures in the first study was employed in determining the feasibility of identifying structural changes using Fourier transform infrared spectroscopy (FTIR) concomitant with the evolution of sediment, the second objective. FTIR successfully detected changes in UHT WM and SM samples stored at and above 40 °C within 14 days. This suggested that it may take as less as 14 days to detect significant changes

using FTIR spectroscopy and accelerated storage stability testing. PCA score and loading plot demonstrated that both SM and WM were classified in different groups according to different storage temperature and time and the changes in the conformation of milk lipids and proteins propelled this classification, respectively. Changes in proteins and carbohydrates due to Maillard reaction were less intense. Furthermore, increase in the sediment was correlated with rise in intermolecular β-sheet formation. Another interesting observation was that SM showed significant changes in FTIR spectra at comparatively lower temperatures of 20 and 30 °C. However, WM samples experienced changes only at 40 °C. To fully establish the reasons related to different behaviour of SM and WM at 20 and 30 °C and to detect specific markers which can be employed for rapid prediction of shelf life, a long-term study was conducted (third objective).

During long term storage at 20 °C, the increase in sediment concentration for both SM and WM (an indicator of the shelf life stability) correlated with the changes in FTIR spectral profiles of the samples. PCA was able to specify marker variables, changes in which could be used to predict build-up of sediment in UHT milk, especially SM. Marker variables corresponded to structural changes in milk lipids, proteins and carbohydrates signifying that storage at 20 °C produced definite changes in these spectral regions. These changes were similar to those observed previously during accelerated shelf life testing. Thus, an earlier concern that different types and rate of reactions at elevated storage temperatures could hinder the application of accelerated shelf life testing in UHT milk appeared to be unfounded. Use of accelerated temperatures could thus assist in reducing time required to detect the changes and estimate sedimentation, a measure of shelf life of this product.

An overall picture of different changes in the secondary structure and related protein interactions leading to storage instability in UHT milk was established. However, conformational adjustments corresponding to individual protein interactions remain largely unknown. This information could assist in identifying the main interactions responsible for this storage instability and improve the predictive ability of a model to predict sedimentation, hence adding further to the main aim of the project to understand and predict storage stability of UHT milk. Therefore, the fourth objective was aimed to evaluate possibility of fingerprinting several selected mechanisms involved in structural changes of proteins using FTIR. Deamidation and dephosphorylation was enzymatically induced in raw skim milk samples followed by heat treatment. Specific changes in the secondary structure of milk proteins was then identified by employing curve fitting and band assignment procedure to FTIR spectral amide I region. FTIR and quantification were able to pick changes in secondary structure specific to the induced modification. In contrast to a decrease in ordered structure in control samples, heated-deamidated and heated-dephosphorylated samples demonstrated increase in ordered structure. However, the latter differed in percentage area of large loops. The increase in ordered structure in enzyme-treated samples was in line with the observation made in the previous storage study recorded in this project, in which increase in sediment during storage of UHT milk at 20 °C was concomitant with the rise in inter- and intramolecular β-sheet and α-helix. However, no significant difference was observed in sediment between control and enzyme treated samples. Thus, it could not be concluded with confidence that changes in the secondary structure observed in this study were exactly similar to the ones observed in the previous storage study. Overall, combination of accelerated temperatures and FTIR spectroscopy could be established as a promising rapid tool for predicting sedimentation in UHT milk, one of the

measures of its shelf life. In addition, FTIR can pick structural changes in milk protein specific to similar changes happening during storage.

7.2 Future research directions

It was interesting observation that sediment produced as a result of the UHT treatment was almost twice in whole milk compared to skim milk. And sediment increased more slowly during storage in whole milk (about 30—40%) over 28 days at elevated temperatures compared to skim milk, where it was over 100%. It would be more informative if in future a sensory evaluation could be done to know whether the levels of sediment were likely to be noticed by the consumer and lead to product being rejected at any point during its subsequent storage. In addition, measurement of sediment in raw milk prior to UHT processing could also add valuable insight.

A model was developed to detect changes in proteins and corresponding levels of sedimentation in UHT milk. Further work is required to develop a model that could forecast sedimentation in advance. In addition, to identify conformational changes specific to interactions known to lead to storage instabilities in UHT milk would probably involve intentional inducement of instabilities in samples and identify corresponding changes in the spectra. In fourth study conducted in this direction as mentioned above, it was demonstrated that FTIR successfully detected changes in secondary structure corresponding to two intentionally induced modifications, known to play role in development of storage instabilities in UHT milk. However, these modifications being induced enzymatically and prior to heat treatment in raw milk followed by heat treatment might have modified the structure of milk proteins in a way that may not really reflect the real-time mechanisms. Moreover, the increase in secondary structure observed in UHT milk samples during storage was combined effect of all known and unknown interactions occurring

during storage. Thus, to closely replicate changes happening during storage of the UHT milk, further work with the basic information and technique developed in this project needs to be extended to different treatment combinations like heat followed by enzymatic treatment and also to the other interactions like Maillard and formation of lysinoalanine occurring during storage of UHT milk. In addition, it would also be useful and interesting to investigate whether the effect of the enzymatic treatments dephosphorylation and deamidation can protect against onset of age-gelation in UHT milk, another predominant storage instability in UHT milk and other UHT dairy and non-dairy high protein beverages

FTIR spectroscopy has demonstrated considerable potential in this study in both understanding and predicting development of sedimentation in UHT milk. It would also be interesting to investigate the potential of the FTIR technique to detect and predict early onset gelation in UHT milk. The research could also be extended to investigating the role of protein stability and aggregation in other biofluids, particularly those of the dairy industry e.g. non-UHT milk, other dairy products and high-protein non-dairy-beverages. Furthermore, understanding storage instabilities in UHT milk and other similar fluids could be expanded by combining FTIR spectroscopy with other complementary spectroscopy techniques like CD and Raman spectroscopy.

CHAPTER 8

References

8.1 References

Al-Attabi, Z., D'Arcy, B. R., & Deeth, H. C. (2014). Volatile sulfur compounds in pasteurised and UHT milk during storage. *Dairy Science & Technology, 94*(3), 241-253.

Al-Saadi, J. M., & Deeth, H. C. (2008). Cross-linking of proteins and other changes in UHT milk during storage at different temperatures. *Australian Journal of Dairy Technology, 63*(3), 93.

Andrews, A. (1975). Properties of aseptically packed ultra-high-temperature milk: III. Formation of polymerized protein during storage at various temperatures. *Journal of Dairy Research, 42*(01), 89-99.

Andrews, A. T., & Cheeseman, G. C. (1971). Properties of aseptically packed UHT milk: casein modification during storage and studies with model systems. *Journal of Dairy Research, 38*(2), 193-207.

Andrews, A., & Cheeseman, G. (1972). Properties of aseptically packed ultra-high-temperature milk: II. Molecular weight changes of the casein components during storage. *Journal of Dairy Research, 39*(03), 395-408.

Anema, S. G. (2008). On heating milk, the dissociation of kappa-casein from the casein micelles can precede interactions with the denatured whey proteins. *Journal of Dairy Research, 75*(4), 415-421.

Anema, S. G. (2014). The whey proteins in milk: Thermal denaturation, physical interactions, and effects on the functional properties of milk. In H. Singh, M. Boland, & A. Thompson

(Eds.), *Milk proteins: From expression to food* (2nd ed., pp. 269-318). San Diego: Academic Press.

Anema, S. G. (2017). Storage stability and age gelation of reconstituted ultra-high temperature skim milk. *International Dairy Journal, 75*, 56-67.

Auldist, M. J., Coats, S. J., Sutherland, B. J., Hardham, J. F., McDowell, G. H., & Rogers, G. L. (1996). Effect of somatic cell count and stage of lactation on the quality and storage life of ultra high temperature milk. *Journal of Dairy Research, 63*(3), 377-386.

Bansal, B., & Chen, X. D. (2006). A critical review of milk fouling in heat exchangers. *Comprehensive Reviews in Food Science and Food Safety, 5*(2), 27-33.

Belec, J., & Jenness, R. (1962). Dephosphorization of casein by heat treatment. II. In skimmilks. *Journal of Dairy Science, 45*(1), 20-26.

Boye, J. I., Ismail, A. A., & Alli, I. (1996). Effects of physicochemical factors on the secondary structure of β-lactoglobulin. *Journal of Dairy Research, 63*(1), 97-109.

Bruun, S. W. (2006). *Protein- lipid- carbohydrate interactions and importance to food quality: Spectroscopic detection of macromolecular interactions* (PhD), Technical University of Denmark, Lyngby, Denmark.

Burton, H. (1988). *Ultra high temperature processing of milk and milk products.* London: Elsevier Applied Science.

Button, P., Roginski, H., Deeth, H., & Craven, H. (2011). Improved shelf life estimation of UHT milk by prediction of proteolysis. *Journal of Food Quality, 34*(4), 229-235.

Byler, D. M., Farrell, H. M., & Susi, H. (1988). Raman spectroscopic study of casein structure. *Journal of Dairy Science, 71*(10), 2622-2629.

Carbonaro, M., & Nucara, A. (2010). Secondary structure of food proteins by Fourier transform spectroscopy in the mid-infrared region. *Amino Acids, 38*(3), 679-690.

Carbonaro, M., Maselli, P., & Nucara, A. (2012). Relationship between digestibility and secondary structure of raw and thermally treated legume proteins: a Fourier transform infrared (FT-IR) spectroscopic study. *Amino Acids, 43*(2), 911-921.

Cattaneo, S., Masotti, F., & Pellegrino, L. (2008). Effects of overprocessing on heat damage of UHT milk. *European Food Research and Technology, 226*(5), 1099-1106.

Chandrapala, J., McKinnon, I., Augustin, M. A., & Udabage, P. (2010). The influence of milk composition on pH and calcium activity measured in situ during heat treatment of reconstituted skim milk. *Journal of Dairy Research, 77*(03), 257-264.

Corradini, C., & Pecchini, G. (1981). Effect on proteinases on different UHT treatments. *Netherlands Milk and Dairy Journal*, 35, 393-395.

Corredig, M., & Dalgleish, D. G. (1996a). Effect of temperature and pH on the interactions of whey proteins with casein micelles in skim milk. *Food Research International, 29*(1), 49-55.

Corredig, M., & Dalgleish, D. G. (1996b). The binding of α-lactalbumin and β-lactoglobulin to casein micelles in milk treated by different heating systems. *Milchwissenschaft, 51*, 123-127.

Corrigan, V., Hedderley, D., & Harvey, W. (2012). Modeling the Shelf Life of Fruit- Filled Snack Bars Using Survival Analysis and Sensory Profiling Techniques. *Journal of Sensory Studies, 27*(6), 403-416.

Dalgleish, D. G. (2011). On the structural models of bovine casein micelles—review and possible improvements. *Soft Matter, 7*(6), 2265-2272.

Datta, N., & Deeth, H. C. (2001). Age gelation of UHT milk—A review. *Food and Bioproducts Processing, 79*(4), 197-210.

Datta, N., & Deeth, H. C. (2003). Diagnosing the cause of proteolysis in UHT milk. *LWT - Food Science and Technology, 36*(2), 173-182.

Datta, N., Elliott, A. J., Perkins, M. L., & Deeth, H. C. (2002). Ultra-high-temperature (UHT) treatment of milk: comparison of direct and indirect modes of heating. *Australian Journal of Dairy Technology, 57*(3), 211-227.

de Kruif, C. G., Huppertz, T., Urban, V. S., & Petukhov, A. V. (2012). Casein micelles and their internal structure. *Advances in Colloid and Interface Science, 171-172*(Supplement C), 36-52.

De Kruif, C., & Holt, C. (2003). Casein micelle structure, functions and interactions. In *Advanced Dairy Chemistry—1 Proteins* (pp. 233-276): New York: Kluwer Academic/Plenum.

Deeth, H. C., & Lewis, M. J. (2017a). Changes during heat treatment of milk. In H. Deeth & M. J. Lewis (Eds.), *High temperature processing of milk and milk products* (pp. 177-260). Chichester, UK: Wiley Blackwell.

Deeth, H. C., & Lewis, M. J. (2017b). Changes during storage of uht milk. In H. Deeth & M. J. Lewis (Eds.), *High temperature processing of milk and milk products* (pp. 261-319). Chichester, UK: Wiley Blackwell.

Deeth, H., & Lewis, M. (2016). Protein Stability in Sterilised Milk and Milk Products. In P. L. H. McSweeney & J. A. O'Mahony (Eds.), *Advanced Dairy Chemistry: Volume 1B: Proteins: Applied Aspects* (pp. 247-286). New York, NY: Springer New York.

Dong, A., Huang, P., & Caughey, W. S. (1990). Protein secondary structures in water from second-derivative amide I infrared spectra. *Biochemistry, 29*(13), 3303-3308.

Downs, M. L., Kabourek, J. L., Baumert, J. L., & Taylor, S. L. (2013). Milk protein allergy. In Y.W. Park & G.F.W. Haenlein (Eds.), *Milk and dairy products in human nutrition* (pp. 111-128).West Sussex, UK: John Wiley & Sons.

Dufour, E., Mazerolles, G., Devaux, M. F., Duboz, G., Duployer, M. H., & Mouhous Riou, N. (2000). Phase transition of triglycerides during semi-hard cheese ripening. *International Dairy Journal, 10*(1–2), 81-93.

Dufour, E., Robert, P., Renard, D., & Llamas, G. (1998). Investigation of β-lactoglobulin gelation in water/ethanol solutions. *International Dairy Journal, 8*(2), 87-93.

Dupont, D., Rolet-Repecaud, O., & Muller-Renaud, S. (2004). Determination of the heat treatment undergone by milk by following the denaturation of alpha-lactalbumin with a biosensor. *Journal of Agricultural and Food Chemistry, 52*(4), 677-681.

Edwards, P. J. B., & Jameson, G. B. (2014). Structure and stability of whey proteins. In *Milk proteins* (2nd ed., pp. 201-242). San Diego: Academic Press.

Esbensen, K. H., Guyot, D., Westad, F., & Houmoller, L. P. (2002). *Multivariate data analysis: in practice: an introduction to multivariate data analysis and experimental design* (5th ed.): CAMO Process AS.

Farrell Jr, H., Brown, E., & Malin, E. (2013). Higher order structures of the caseins: A paradox? In P. L. H. McSweeney & P. F. Fox (Eds.), *Advanced Dairy Chemistry* (Vol. 1A, 4th ed., pp. 161-184). Boston, MA: Springer.

Farrell, H. M., Kumosinski, T. F., Cooke, P. H., King, G., Hoagland, P. D., Wickham, E. D., Groves, M. L. (1996). Particle sizes of purified κ-casein: metal effect and correspondence with predicted three-dimensional molecular models. *Journal of Protein Chemistry, 15*(5), 435-445.

Farrell, H. M., Malin, E. L., Brown, E. M., & Mora-Gutierrez, A. (2009). Review of the chemistry of αS2-casein and the generation of a homologous molecular model to explain its properties1. *Journal of Dairy Science, 92*(4), 1338-1353.

Farrell, H. M., Wickham, E. D., Unruh, J. J., Qi, P. X., & Hoagland, P. D. (2001). Secondary structural studies of bovine caseins: temperature dependence of β-casein structure as analyzed by circular dichroism and FTIR spectroscopy and correlation with micellization. *Food Hydrocolloids, 15*(4), 341-354.

Fox P.F., Uniacke-Lowe T., McSweeney P.L.H., O'Mahony J.A. (2015a). Milk Proteins. In: *Dairy Chemistry and Biochemistry* (pp.145-239). Cham: Springer International Publishing.

Fox, P. F., Uniacke-Lowe, T., McSweeney, P. L. H., & O'Mahony, J. A. (2015b). Salts of milk. In *Dairy chemistry and biochemistry* (pp.241-270). Cham: Springer International Publishing.

Friedman, M. (1999). Chemistry, biochemistry, nutrition, and microbiology of lysinoalanine, lanthionine, and histidinoalanine in food and other proteins. *Journal of Agricultural and Food Chemistry, 47*(4), 1295-1319.

Fritsch, R. J., Hoffmann, H., & Klostermeyer, H. (1983). Formation of lysinoalanine during heat treatment of milk. *Zeitschrift Fur Lebensmittel-Untersuchung Und -Forschung, 176*(5), 341-345.

Fu, F.-N., Deoliveira, D. B., Trumble, W. R., Sarkar, H. K., & Singh, B. R. (1994). Secondary structure estimation of proteins using the amide III region of Fourier transform infrared spectroscopy: Application to analyze calcium-binding-induced structural changes in calsequestrin. *Applied Spectroscopy, 48*(11), 1432-1441.

Garcia-Risco, M. R., Ramos, M., & Lopez-Fandino, R. (1999). Proteolysis, protein distribution and stability of UHT milk during storage at room temperature. *Journal of the Science of Food and Agriculture, 79*(9), 1171-1178.

Garcia-Risco, M. R., Ramos, M., & Lopez-Fandino, R. (1999). Proteolysis, protein distribution and stability of UHT milk during storage at room temperature. *Journal of the Science of Food and Agriculture, 79*(9), 1171-1178.

Garnier, J., Osguthorpe, D. J., & Robson, B. (1978). Analysis of the accuracy and implications of simple methods for predicting the secondary structure of globular proteins. *Journal of Molecular Biology, 120*(1), 97-120.

Gaucher, I., Boubellouta, T., Beaucher, E., Piot, M., Gaucheron, F., & Dufour, E. (2008). Investigation of the effects of season, milking region, sterilisation process and storage conditions on milk and UHT milk physico-chemical characteristics: A multidimensional statistical approach. *Dairy Science & Technology, 88*(3), 291-312.

Gaucher, I., Mollé, D., Gagnaire, V., & Gaucheron, F. (2008). Effects of storage temperature on physico-chemical characteristics of semi-skimmed UHT milk. *Food Hydrocolloids, 22*(1), 130-143.

Gaucher, I., Tanguy, G., Fauquant, J., Jardin, J., Rousseau, F., Robert, B., . . . Gaucheron, F. (2011). Proteolysis of casein micelles by Pseudomonas fluorescens CNRZ 798 contributes to the destabilisation of UHT milk during its storage. *Dairy Science & Technology, 91*(4), 413.

Gaucheron, F. (2005). The minerals of milk. *Reproduction Nutrition Development, 45*(4), 473-483.

Gaur, V., Schalk, J., & Anema, S. G. (2018). Sedimentation in UHT milk. *International Dairy Journal, 78*(Supplement C), 92-102.

Gebhardt, R., Takeda, N., Kulozik, U., & Doster, W. (2011). Structure and stabilizing interactions of casein micelles probed by high-pressure light scattering and FTIR. *The Journal of Physical Chemistry B, 115*(10), 2349-2359.

Geerts, J., Bekhof, J., & Scherjon, J. (1983). Determination of calcium ion activities in milk with an ion-selective electrode. A linear relationship between the logarithm of time and the recovery of the calcium ion activity after heat treatment. *Netherlands Milk and Dairy Journal, 37, 197-211*.

Granato, D., & Ares G. (Eds.) (2014). *Mathematical and statistical methods in food science and technology*. Los Angeles, CA: John Wiley & Sons.

Hawran, L. J., Jones, V. A., & Swartzel, K. R. (1985). Sediment formation in aseptically processed and packaged milk. *Journal of Food Processing and Preservation, 9*(3), 189-207.

Hedegaard, R. V., Kristensen, D., Nielsen, J. H., Frøst, M. B., Østdal, H., Hermansen, J. E., . . . Skibsted, L. H. (2006). Comparison of Descriptive Sensory Analysis and Chemical Analysis for Oxidative Changes in Milk. *Journal of Dairy Science, 89*(2), 495-504.

Heid, H. W., & Keenan, T. W. (2005). Intracellular origin and secretion of milk fat globules. *European Journal of Cell Biology, 84*(2), 245-258.

Henle, T., Schwarzenbolz, U., & Klostermeyer, H. (1996). *Irreversibles crosslinking of casein during storage of UHT-treated skim milk.* Paper presented at the Heat treatments and alternative methods. IDF Symposium, Vienna (Austria), 6-8 Sep 1995.

Hoagland, P., Unruh, J., Wickham, E., & Farrell, H. (2001). Secondary structure of bovine αS2-casein: Theoretical and experimental approaches. *Journal of Dairy Science, 84*(9), 1944-1949.

Holland, J. W., Gupta, R., Deeth, H. C., & Alewood, P. F. (2011). Proteomic analysis of temperature-dependent changes in stored UHT milk. *Journal of Agricultural and Food Chemistry, 59*(5), 1837-1846.

Holland, J. W., Gupta, R., Deeth, H. C., & Alewood, P. F. (2012). UHT milk contains multiple forms of αs1-CN that undergo degradative changes during storage. *Food Chemistry, 133*(3), 689-696.

Holt, C. (1992). Structure and stability of bovine casein micelles. In C. B. Anfinsen, F. M. Richards, J. T. Edsall, & D. S. Eisenberg (Eds.), *Advances in protein chemistry* (Vol. 43, pp. 63-151): Academic Press.

Holt, C. (1998). Casein micelle substructure and calcium phosphate interactions studied by sephacryl column chromatography. *Journal of Dairy Science, 81*(11), 2994-3003.

Holt, C., & Horne, D. S. (1996). The hairy casein micelle: Evolution of the concept and its implications for dairy technology. *Netherlands Milk and Dairy Journal, 50*(2), 85-111.

Holt, C., & Jenness, R. (1984). Interrelationships of constituents and partition of salts in milk samples from eight species. *Comparative Biochemistry and Physiology*, 77, 275–282.

Holt, C., & Sawyer, L. (1993). Caseins as rheomorphic proteins: Interpretation of primary and secondary structures of the α S1-, β-and κ-caseins. *Journal of the Chemical Society, Faraday Transactions, 89*(15), 2683-2692.

Horne, D. S. (1998). Casein interactions: Casting light on the black boxes, the structure in dairy products. *International Dairy Journal, 8*(3), 171-177.

Horne, D. S. (2002). Casein structure, self-assembly and gelation. *Current Opinion in Colloid & Interface Science, 7*(5), 456-461.

Horne, D. S. (2006). Casein micelle structure: Models and muddles. *Current Opinion in Colloid & Interface Science, 11*(2–3), 148-153.

Horne, D. S. (2008). Casein micelle structure and stability In M. Boland, H. Singh, & A. Thompson (Eds.), *Milk Proteins* (pp. 133-162). San Diego: Academic Press.

Horne, D. S. (2014). Casein micelle structure and stability. In H. Singh, M. Boland, & A. Thompson (Eds.), *Milk proteins from expression to food* (2nd ed., pp. 169-200). San Diego: Academic Press.

Huijs, G., van Asselt, A., Verdurmen, R., & De Jong, P. (2004). High speed milk. *Dairy Industries International, 69*(11), 30-32.

Huppertz, T. (2013). Chemistry of the Caseins. In P. L. H. McSweeney & P. F. Fox (Eds.), *Advanced Dairy Chemistry* (Vol.1A, 4th ed., pp. 135-160). Boston, MA: Springer.

Hurley, W. L., & Theil, P. K. (2013). Immunoglobulins in mammary secretions. In P. L. H. McSweeney & P. F. Fox (Eds.), *Advanced Dairy Chemistry* (Vol. 1, 4th ed., pp. 275-294). Boston, MA: Springer.

Iñón, F. A., Garrigues, S., & de la Guardia, M. (2004). Nutritional parameters of commercially available milk samples by FTIR and chemometric techniques. *Analytica Chimica Acta, 513*(2), 401-412.

Jaiswal, P., Jha, S. N., Borah, A., Gautam, A., Grewal, M. K., & Jindal, G. (2015). Detection and quantification of soymilk in cow–buffalo milk using Attenuated Total Reflectance Fourier Transform Infrared spectroscopy (ATR–FTIR). *Food Chemistry, 168*, 41-47.

Karoui, R., & De Baerdemaeker, J. (2007). A review of the analytical methods coupled with chemometric tools for the determination of the quality and identity of dairy products. *Food Chemistry, 102*(3), 621-640.

Karoui, R., Downey, G., & Blecker, C. (2010). Mid-infrared spectroscopy coupled with chemometrics: A tool for the analysis of intact food systems and the exploration of their molecular structure− Quality relationships− A review. *Chemical reviews, 110*(10), 6144-6168.

Karoui, R., Mazerolles, G., & Dufour, É. (2003). Spectroscopic techniques coupled with chemometric tools for structure and texture determinations in dairy products. *International Dairy Journal, 13*(8), 607-620.

Kelly, A. L., & Foley, J. (1997). Proteolysis and storage stability of UHT milk as influenced by milk plasmin activity, plasmin/β-lactoglobulin complexation, plasminogen activation and somatic cell count. *International Dairy Journal, 7*(6-7), 411-420.

Kher, A., Udabage, P., McKinnon, I., McNaughton, D., & Augustin, M. A. (2007). FTIR investigation of spray-dried milk protein concentrate powders. *Vibrational Spectroscopy, 44*(2), 375-381.

Kocak, H., & Zadow, J. (1985). The effect of low-temperature-inactivation treatment on age gelation of UHT whole milk. *Australian Journal of Dairy Technology, 40*(2), 53.

Kumosinski, T. F., Brown, E. M., & Farrell, H. M. (1993). Three-dimensional molecular modeling of bovine caseins: An energy-minimized β-casein structure. *Journal of Dairy Science, 76*(4), 931-945.

Kumosinski, T., Brown, E., & Farrell, H. (1991). Three-dimensional molecular modeling of bovine caseins: αs1-casein. *Journal of Dairy Science, 74*(9), 2889-2895.

Le, T. T., Holland, J. W., Bhandari, B., Alewood, P. F., & Deeth, H. C. (2013). Direct evidence for the role of Maillard reaction products in protein cross-linking in milk powder during storage. *International Dairy Journal, 31*(2), 83-91.

Leser, M. E., & Michel, M. (2008). Colloids in milk products. *Chimia, 62*(10), 783-788.

Lewis, M. J., & Deeth, H. C. (2009). Heat treatment of milk. In A.Y. Tamine (Ed.) *Milk processing and quality management* (pp. 168-204). Chichester: Wiley-Blackwell.

Lewis, M., Grandison, A., Mei-Jen, L., & Tsioulpas, A. (2011). Ionic calcium and pH as predictors of stability of milk to UHT processing. *Milchwissenschaft, 66*(2), 197-200.

López-Fandiño, R., Olano, A., Corzo, N., & Ramos, M. (1993). Proteolysis during storage of UHT milk: differences between whole and skim milk. *Journal of Dairy Research, 60*(03), 339-347.

López-Fandiño, R., Olano, A., Corzo, N., & Ramos, M. (1993). Proteolysis during storage of UHT milk: differences between whole and skim milk. *Journal of Dairy Research, 60*(03), 339-347.

Losito, I., Stringano, E., Carulli, S., & Palmisano, F. (2010). Correlation between lactosylation and denaturation of major whey proteins: an investigation by liquid chromatography–

electrospray ionization mass spectrometry. *Analytical and Bioanalytical Chemistry, 396*(6), 2293-2306.

Lucey, J. A., & Singh, H. (2003). Acid coagulation of milk. In P. F. Fox & P. L. H. McSweeney (Eds.) *Advanced Dairy Chemistry—2 Proteins* (pp. 1001−1025). New York, Kluwer Academic/Plenum.

Malin, E. L., Brown, E. M., Wickham, E. D., & Farrell, H. M. (2005). Contributions of terminal peptides to the associative behavior of αs1-casein. *Journal of Dairy Science, 88*(7), 2318-2328.

Malmgren, B., Ardö, Y., Langton, M., Altskär, A., Bremer, M. G., Dejmek, P., & Paulsson, M. (2017). Changes in proteins, physical stability and structure in directly heated UHT milk during storage at different temperatures. *International Dairy Journal, 71*, 60-75.

Manji, B., Kakuda, Y., & Arnott, D. (1986). Effect of storage temperature on age gelation of ultra-high temperature milk processed by direct and indirect heating systems. *Journal of Dairy Science, 69*(12), 2994-3001.

Martens, H., & Martens, M. (2001). *Multivariate analysis of quality. An introduction*. Chichester: John Wiley & Sons.

Masmoudi, H., Dréau, Y. L., Piccerelle, P., & Kister, J. (2005). The evaluation of cosmetic and pharmaceutical emulsions aging process using classical techniques and a new method: FTIR. *International Journal of Pharmaceutics, 289*(1–2), 117-131.

Mather, I. H., & Keenan, T. W. (1998). Origin and secretion of milk lipids. *Journal of Mammary Gland Biology and Neoplasia, 3*(3), 259-273.

Mazerolles, G., Devaux, M.-F., Duboz, G., Duployer, M.-H., Riou, N. M., & Dufour, É. (2001). Infrared and fluorescence spectroscopy for monitoring protein structure and interaction changes during cheese ripening. *Le Lait, 81*(4), 509-527.

McMahon, D. J. (1996). *Age-gelation of UHT milk: changes that occur during storage, their effect on shelf life and the mechanism by which age-gelation occurs.* Paper presented at the Heat treatments and alternative methods. IDF Symposium, Vienna (Austria), 6-8 Sep 1995.

McMahon, D. J., & McManus, W. R. (1998). Rethinking casein micelle structure using electron microscopy. *Journal of Dairy Science, 81*(11), 2985-2993.

Mendelsohn, R., Mao, G., & Flach, C. R. (2010). Infrared reflection–absorption spectroscopy: Principles and applications to lipid–protein interaction in Langmuir films. *Biochimica et Biophysica Acta (BBA) - Biomembranes, 1798*(4), 788-800.

Metwalli, A., & Van Boekel, M. (1998). On the kinetics of heat-induced deamidation and breakdown of caseinate. *Food Chemistry, 61*(1), 53-61.

Miwa, N., Yokoyama, K., Wakabayashi, H., & Nio, N. (2010). Effect of deamidation by protein-glutaminase on physicochemical and functional properties of skim milk. *International Dairy Journal, 20*(6), 393-399.

Mulvihill, D. M., & Donovan, M. (1987). Whey proteins and their thermal denaturation - a review. *Irish Journal of Food Science and Technology, 11*(1), 43-75.

Murphy, E. G., Fenelon, M. A., Roos, Y. H., & Hogan, S. A. (2014). Decoupling macronutrient interactions during heating of model infant milk formulas. *Journal of Agricultural and Food Chemistry, 62*(43), 10585-10593.

Newstead, D., Groube, G., Smith, A., & Eiger, R. (1998). Fouling of UHT plants by recombined and fresh milk: some effects of preheat treatment. In D.I. Wilson, P.J. Fryer & A.P.M. Hasting (Eds.). *Fouling and Cleaning in Food Processing* (pp. 17–24). Cambridge, U.K.: Jesus College.

Newstead, D., Paterson, G., Anema, S., Coker, C., & Wewala, A. (2006). Plasmin activity in direct-steam-injection UHT-processed reconstituted milk: Effects of preheat treatment. *International Dairy Journal, 16*(6), 573-579.

Newswire, P. R. (2014). UHT milk market - global industry analysis, size, share, growth, trends and forecast, 2013 - 2019. *NY-Reportlinker*. Retrieved from http://0-search.ebscohost.com.library.vu.edu.au/login.aspx?direct=true&db=bwh&AN=201406091241PR.NEWS.USPR.BR44785&site=eds-live

Nicolaou, N., Xu, Y., & Goodacre, R. (2010). Fourier transform infrared spectroscopy and multivariate analysis for the detection and quantification of different milk species. *Journal of Dairy Science, 93*(12), 5651-5660.

Nielsen, S. S. (2002). Plasmin system and microbial proteases in milk: characteristics, roles, and relationship. *Journal of Agricultural and Food Chemistry, 50*(22), 6628-6634.

Nieuwenhuijse, J. A., & van Boekel, M. A. (2003). Protein stability in sterilised milk and milk products. In F. PF & M. PLH (Eds.), *Advanced Dairy Chemistry 1-Proteins* (3 ed., Vol. 1, pp. 947-974). New York: Kluwer Academic/Plenum.

O'connell, J.E., & Fox, P.F. (2003). Heat-induced coagulation of milk. In P. F. Fox & P. McSweeney (Eds.) *Advanced Dairy Chemistry* (pp. 879-945). New York, USA: Kluwer Academic/Plenum.

O'Mahony, J. A., & Fox, P. F. (2014). Milk: An overview. In *Milk proteins (2nd ed.)* (pp. 19-73). San Diego, USA: Academic Press.

Oberg, K. A., Ruysschaert, J. M., & Goormaghtigh, E. (2004). The optimization of protein secondary structure determination with infrared and circular dichroism spectra. *The FEBS Journal, 271*(14), 2937-2948.

On-Nom, N., Grandison, A. S., & Lewis, M. J. (2010). Measurement of ionic calcium, pH, and soluble divalent cations in milk at high temperature. *Journal of Dairy Science, 93*(2), 515-523.

Ozen, B. F., Hayes, K. D., & Mauer, L. J. (2003). Measurement of plasminogen concentration and differentiation of plasmin and plasminogen using Fourier-transform infrared spectroscopy. *International Dairy Journal, 13*(6), 441-446.

Parris, N., Purcell, J. M., & Ptashkin, S. M. (1991). Thermal denaturation of whey proteins in skim milk. *Journal of Agricultural and Food Chemistry, 39*(12), 2167-2170.

Pedro, A. M., & Ferreira, M. (2006). Multivariate accelerated shelf- life testing: a novel approach for determining the shelf- life of foods. *Journal of Chemometrics, 20*(1- 2), 76-83.

Perkins, M. L., Elliott, A. J., D'Arcy, B. R., & Deeth, H. C. (2005). Stale flavour volatiles in Australian commercial UHT milk during storage. *Australian Journal of Dairy Technology, 60*(3), 231.

Powell, J., Wasacz, F., & Jakobsen, R. (1986). An algorithm for the reproducible spectral subtraction of water from the FT-IR spectra of proteins in dilute solutions and adsorbed monolayers. *Applied Spectroscopy, 40*(3), 339-344.

Qi, P. X., Ren, D., Xiao, Y., & Tomasula, P. M. (2015). Effect of homogenization and pasteurization on the structure and stability of whey protein in milk. *Journal of Dairy Science, 98*(5), 2884-2897.

Qi, P. X., Wickham, E. D., & Garcia, R. A. (2014). Structural and thermal stability of β-lactoglobulin as a result of interacting with sugar beet pectin. *Journal of Agricultural and Food Chemistry, 62*(30), 7567-7576.

Ramsey, J. A., & Swartzel, K. R. (1984). Effect of ultra high temperature processing and storage conditions on rates of sedimentation and fat separation of aseptically packaged milk. *Journal of Food Science, 49*(1), 257-262.

Richards, M., De Kock, H. L., & Buys, E. M. (2014). Multivariate accelerated shelf-life test of low fat UHT milk. *International Dairy Journal, 36*(1), 38-45.

Robins, M. M. (2000). Emulsions — creaming phenomena. *Current Opinion in Colloid & Interface Science, 5*(5–6), 265-272.

Samel, R., Weaver, R. W. V., & Gammack, D. B. (1971). Changes on storage in milk processed by ultra-high-temperature sterilization. *Journal of Dairy Research, 38*(3), 323-332.

Sawyer, L. (2003). β-Lactoglobulin. In P. F. Fox & P. McSweeney (Eds.) *Advanced Dairy Chemistry* (Vol.1, pp. 319-386). New York, USA: Kluwer Academic/Plenum.

Schmidt, D.G. (1982). Association of caseins and casein micelle structure. In P. F. Fox (Ed.) *Developments in dairy chemistry* (Vol. 1, pp. 61-86). London: Applied Science Publishers.

Sharma, S. K., & Dalgleish, D. G. (1993). Interactions between milk serum proteins and synthetic fat globule membrane during heating of homogenized whole milk. *Journal of Agricultural and Food Chemistry, 41*(9), 1407-1412.

Sharma, S. K., & Dalgleish, D. G. (1993). Interactions between milk serum proteins and synthetic fat globule membrane during heating of homogenized whole milk. *Journal of Agricultural and Food Chemistry, 41*(9), 1407-1412.

Singh, H. (1991). Modification of food proteins by covalent crosslinking. *Trends in Food Science & Technology, 2*, 196-200.

Singh, H., Boland, M., &. Thompson, A. (Eds.) (2014). *Milk proteins : From expression to food* (2nd ed.). London: Academic Press.

Singh, H., & Gallier, S. (2017). Nature's complex emulsion: The fat globules of milk. *Food Hydrocolloids, 68* (Supplement C), 81-89.

Singh, H., & Latham, J. M. (1993). Heat stability of milk: Aggregation and dissociation of protein at ultra-high temperatures. *International Dairy Journal, 3*(3), 225-237.

Swaisgood, H. E. (2003). Chemistry of the caseins. In *Advanced Dairy Chemistry—1 Proteins* (pp. 139-201): New York: Kluwer Academic/Plenum.

Tessier, H., & Rose, D. (1958). Calcium ion concentration in milk. *Journal of Dairy Science, 41*(3), 351-359.

Thompson, A., Boland, M., & Singh, H. (Eds.) (2009). *Milk proteins: From expression to food*. London, UK: Academic Press.

Tobin, J. T., Fitzsimons, S. M., Kelly, A. L., & Fenelon, M. A. (2011). The effect of native and modified konjac on the physical attributes of pasteurized and UHT-treated skim milk. *International Dairy Journal, 21*(10), 790-797.

Topçu, A., Numanoğlu, E., & Saldamlı, İ. (2006). Proteolysis and storage stability of UHT milk produced in Turkey. *International Dairy Journal, 16*(6), 633-638.

Tran, H., Datta, N., Lewis, M. J., & Deeth, H. C. (2008). Predictions of some product parameters based on the processing conditions of ultra-high-temperature milk plants. *International Dairy Journal, 18*(9), 939-944.

Trejo, R., Dokland, T., Jurat-Fuentes, J., & Harte, F. (2011). Cryo-transmission electron tomography of native casein micelles from bovine milk. *Journal of Dairy Science, 94*(12), 5770-5775.

Valero, E., Villamiel, M., Miralles, B., Sanz, J., & Martínez-Castro, I. (2001). Changes in flavour and volatile components during storage of whole and skimmed UHT milk. *Food Chemistry, 72*(1), 51-58.

Van Asselt, A., Sweere, A., Rollema, H., & De Jong, P. (2008). Extreme high-temperature treatment of milk with respect to plasmin inactivation. *International Dairy Journal, 18*(5), 531-538.

Van Boekel, M. (1998). Effect of heating on Maillard reactions in milk. *Food Chemistry, 62*(4), 403-414.

van Boekel, M. A. (1999). Heat-induced deamidation, dephosphorylation and breakdown of caseinate. *International Dairy Journal, 9*(3), 237-241.

van der Ven, C., Muresan, S., Gruppen, H., de Bont, D. B., Merck, K. B., & Voragen, A. G. (2002). FTIR spectra of whey and casein hydrolysates in relation to their functional properties. *Journal of Agricultural and Food Chemistry, 50*(24), 6943-6950.

Varnam, A., & Sutherland, J. P. (2001). *Milk and milk products Technology, chemistry and microbiology.* Maryland, USA: Aspen publishers.

Vazquez-Landaverde, P. A., Torres, J., & Qian, M. (2006). Quantification of trace volatile sulfur compounds in milk by solid-phase microextraction and gas chromatography–pulsed flame photometric detection. *Journal of Dairy Science, 89*(8), 2919-2927.

Vesconsi, C. N., Valduga, A. T., & Cichoski, A. J. (2012). Particle sedimentation in semi-skimmed, skimmed on whole milk UHT, during storage. *Ciência Rural, 42*(4), 730-736.

Walstra P. (1999). Casein sub-micelles: do they exist? *International Dairy Journal, 9*(3), 189-192.

Walstra, P., Jenness, R., & Badings, H. T. (1984). *Dairy chemistry and physics*. New York, USA: John Wiley & Sons.

Walstra, P., Wouters, J. T. M., & Geurts, T. J. (2005). *Dairy science and technology* (2nd ed.). Boca Raton, Florida, USA: CRC Press.

Wang, Q., He, L., Labuza, T. P., & Ismail, B. (2013). Structural characterisation of partially glycosylated whey protein as influenced by pH and heat using surface-enhanced Raman spectroscopy. *Food Chemistry, 139* (1–4), 313-319.

Wang, W., Nema, S., & Teagarden, D. (2010). Protein aggregation—Pathways and influencing factors. *International Journal of Pharmaceutics, 390*(2), 89-99.

Whittinghill, J. M., Norton, J., & Proctor, A. (1999). A fourier transform infrared spectroscopy study of the effect of temperature on soy lecithin-stabilized emulsions. *Journal of the American Oil Chemists' Society, 76*(12), 1393-1398.

Wynn, P. C., & Sheehy, P. A. (2013). Minor proteins, including growth factors. In P. L. H. McSweeney & P. F. Fox (Eds.), *Advanced Dairy Chemistry* (pp. 317-335). Boston, MA: Springer US.

Yagi, M., Sakurai, K., Kalidas, C., Batt, C. A., & Goto, Y. (2003). Reversible unfolding of bovine β-lactoglobulin mutants without a free thiol group. Journal of Biological Chemistry, 278(47), 47009-47015.

Yang, H., Yang, S., Kong, J., Dong, A., & Yu, S. (2015). Obtaining information about protein secondary structures in aqueous solution using Fourier transform IR spectroscopy. *Nature Protocols, 10*(3), 382-396.

Zhou, Q., Sun, S.-Q., Yu, L., Xu, C.-H., Noda, I., & Zhang, X.-R. (2006). Sequential changes of main components in different kinds of milk powders using two-dimensional infrared correlation analysis. *Journal of Molecular Structure, 799*(1–3), 77-84.